

KNOTS AND CHAOS IN THE RÖSSLER SYSTEM

ERAN IGRA

ABSTRACT. The Rössler System is one of the best known chaotic dynamical systems, exhibiting a plethora of complex phenomena - and yet, only a few studies tackled its complexity analytically. In this paper we find sufficient conditions for the existence of chaotic dynamics for the Rössler System at some specific parameter values at which the flow satisfies a certain heteroclinic condition. This will allow us to prove the existence of infinitely many periodic trajectories for the flow, and study their bifurcations in the parameter space of the Rössler system.

Keywords - The Rössler Attractor, Chaos Theory, Heteroclinic bifurcations, Topological Dynamics

1. INTRODUCTION

In 1976, Otto E. Rössler introduced the following system of Ordinary Differential Equations, depending on parameters $A, B, C \in \mathbf{R}^3$ [6]:

$$\begin{cases} \dot{X} = -Y - Z \\ \dot{Y} = X + AY \\ \dot{Z} = B + Z(X - C) \end{cases} \quad (1)$$

Unlike many other dynamical systems, the Rössler system was not introduced in order to model any specific natural phenomena. Rather, inspired by the Lorenz attractor (see [2]), Otto E. Rössler attempted to find the simplest non-linear flow exhibiting chaotic dynamics. This is realized by the vector field above, as it has precisely one non-linearity, XZ in the \dot{Z} component - and as observed by Rössler, the vector field appears to generate a chaotic attractor for $(A, B, C) = (0.2, 0.2, 5.7)$. In more detail, at these parameter values Rössler observed the first return map of the flow has the shape of a horseshoe (i.e., numerically), which is known to be chaotic (see [4]).

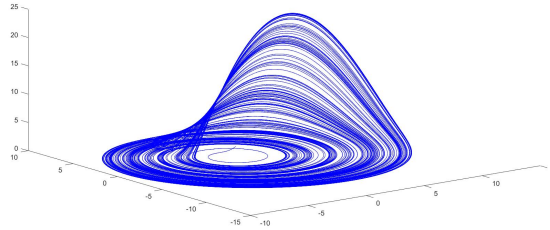


FIGURE 1. The Rössler attractor at $(A, B, C) = (0.2, 0.2, 5.7)$

Since its introduction in 1976, the Rössler system was the focus of many numerical studies - despite the simplicity of the vector field, the flow gives rise to many non-linear phenomena (see, for example: [27], [22], [20], [24], [23]). One particular feature is that varying the parameters A, B, C often leads to a change in the complexity of the system: that is, as the parameters are varied, more and more symbols appear in the first-return map of the flow (for more details, see [27], [22],[12],[25]). In a topological context, several numerical studies noted this variation of parameters changes the topology of the attractor - see, for example, [12],[25].

In contrast to the vast corpus of numerical studies, analytical results on the Rössler system are sparse. For example, in [15], the existence of periodic trajectories at some parameters was established; in [26] the existence of an invariant Torus (and its breakdown) at some parameters was proven; and in [21] the dynamics of the flow at ∞ were analyzed. As far as chaotic dynamics go, their existence at $(A, B, C) = (0.2, 0.2, 5.7)$ was proven with rigorous numerical methods - see [13],[18]. To our knowledge, no studies on the Rössler system attempted to prove its nonlinear phenomena (and in particular, its chaotic dynamics) by analytical tools. It is precisely this gap that this paper aims to address. In this paper we prove analytically, for the first time, sufficient conditions for the existence of complex dynamics in the Rössler system.

The key idea in everything that is to follow is that the existence of a certain heteroclinic knot at some parameters (A, B, C) forces the creation of complex dynamics for the first-return map (see Def.1.1 and Th.3.1 for the precise formulation). We denote such parameters as **trefoil parameters** (for a precise definition, see Def.3.2). In [28] it was proven the existence of a similar heteroclinic knot for the Lorenz system also implies similar results - as such, this study and [28] lend further credence to the role of heteroclinic knots in the onset of complex dynamics. As must be stated, these heteroclinic knots and their connection to the onset of chaotic dynamics play a similar role to that of the homoclinic trajectories in Shilnikov's Theorem (see [3] for more details).

To state our main results, given parameter values $p = (A, B, C)$, denote by F_p the corresponding vector field. As we will see later on, there exists an open set of parameters $P \subseteq \mathbf{R}^3$, s.t. $\forall p \in P$, F_p generates a cross-section U_p which varies smoothly in p . Now, denote by $f_p : \overline{U_p} \rightarrow \overline{U_p}$ the first return map of F_p (wherever defined), and denote by $\sigma : \{1, 2\}^{\mathbf{N}} \rightarrow \{1, 2\}^{\mathbf{N}}$ the one sided-shift. We first prove the following result, about the global dynamics of F_p (see the discussion before Lemma 2.2 and Th.2.1):

Theorem 1. *There exists an open set of parameters $O \subseteq \mathbf{R}^3$ s.t. F_p can be extended to a vector field on S^3 with precisely three fixed points - two saddle-foci P_{In}, P_{Out} (of opposing indices) and a degenerate fixed point at ∞ . Moreover, both P_{In}, P_{Out} admit heteroclinic trajectories connecting them to ∞ .*

Th.1 would be proven in Section 2.1 - as we will discover, Th.1 and its corollaries serve as the backbone of almost all the results which come next. In particular, Th.1 will allow us to find a cross-section, $H_p \subseteq U_p$ on which the first-return map $f_p : \overline{H_p} \rightarrow \overline{H_p}$ is well-defined at every initial condition $x \in \overline{H_p}$ (see Lemma 2.2.1 and Prop.2.3). These results (as well as the other corollaries of Th.1) would allow us to state and prove the following criterion for the existence of complex dynamics for the Rössler system at trefoil parameters (see Th.3.1):

Theorem 2. *Let $p = (A, B, C) \in P$ be a trefoil parameter as given in Def.3.2. Then, there exists an f_p -invariant $Q \subseteq \overline{U_p}$ and a continuous $\pi : Q \rightarrow \{1, 2\}^{\mathbf{N}}$ such that:*

- $\pi \circ f_p = \sigma \circ \pi$.
- f_p is continuous on Q .
- $\pi(Q)$ includes every periodic symbol $s \in \{1, 2\}^{\mathbf{N}}$.
- Given any periodic $s \in \{1, 2\}^{\mathbf{N}}$ of minimal period $k > 0$, $\pi^{-1}(s)$ includes at least one periodic point for f_p of minimal period k .

The proof of Th.2 would take up most of Section 3, and will be carried by directly analyzing the vector field using (mostly) elementary methods. Despite the relative complexity and the many details and technicalities involved, the idea behind the proof of Th.2 is fairly simple - inspired by [18] and [16], we prove the existence of the heteroclinic trefoil knot forces the first-return map to have dynamics similar (though not the same) to those of a topological horseshoe (see [16] for a precise definition). Once Th.2 is proven, we apply it to analyze the dynamical complexity of the flow in and around trefoil parameters. Inspired by [13] and using both Th.2 and a Fixed-Point Index argument (see Ch.VII.5 in [5]), we prove the following Theorem in Section 4 (see Th.4.1):

Theorem 3. *Let $p \in P$ be a trefoil parameter, and let $v \in P$ s.t. $v \neq p$, and choose some $k > 0$. Then, provided v is sufficiently close to p , $f_v : \overline{U_v} \rightarrow \overline{U_v}$ has at least one periodic orbit of minimal period k .*

Or, in other words, Theorem 3 has the following meaning - the closer a parameter $v \in P$ is to a trefoil parameter p , the more complex its dynamics become. With these ideas in mind, we must remark that when the parameter space of the Rössler system was analyzed numerically, spiral bifurcation structures were observed (see, for example [27], [22], [20], [24]). In all these studies, these spiral structures always accumulated at some point p_0 , often referred to as a **periodicity hub**, which lies on the Shilnikov homoclinic curve (see [3]). As was observed in [23] (see pg. 430), the dynamics around some periodicity hubs may, in fact, be heteroclinic. This suggests Th.2 and 3 possibly have a part in explaining the emergence of such complex phenomena.

Finally, we must also stress that even though the results in this study all relate to the Rössler system, in practice most of our arguments in Section 3 and 4 are purely topological. As such, they can be generalized and applied to study nonlinear phenomena in a much wider class of smooth flows on \mathbf{R}^3 . In particular, they exemplify the potential of topological methods for explaining the emergence of nonlinear, chaotic phenomena - and moreover, they attest to the importance of bounded heteroclinic trajectories to the emergence of chaotic and complex dynamics in three-dimensional flows. As such, our results (and in particular Th.2, Th.3 and Prop.4.2) should be compared with those of [14], where the bifurcations scenario around heteroclinic connections was studied in a two-parameter family of vector fields.

PRELIMINARIES

Let X be a metric space, with a metric d . For any $A \subseteq X$, we will denote by \overline{A} the closure of A , and by ∂A the boundary of A . Given any $x \in X, r > 0$, we denote the ball of radius r around x by $B_r(x)$. Also, given

$A, B, C, D \subseteq X$, we say that C **connects** A, B if C is connected and $A \cap C, B \cap C \neq \emptyset$. We say that D **separates** A, B if given any connected C which connects A, B , we also have $D \cap C \neq \emptyset$ - see the illustration in Fig.2. Moreover, we say a curve $\gamma : [0, 1] \rightarrow \mathbf{R}^3$ is **simple** or **not self intersecting** if for every $x, y \in [0, 1]$, $x \neq y$, $\gamma(x) \neq \gamma(y)$. Given a topological disc $D \subseteq \mathbf{R}^2$, we say D is a **Jordan domain** if its boundary ∂D can be parameterized by some $\gamma[0, 1]$ s.t. $\gamma(0) = \gamma(1)$ and for every other $x, y \in (0, 1)$, $\gamma(x) \neq \gamma(y)$.

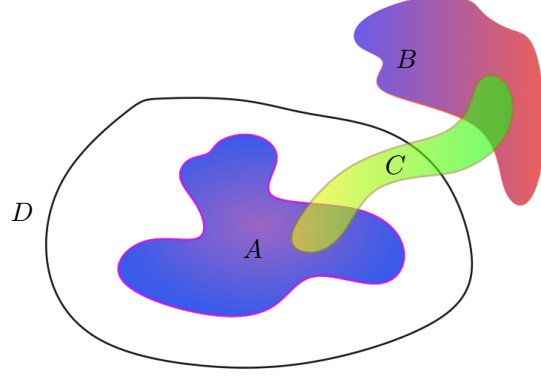


FIGURE 2. The set C connects A and B , while D separates them.

From now on given $(a, b, c) \in \mathbf{R}^3$, we switch to the more convenient form of the Rössler system, given by the following system of ODEs:

$$\begin{cases} \dot{x} = -y - z \\ \dot{y} = x + ay \\ \dot{z} = bx + z(x - c) \end{cases} \quad (2)$$

Denote this vector field corresponding to $(a, b, c) \in \mathbf{R}^3$ by $F_{a,b,c}$. This definition is slightly different from the one presented in Eq.1 - however, setting $p_1 = \frac{-C + \sqrt{C^2 - 4AB}}{2A}$, it is easy to see that whenever $C^2 - 4AB > 0$, $(X, Y, Z) = (x - ap_1, y + p_1, z - p_1)$ defines a change of coordinates between the vector fields in Eq.1 and Eq.2.

Before we continue, we must introduce a definition for chaotic dynamics:

Definition 1.1. Chaotic Dynamics Let Y be some topological space, and let $g : Y \rightarrow Y$ be continuous. We say g is **properly chaotic** provided the periodic orbits of g in Y are dense, and $\exists y \in Y$ s.t. $\{g^n(y)\}_{n \geq 0} = Y$. We say a first-return map $f : S \rightarrow S$ for a smooth flow on \mathbf{R}^3 is **chaotic** on some bounded invariant set $X \subseteq S$, if f is continuous on X and there exists a topological space Y , a properly chaotic $g : Y \rightarrow Y$ and a continuous, surjective, $\pi : X \rightarrow Y$ s.t. $\pi \circ f = g \circ \pi$.

For example, the Smale Horseshoe map (see [4]) is a properly chaotic map, while the first-return map of the Geometric Lorenz Attractor (see, for example, Ch.3 in [19]) is chaotic. As must be remarked, this definition is inspired (yet more complicated) from the one originally given in [11] - however, as we will see, it is the one necessary for the proof of existence of complex dynamics in Th.3.1.

To conclude this section, since the vector field in Eq.2 depends on three parameters, (a, b, c) , we must specify the region in the parameter space in which we prove our results. As observed in several numerical studies (see, for example, [22],[27],[20] and [23]), many interesting bifurcation phenomena occur at a very specific **open region** in the parameter space. In that parameter space the a, b, c parameters **always** satisfy $a, b \in (0, 1)$, $c > 1$ - and moreover, the vector field F_p always generates precisely two fixed points, P_{In}, P_{Out} , s.t. **both** are saddle-foci. Additionally, in these studies the eigenvalues of the linearization at P_{In} satisfy a resonance condition known as the **Shilnikov condition** (see [3] or below for a definition) - and moreover, this resonance condition is stable in the parameter space. Therefore, to make everything clear, let us write down the assumption we impose on our parameter space P :

- **Assumption 1** - $\forall p \in P, p = (a, b, c)$ the parameters satisfy $a, b \in (0, 1)$ and $c > 1$. As can be seen, for every choice of such p , the vector field F_p generates precisely two fixed points - $P_{In} = (0, 0, 0)$ and $P_{Out} = (c - ab, b - \frac{c}{a}, \frac{c}{a} - b)$.
- **Assumption 2** - We assume that for every $p \in P$ the fixed points P_{In}, P_{Out} are both saddle-foci of opposing indices. In more detail, we always assume that P_{In} has a one-dimensional stable manifold, W_{In}^s , and a two-dimensional unstable manifold, W_{In}^u . Conversely, we assume P_{Out} has a one-dimensional

unstable manifold, W_{Out}^u , and a two-dimensional stable manifold, W_{Out}^s - that is, the linearization of F_p at P_{Out} , $J_p(P_{Out})$ has one **positive**, real eigenvalue γ_{Out} , and two complex-conjugate eigenvalues $\rho_{Out} \pm i\omega_{Out}$ s.t. $\rho_{Out} > 0$.

- **Assumption 3** - For every $p \in P$, let set $\gamma_{In} < 0$ and $\rho_{In} \pm i\omega_{In}$, $\rho_{In} > 0$ denote the eigenvalues of $J_p(P_{In})$, the linearization of P_{In} , and set $\nu_{In} = |\frac{\rho_{In}}{\gamma_{In}}|$. Conversely, let $\gamma_{Out} > 0$, $\rho_{Out} \pm i\omega_{Out}$ s.t. $\rho_{Out} > 0$ denote the eigenvalues of $J_p(P_{Out})$ and define $\nu_{Out} = |\frac{\rho_{Out}}{\gamma_{Out}}|$. We will refer to ν_{In}, ν_{Out} as the respective saddle indices at P_{In}, P_{Out} , and we will always assume $(\nu_{In} < 1) \vee (\nu_{Out} < 1)$ - that is, for every $p \in P$ **at least** one of the fixed points satisfies the Shilnikov condition (see [3] for more details).

As must be remarked, the parameter space P we are considering is not only open in the parameter space, but in fact but also **includes** the region considered in numerical studies. Additionally, it should also be stated that later in this paper, **after** the proof of Th.2.1 we will impose another, less trivial (yet stable), assumption on the dynamics of $F_{a,b,c}$, $a, b, c \in P$ - which, nevertheless, can be justified numerically (see the discussion in page 16). At the moment, however, we will be content with Assumptions 1 – 3.

2. THE GLOBAL DYNAMICS VECTOR FIELD F_p , $p \in P$.

A central theme in this paper is that parameters in P at which there exist certain heteroclinic connections force the creation of chaotic dynamics in the Rössler System. Generically, one cannot expect heteroclinic trajectories for the vector field in Eq.2 to be stable in the parameter space P - however, as we will prove in this section, in a sense this is **almost** the case. More precisely, in this section we will prove that given any $p = (a, b, c) \in P$, the vector field F_p **always** generates two unbounded, invariant one-dimensional separatrices in the parameter space, connecting each fixed point to ∞ (in S^3) - see Th.2.1. As Th.2.1 gives us information on the global dynamics of the flow, later on in Sections 3 and 4 Th.2.1 and its corollaries will form a major element in many of our results.

This section is organized as follows - we begin subsection 2.1 with a quick analysis of the vector field. Following that, we first prove the existence of a cross-section U_p , a half-plane which intersects transversely every periodic trajectory generated by F_p (see Lemma 2.1). Having done so, we turn to analyze the behavior of F_p on its unbounded trajectories - i.e., we analyze the global dynamics of F_p , which will be done in Th.2.1. The proof of Th.2.1 will be relatively long, forming the bulk of subsection 2.1. Once Th.2.1 is proven, we apply it in Subsection 2.2 to derive certain Corollaries on both the dynamical complexity of F_p around ∞ (see Cor.2.1.5), and about the first-return map and its dynamics (see Cor.2.1.6). Later in this paper, Cor.2.1.6 will allow us to locate a cross-section, $\overline{D_\alpha}$, which is a topological disc on which the first-return map $f_p : \overline{D_\alpha} \rightarrow \overline{D_\alpha}$ is well-defined (see Th.2.2, Prop.2.3 and Cor.2.2.1).

2.1. A heteroclinic connection through ∞ . To begin, fix some parameter $p = (a, b, c) \in P$ and consider the plane $Y_p = \{(x, -\frac{x}{a}, z) | x, z \in \mathbf{R}\} = \{\dot{y} = 0\}$ (with \dot{y} taken w.r.t. F_p - see Eq.2). Let $N_p = (1, a, 0)$ denote the normal vector to Y_p , - by computation F_p is tangent to Y_p **precisely** at the straight line $l_p = \{(t, -\frac{t}{a}, \frac{x}{a}) | t \in \mathbf{R}\}$. Hence, $Y_p \setminus l_p$ consists of precisely two components, both half-planes - let $U_p = \{(x, -\frac{x}{a}, z) | x, z \in \mathbf{R}, -z + \frac{x}{a} < 0\}$ denote the upper half of $Y_p \setminus l_p$, and denote by $L_p = \{(x, -\frac{x}{a}, z) | x, z \in \mathbf{R}, -z + \frac{x}{a} > 0\}$ the lower half. As l_p is a straight line, we immediately conclude the following, useful fact:

Lemma 2.1. *Every bounded, invariant set generated by F_p that is **not** a fixed point (or limits to one) has to intersect U_p transversely **at least** once. In particular, any periodic trajectory intersects U_p transversely at least once.*

Now, denote by $f_p : \overline{U_p} \rightarrow \overline{U_p}$ the first-return map, wherever defined - by Lemma 2.1, it is defined at least around every periodic trajectory for F_p . We are thus led to the following question - on which initial conditions in $\overline{U_p}$ the first-return map g_p is defined? If we could answer this question, we could analyze the flow dynamics generated by F_p . By Lemma 2.1, the only initial conditions $x \in \overline{U_p}$ on which f_p is possibly undefined are those whose trajectories either limit to fixed points, or blow up to ∞ . This implies that in order to analyze the first-return map, we must study the unbounded dynamics of F_p - and in particular, its dynamics around ∞ - that is, its global dynamics.

To make this discussion more precise, let us consider the flow generated by the extension of F_p to the one-point compactification of \mathbf{R}^3 , S^3 . We first recall Th.1 in [21], where the dynamics of F_p around ∞ were analyzed by the means of the Poincaré sphere. In that paper it was proven the behaviour of F_p on $\{(x, y, z) | x^2 + y^2 + z^2 > r\}$ is independent of $r > 0$ (for any sufficiently large r) - which proves we can extend F_p to S^3 by adding ∞ as a fixed point for the flow. Therefore, from now on, **unless said otherwise**, we always consider F_p to be a vector field on S^3 with precisely three fixed points - P_{In}, P_{Out} and ∞ . This leads us to ask - just how well behaved is F_p around ∞ ? To answer this question, we now quickly prove:

Lemma 2.2. *For any $p \in P$, F_p is not C^1 at ∞ .*

Proof. For any $(x, y, z) = v \in \mathbf{R}^3$ consider the linearized vector field $J_p(v)$ at v - namely, the Jacobian matrix of F_p at $v \in \mathbf{R}^3$ (see Eq.2.) Now, choose some $\lambda \in \mathbf{R}$ and note the equation $\det(J_p(v)) = \lambda$ can be rewritten as $z = \frac{\lambda + c - x - ab}{a}$. This proves the set $S_\lambda = \{\det(J_p(v)) = \lambda\}$ is a plane in \mathbf{R}^3 - which implies that when we extend \mathbf{R}^3 to S^3 we have $\infty \in \partial S_\lambda$ (with ∂S_λ taken in S^3). We conclude that for any $\lambda_1 \neq \lambda_2$, we have $\{\infty\} = \partial S_{\lambda_1} \cap \partial S_{\lambda_2}$ - which proves $\det(J_p(v))$ takes infinitely many values at any neighborhood of ∞ . As such F_p cannot be C^1 at ∞ and the Lemma follows. \square

Lemma 2.2 teaches us we **cannot** analyze F_p as a smooth vector field on S^3 . However, even though F_p is not C^1 at ∞ , it still is C^1 in \mathbf{R}^3 , i.e. on $S^3 \setminus \{\infty\}$. This motivates us to prove Th.2.1 - as we will see in Section 3 and 4, Th.2.1 allows us to bypass the obstacle posed by Lemma 2.2 by reducing the dynamics of F_p by those of R_p : a smooth vector field on S^3 , whose first-return map is well defined (see Cor.??). To state it, recall W_{In}^s is the stable, one-dimensional invariant manifold of the saddle focus P_{In} - and that W_{Out}^u is the unstable, one dimensional manifold of the saddle focus P_{Out} . We now prove:

Theorem 2.1. *For every $p \in P$, F_p generates two heteroclinic trajectories:*

- $\Gamma_{In} \subseteq W_{In}^s$, which connects P_{In}, ∞ in S^3 .
- $\Gamma_{Out} \subseteq W_{Out}^u$, which connects P_{Out}, ∞ in S^3 .

As a consequence, for every sufficiently large $r > 0$, there exists a smooth vector field on S^3 , R_p , s.t.:

- R_p coincides with F_p on the open ball $B_r(P_{In})$.
- R_p has precisely two fixed points in S^3 - P_{In}, P_{Out} .
- R_p generates a heteroclinic trajectory which connects P_{In}, P_{Out} and passes through ∞ .

Proof. Let $(a, b, c) = p \in P$ be a parameter, and recall we denote by F_p the corresponding vector field (see Eq.2). Due to the length of the argument and the amount of details involved, we will split the proof into several stages - however, despite the length of the argument, the idea behind the proof of Th.2.1 is relatively straightforward. The sketch of the proof is as follows:

- In Stages *I* we analyze the local dynamics of F_p on two cross-sections: $\{\dot{x} = 0\}$ and $\{\dot{y} = 0\}$.
- In Stages *II* we use the results from Stage *I* and the interplay between the two cross-sections $\{\dot{x} = 0\}$ and $\{\dot{y} = 0\}$ to construct a three-dimensional body, C_{In} which traps Γ_{In} , a component of W_{In}^s . As we will prove, $C_{In} \subseteq \{\dot{y} \leq 0\}$, from which it would follow that Γ_{In} is a heteroclinic connection between P_{In}, ∞ .
- In Stage *III* we do the same for the outer fixed-point, P_{Out} - that is, we prove, using an almost symmetrical argument to Stage *II*, the existence of a three-dimensional body $C_{Out} \subseteq \{\dot{y} \leq 0\}$, trapping Γ_{Out} , a component of W_{Out}^u which is also a heteroclinic connection between P_{Out}, ∞ .
- In Stage *IV* we conclude the proof of Th.2.1 by constructing the vector field R_p . We do so by using the Poincare-Hopf Theorem to smoothen F_p around ∞ , thus constructing the vector field R_p . As we will prove, R_p can be constructed s.t. it coincides with F_p on an arbitrarily large set in \mathbf{R}^3 . Furthermore, by the existence of $\Gamma_{In}, \Gamma_{Out}$, we will construct R_p s.t. it has precisely two fixed points in S^3 , P_{In} and P_{Out} - connected by an unbounded heteroclinic trajectory.

To begin, following the sketch of proof above, our first objective is to analyze the local dynamics of F_p on the following cross-sections - $\{\dot{x} = 0\}$ and $\{\dot{y} = 0\}$ (both considered w.r.t. the vector field in Eq.2).

2.1.1. Stage I - a tale of two cross-sections. We begin with the cross-section $\{\dot{x} = 0\}$, given by the parameterization $\{(x, y, -y) | x, y \in \mathbf{R}\}$ (see Eq.2). From this parameterization $\{\dot{x} = 0\}$ is a plane, which proves $\mathbf{R}^3 \setminus \{\dot{x} = 0\}$ is composed of two open regions. The first is $\{\dot{x} > 0\}$, defined by $\{(x, y, -z) | x, y, z \in \mathbf{R}, y < -z\}$ and lying **below** $\{\dot{x} = 0\}$ - the second is $\{\dot{x} < 0\}$, given by the parameterization $\{(x, y, -z) | x, y, z \in \mathbf{R}, y > -z\}$ and lying **above** $\{\dot{x} = 0\}$ (see Fig.5 for an illustration). Now, recall we denote by W_{In}^s the one-dimensional stable invariant manifold of P_{In} , and by W_{In}^u the two-dimensional unstable invariant manifold of P_{In} . Similarly, we denote by W_{Out}^u the unstable one-dimensional invariant manifold of P_{Out} , and by W_{Out}^s the stable two-dimensional, invariant manifold of P_{Out} . We first prove:

Lemma 2.3. *The two-dimensional W_{Out}^s, W_{In}^u and the one dimensional W_{Out}^u, W_{In}^s are non-tangent to $\{\dot{x} = 0\}$ at P_{In}, P_{Out} , respectively. In particular, W_{Out}^s, W_{In}^u are transverse to $\{\dot{x} = 0\}$ at P_{Out}, P_{In} , respectively.*

Proof. The normal vector to $\{\dot{x} = 0\}$ is $(0, 1, 1)$ - therefore, for every point $v \in \{\dot{x} = 0\}$, the dot-product is $F_p(v) \bullet (0, 1, 1) = x + ay + bx - xy + cy$ - as such, $F_p(v) \bullet (0, 1, 1) \neq 0$ precisely when $y \neq \frac{-x(b+1)}{a+c-x}$. This proves the set $\{\dot{x} = 0\} \setminus \{(x, y, -y) | y = \frac{-x(b+1)}{a+c-x}\}$ is composed of three components, A_1, A_2, A_3 , defined thus:

- For $v \in A_1 \cup A_2$ we have $F_p(v) \bullet (0, 1, 1) < 0$.
- For $v \in A_3$ we have $F_p(v) \bullet (0, 1, 1) > 0$.

See Fig.3 for an illustration. That is, on A_1, A_2 the vector field F_p points inside $\{\dot{x} > 0\}$, while on A_3 it points inside $\{\dot{x} < 0\}$. The sets A_1, A_2, A_3 are separated from one another by the curve $\sigma(x) = (x, -\frac{x(b+1)}{a+c-x}, \frac{x(b+1)}{a+c-x})$,

$x \neq c + a$, on which F_p is tangent to $\{\dot{x} = 0\}$ (see Fig.3 for a illustration). By computation, the tangent vectors to $\sigma(x), x \neq c + a$ are given by $\sigma'(x) = (1, \frac{-(b+1)(a+c)}{(a+c-x)^2}, \frac{(b+1)(a+c)}{(a+c-x)^2})$, $x \neq c + a$.

Now, consider the linearization of F_p at P_{In} , denoted by $J_p(P_{In})$ - by direct computation, $\sigma'(x)$ is not an eigenvector for $J_p(P_{In})$ (for every $t \neq c + a$). Hence, since $P_{In} = \sigma(0)$, W_{In}^u must be transverse to $\{\dot{x} = 0\}$ at P_{In} - a similar argument now proves W_{In}^s cannot be tangent to σ at P_{In} . Finally, by considering $J_p(P_{Out})$ - the linearization of F_p at P_{Out} - the same arguments prove W_{Out}^s is transverse to $\{\dot{x} = 0\}$ at P_{Out} , and that W_{Out}^u is non-tangent to σ at P_{Out} . \square

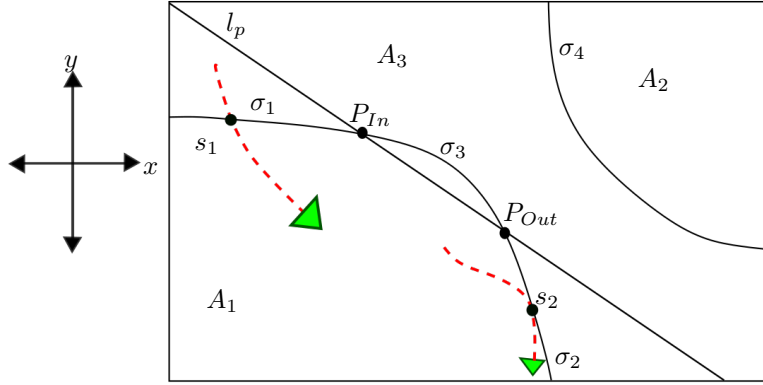


FIGURE 3. the geography of $\{\dot{x} = 0\}$. Observe the flow lines arriving from below $\{\dot{x} = 0\}$.

Having proven Lemma 2.3, we now proceed by characterizing the local behaviour of F_p on initial conditions lying in σ , the tangency curve of F_p to $\{\dot{x} = 0\}$ (see the proof of Lemma 2.3 for the definition, and Fig.3 for an illustration). As computed in the proof of Lemma 2.3, σ is parameterized by $\sigma(x) = (x, -\frac{x(b+1)}{a+c-x}, \frac{x(b+1)}{a+c-x})$, $x \neq c + a$, and it separates the regions A_1, A_2, A_3 on $\{\dot{x} = 0\}$ (see the definition in the proof of Lemma 2.3, and the illustration in Fig.3). Now, recall $P_{Out} = (c - ab, b - \frac{c}{a}, \frac{c}{a} - b)$ - since $c + a > c - ab$, from $P_{In} = (0, 0, 0)$ we conclude P_{Out}, P_{In} lie on the same component in σ . Set A_1 as the component of $\{v \in \{\dot{x} = 0\} | F_p(v) \bullet (0, 1, 1) < 0\}$ s.t. $P_{In}, P_{Out} \in \partial A_1$ - by this discussion, ∂A_1 is a component of σ .

From now on, given any $s \in \mathbf{R}^3$ denote by γ_s its trajectory, $\gamma_s(0) = s$. By computation, $\sigma \setminus \{P_{In}, P_{Out}\}$ is composed of four components, $\sigma_1, \sigma_2, \sigma_3, \sigma_4$ s.t. σ_1 connects P_{In}, ∞ , and σ_2 connects P_{Out}, ∞ , and σ_3 connects P_{In}, P_{Out} (see the illustration in Fig.3). We now prove the following fact about the local dynamics of F_p on σ , thus concluding our analysis of $\{\dot{x} = 0\}$:

Lemma 2.4. *For every initial condition $s \in \sigma_1, \sigma_2$, there exists $\epsilon > 0$ s.t. for every time $t \in (-\epsilon, \epsilon), t \neq 0$, we have $\gamma_s(t) \in \{\dot{x} > 0\} \cap \{\dot{y} < 0\} \cap \{\dot{z} > 0\}$. Additionally, $\sigma_3, \sigma_4 \subseteq \{\dot{y} > 0\}$.*

Proof. We first prove that for every $s \in \sigma_1, \sigma_2$, there exists $\epsilon > 0$ s.t. given $t \in (-\epsilon, \epsilon), t \neq 0$ we have $\gamma_s(t) \in \{\dot{x} > 0\} \cap \{\dot{y} < 0\} \cap \{\dot{z} > 0\}$. To this end, recall Eq.2. By the discussion above, ∂A_1 is parameterized by $\sigma(x) = (x, -\frac{x(b+1)}{a+c-x}, \frac{x(b+1)}{a+c-x})$, $x < c + a$. By computation, $F_p(x, -\frac{x(b+1)}{a+c-x}, \frac{x(b+1)}{a+c-x}) = (0, \frac{-x^2+cx-abx}{a+c-x}, \frac{x^2-cx+abx}{a+c-x})$ -therefore, for $x < 0$ or $c - ab < x < c + a$ we have $\frac{-x^2+cx-abx}{a+c-x} < 0$. Hence, for $x < 0$ or $c - ab < x < c + a$, $F_p(\sigma(x))$ points in the negative y -direction and positive z -direction - which proves the trajectory of an initial condition $\sigma(x)$ with $x < 0$ or $c - ab < x < c + a$ leaves ∂A_1 and enters the region $\{\dot{x} > 0\} \cap \{\dot{y} < 0\} \cap \{\dot{z} > 0\}$ (see Fig.3 for an illustration). Since points on σ_1, σ_2 correspond to initial conditions $\sigma(x)$ s.t. $x < 0$ and $c - ab < x < c + a$ (respectively), we conclude the flow lines arrive at σ_1, σ_2 from $\{\dot{x} > 0\} \cap \{\dot{y} < 0\} \cap \{\dot{z} > 0\}$ - that is, writing $s = \sigma(x)$, $\exists \epsilon_1 > 0$ s.t. $\forall t \in (-\epsilon_1, 0), \gamma_s(t) \in \{\dot{x} > 0\} \cap \{\dot{y} < 0\} \cap \{\dot{z} > 0\}$.

A similar argument applied to $-F_p$ (i.e. to the inverse flow) proves that $\forall s \in \sigma_1 \cup \sigma_2$ there exists some $\epsilon_2 > 0$ s.t. $\gamma_s(t) \in \{\dot{x} > 0\} \cap \{\dot{y} < 0\} \cap \{\dot{z} > 0\}$ whenever $t \in (0, \epsilon_2)$ (see Fig.3 for an illustration). Hence, we conclude that given any $s \in \sigma_1, \sigma_2$, there exists $\epsilon > 0$ s.t. given $t \in (-\epsilon, \epsilon), t \neq 0$ we have $\gamma_s(t) \in \{\dot{x} > 0\} \cap \{\dot{y} < 0\} \cap \{\dot{z} > 0\}$. To conclude the proof of Lemma 2.4 we need now prove that $\sigma_3, \sigma_4 \subseteq \{\dot{y} > 0\}$. To do so, recall we have $F_p(x, -\frac{x(b+1)}{a+c-x}, \frac{x(b+1)}{a+c-x}) = (0, \frac{-x^2+cx-abx}{a+c-x}, \frac{x^2-cx+abx}{a+c-x})$, which proves that for $x \in (0, c - ab)$ or $x > a + c$ we have $\frac{-x^2+cx-abx}{a+c-x} > 0$ - since σ_3, σ_4 correspond to points $\sigma(x)$ where $x \in (0, c - ab)$ or $x > a + c$ respectively, we're done. \square

We now turn our attention to the local dynamics of F_p on the cross section $\{\dot{y} = 0\}$. To do so, first recall the cross-sections $Y_p = \{\dot{y} = 0\}$, U_p, L_p , analyzed in the discussion preceding Lemma 2.1 - in particular, recall $(1, a, 0)$ is the normal vector to Y_p , and that for $v \in U_p$, $F_p(v) \bullet (1, a, 0) < 0$, while for $v \in L_p$, $F_p(v) \bullet (1, a, 0) > 0$. We will now quickly replicate the arguments of Lemmas 2.3 and 2.4 to describe the local dynamics of F_p on Y_p . First, let us make some general remarks - since $\{\dot{y} = 0\}$ is a plane, $\mathbf{R}^3 \setminus \{\dot{y} = 0\}$ is composed of two components - $\{\dot{y} > 0\}$ parameterized by $\{(x, y, z) | x, y, z \in \mathbf{R}^3, x > -ay\}$ and $\{\dot{y} < 0\}$, given by $\{(x, y, z) | x, y, z \in \mathbf{R}^3, x < -ay\}$ - both are open, connected regions in \mathbf{R}^3 (see the illustration in Fig.5). By this discussion we conclude that on U_p , F_p points inside $\{\dot{y} < 0\}$, while on L_p it points inside $\{\dot{y} > 0\}$. In fact, we can say more - by direct computation it also follows that $U_p = \{\dot{y} = 0\} \cap \{\dot{x} < 0\}$ and $L_p = \{\dot{y} = 0\} \cap \{\dot{x} > 0\}$. In addition, it also follows that on U_p the vector field F_p points inside the quadrant $\{\dot{x} < 0\} \cap \{\dot{y} < 0\}$ and on L_p inside the quadrant $\{\dot{x} > 0\} \cap \{\dot{y} > 0\}$.

As proven in the discussion preceding Lemma 2.1, the tangency set of F_p to Y_p is a curve parameterized by $l_p(x) = (x, -\frac{x}{a}, \frac{x}{a})$, $x \in \mathbf{R}$. By computation, the tangent vector to $l_p(x)$ is $l'_p(x) = (1, -\frac{1}{a}, \frac{1}{a})$. Therefore, using the Jacobian matrix precisely like we did in Lemma 2.3 we conclude (see the illustration in Fig.4):

Corollary 2.1.1. *The two dimensional, invariant manifolds W_{In}^u, W_{Out}^s are transverse to U_p, L_p at both P_{In}, P_{Out} .*

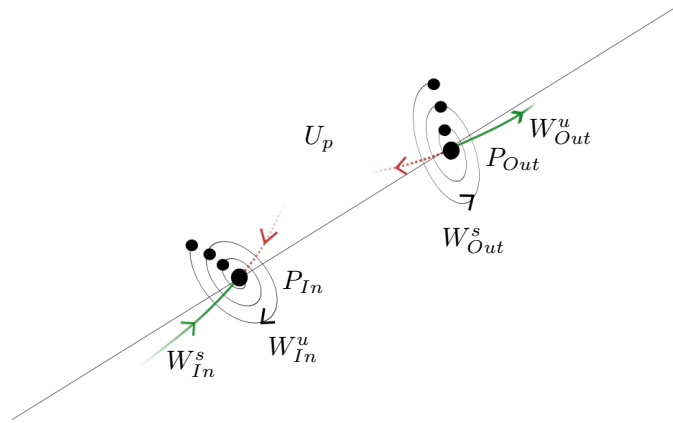


FIGURE 4. The local dynamics around the fixed points. The green and red flow lines are the one-dimensional separatrices in W_{In}^s, W_{Out}^u .

Similarly to Lemma 2.4, we now characterize the local behavior of F_p on l_p . Recall that given any $s \in \mathbf{R}^3$, we denote by γ_s its trajectory, $\gamma_s(0) = s$. We now prove:

Lemma 2.5. $l_p = \{\dot{x} = 0\} \cap \{\dot{y} = 0\}$. Additionally, given $s \in l_p$, $s = (x, -\frac{x}{a}, \frac{x}{a})$, $x \in \mathbf{R}$, then for $x < 0$ or $x > c - ab$, there exists some $\epsilon > 0$ s.t. $\gamma_s(t) \in \{\dot{y} < 0\} \cap \{\dot{z} > 0\}$ for all $t \neq 0, t \in (-\epsilon, \epsilon)$. Conversely, when $x \in (0, c - ab)$ we have $s \in \{\dot{z} < 0\}$, and there exists an $\epsilon > 0$ s.t. for $t \in (-\epsilon, \epsilon), t \neq 0$ we have $\gamma_s(t) \in \{\dot{y} > 0\} \cap \{\dot{z} < 0\}$.

Proof. From $F_p(l_p(x)) = (0, 0, bx + \frac{x^2}{a} - \frac{cx}{a})$ we conclude $l_p = \{\dot{y} = 0\} \cap \{\dot{x} = 0\}$ (see Fig.5 for an illustration). Now, $bx + \frac{x^2}{a} - \frac{cx}{a}$ is a quadratic polynomial vanishing precisely at P_{In}, P_{Out} - therefore $F_p(l_p(x))$ points in the positive z -direction precisely when $x < 0$ or $x > c - ab$ - in particular, at such x , the vector $F_p(l_p(x))$ is tangent to H_p . Now, recall the normal vector to U_p is $(1, a, 0)$, and that by computation, for all $v \in U_p$ we have $F_p(v) \bullet (1, a, 0) < 0$ (see the discussion preceding Lemma 2.1). We therefore conclude the vector field F_p points on U_p inside $\{\dot{y} < 0\}$. As such, by previous discussion we conclude that for $x < 0$ or $x > c - ab$ the trajectory of $l_p(x)$ arrives at $l_p(x)$ from $\{\dot{y} < 0\} \cap \{\dot{z} > 0\}$ (the region in the front of Fig.5) and flows back straight back inside $\{\dot{y} < 0\} \cap \{\dot{z} > 0\}$ (see Fig.5 for an illustration). Hence, all in all, given $s = l_p(x)$, $x < 0$ or $x > c - ab$, there exists an $\epsilon > 0$ s.t. $\gamma_s(t) \in \{\dot{y} < 0\} \cap \{\dot{z} > 0\}$ for all $t \neq 0, t \in (-\epsilon, \epsilon)$.

Finally, from $F_p(l_p(x)) = (0, 0, bx + \frac{x^2}{a} - \frac{cx}{a})$ we conclude that for $x < 0, x > c - ab$ we have $l_p(x) \in \{\dot{z} > 0\}$ - and for $x \in (0, c - ab)$, $l_p(x) \in \{\dot{z} < 0\}$. A similar argument to the one used in the previous paragraph now proves that for $s = l_p(x)$, $0 < x < c - ab$ there exists some $\epsilon > 0$ s.t. for $t \neq 0, t \in (-\epsilon, \epsilon)$ we have $\gamma_s(t) \in \{\dot{y} > 0\} \cap \{\dot{z} < 0\}$ and Lemma 2.5 now follows. \square

Having completed the analysis of $\{\dot{x} = 0\}$ and $\{\dot{y} = 0\}$, we are now ready to prove the existence of Γ_{In} , a separatrix in the one-dimensional stable manifold W_{In}^s which connects P_{In}, ∞ .

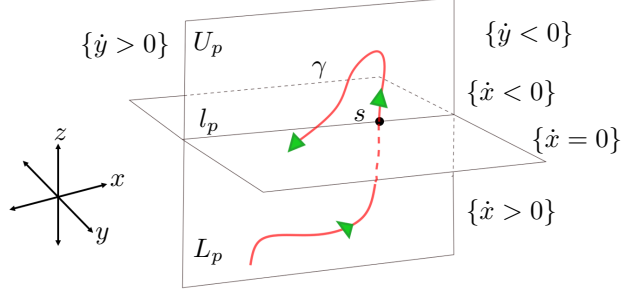


FIGURE 5. The trajectory of an initial condition $s = l_p(x)$, $x < 0$ or $x > c - ab$.

2.1.2. Stage II - the existence of Γ_{In} . In this section we prove the existence of Γ_{In} - an unbounded component of the one-dimensional invariant manifold of P_{In} , W_{In}^s . We do so as follows - using the results proven in Stage I, we first prove the existence of Γ_{In} by constructing a three-dimensional body $C_{In} \subseteq \{y \geq 0\} \cap \{x \geq 0\}$ s.t. no trajectories can enter C_{In} in forward time (see Prop.2.1). As we will see, this would imply C_{In} traps Γ_{In} , a component of W_{In}^s . Thus, reversing the flow, we will conclude the trajectory of every initial condition on Γ_{In} blows up to ∞ under the **inverse** flow (see Cor.2.1.3) - from which it would follow that P_{In}, ∞ are connected by a heteroclinic trajectory in W_{In}^s .

To begin, first consider the plane $\{x = 0\} = \{(0, y, z) | y, z \in \mathbf{R}\}$. Its normal vector is $(1, 0, 0)$, which, by computation (and Eq.2), proves $F_p(0, y, z) \bullet (1, 0, 0) = -y - z = \dot{x}$. Therefore, since $(1, 0, 0)$ points inside the region $\{(x, y, z) | x > 0\} = \{x > 0\}$ we immediately conclude:

Lemma 2.6. *For every $v \in \{x = 0\}$, $F_p(v) \bullet (1, 0, 0) \geq 0$ if and only if $v \in \{\dot{x} \geq 0\} \cap \{x = 0\}$. In particular, on $\{x = 0\} \cap \{\dot{x} > 0\}$ the vector field F_p points inside $\{x > 0\}$ - and on $\{x = 0\} \cap \{\dot{x} < 0\}$, F_p points inside $\{x < 0\}$ (see the illustration in Fig.6).*

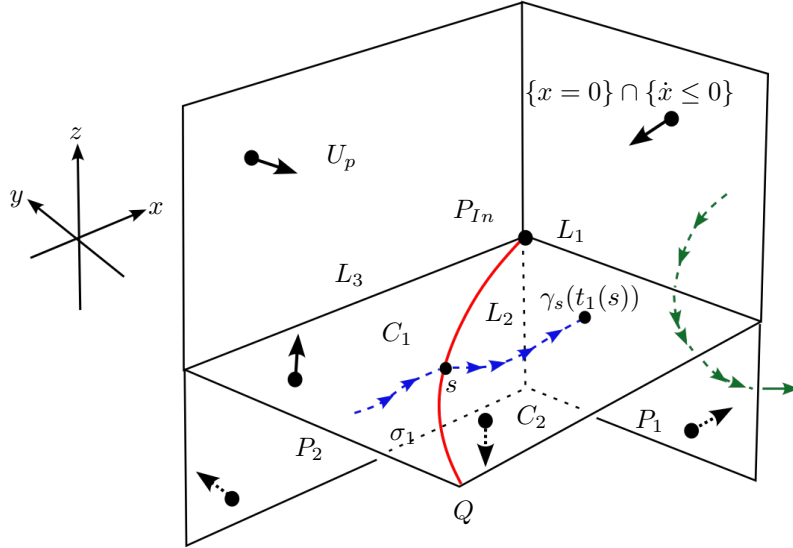


FIGURE 6. The set Q , along with the directions of F_p on P_1, P_2 , and $P_3 = C_1 \cup C_2$. The blue line is the trajectory of an initial condition $s \in \sigma_1$, while the green is a trajectory of some initial condition in L_1 . Q is the quadrant trapped between P_1, P_2 and P_3 .

We are now ready to state and prove Prop.2.1. To begin, first recall we proved in Stage I that both $\{\dot{x} = 0\}, \{\dot{y} = 0\}$ are planes transverse to one another (see Lemma 2.5 and the illustration in Fig.5). As we proved in Stage I, $\mathbf{R}^3 \setminus \{\dot{x} = 0\}$ is composed of two connected regions - $\{\dot{x} > 0\}$ and $\{\dot{x} < 0\}$ - and similarly, $\mathbf{R}^3 \setminus \{\dot{y} = 0\}$ is also composed of two regions, $\{\dot{y} > 0\}$ and $\{\dot{y} < 0\}$. Since $\{\dot{x} = 0\} \cap \{\dot{y} = 0\}$ is a transverse intersection, $\mathbf{R}^3 \setminus (\{\dot{x} = 0\} \cup \{\dot{y} = 0\})$ is made up of four connected regions (see the illustration in Fig.5). Now, consider the quadrant $Q = \{\dot{x} \geq 0\} \cap \{\dot{y} \leq 0\} \cap \{x \leq 0\}$, trapped between the three planes $\{\dot{x} = 0\}, \{\dot{y} = 0\}$ and $\{x = 0\}$ (see the illustration in Fig.6). We now prove:

Proposition 2.1. *There exists a three-dimensional, connected set C_{In} , s.t.:*

- $P_{In} \in \partial C_{In}$, $P_{Out} \notin \partial C_{In}$.
- $C_{In} \subseteq \{\dot{y} \leq 0\} \cap \{\dot{x} \geq 0\}$.
- For every $v \in \partial C_{In}$, $F_p(v)$ is either tangent or points into $\mathbf{R}^3 \setminus C_{In}$ - that is, given any initial condition $s \notin C_{In}$, its forward trajectory never enters C_{In} .

Proof. We prove Prop.2.1 as a sequence of interconnected short, technical Lemmas and their Corollaries. The idea behind the proof is as follows - recall the curve σ_1 introduced at Stage I (see the discussion after Lemma 2.3, and Fig.3 for an illustration). By studying the behaviour of F_p on ∂Q we will infer that given any $s \in \sigma_1$, the forward trajectory of s eventually hits ∂Q transversely (see Lemma 2.9). This will allow us to define the region C_{In} , trapped between the said flow lines and ∂Q - as we will prove, given any $v \in \partial C_{In}$, $F_p(v)$ is either tangent to ∂C_{In} at v or points outside of C_{In} (see Lemma 2.10), from which Prop.2.1 will follow.

Therefore, per this sketch of proof, we begin by studying the behaviour of F_p on ∂Q . By its definition above, the set Q is a quadrant trapped by three planes, given by the following parameterizations:

- $\{\dot{x} = 0\} = \{(x, y, -y) | x, y \in \mathbf{R}\}$.
- $\{\dot{y} = 0\} = \{(x, -\frac{x}{a}, z) | x, z \in \mathbf{N}\}$.
- $\{x = 0\} = \{(0, y, z) | y, z \in \mathbf{R}\}$.

In order to study the behaviour of F_p on ∂Q , we now define the following three curves, all of which lie in ∂Q and consist of transverse intersections (see the illustration in Fig.6):

- $L_1 = \{x = 0\} \cap \{\dot{x} = 0\} \cap \{\dot{y} \leq 0\}$, which is parameterized by $\{(0, y, -y) | y \leq 0\}$.
- $L_2 = \{x = 0\} \cap \{\dot{y} = 0\} \cap \{\dot{x} \geq 0\}$, which is parameterized by $\{(0, 0, z) | z \leq 0\}$.
- $L_3 = \{\dot{y} = 0\} \cap \{\dot{x} = 0\} \cap \{x \leq 0\}$, parameterized by $\{(x, -\frac{x}{a}, \frac{x}{a}) | x \leq 0\}$. In particular, recalling the curve l_p from Stage I and its parameterization (the tangency curve to $\{\dot{y} = 0\}$ - see Lemma 2.5), we conclude $L_3 = \{l_p(x) | x \leq 0\}$.

By definition, the curves L_1, L_2, L_3 all connect the fixed point $P_{In} = (0, 0, 0)$ to ∞ - moreover, since $P_{Out} = (c - ab, \frac{ab-c}{a}, \frac{c-ab}{a})$, by $c - ab > 0$ (see the discussion in page 3), we conclude $P_{Out} \notin L_1 \cup L_2 \cup L_3$ (see Fig.6 for an illustration). Additionally, $\partial Q \setminus (L_1 \cup L_2 \cup L_3)$ is composed of three disjoint planar sets, P_1, P_2, P_3 , defined as follows (see the illustration in Fig.6):

- P_1 is the interior of the convex hull of L_1 and L_2 - by definition, P_1 is a subset of $\{x = 0\} \cap \{\dot{x} \geq 0\}$. By Cor.2.6, F_p points inside $\{x > 0\}$ on P_1 .
- P_2 is the interior of convex hull of L_2 and L_3 - as such, it is a subset of $L_p = \{\dot{y} = 0\} \cap \{\dot{x} > 0\}$ (see the discussion before Lemma 2.1). By the discussion preceding Cor.2.1.1, on P_2 the vector field F_p points into $\{\dot{y} > 0\}$.
- P_3 is the convex hull of L_1 and L_3 - as such, it is a subset of $\{\dot{x} = 0\}$.

As a consequence from the definitions of P_1, P_2, P_3 above, we now prove:

Lemma 2.7. *Assume $v \in \partial Q \setminus (P_3 \cup L_1)$ is **not** a fixed-point for F_p . Then, $F_p(v)$ points outside of Q (see the illustration in Fig.6).*

Proof. First, recall we defined Q as the quadrant $Q = \{\dot{x} \geq 0\} \cap \{\dot{y} \leq 0\} \cap \{x \leq 0\}$. By the discussion above, if $v \in \partial Q \setminus (P_3 \cup L_1)$, there are precisely three possibilities:

- $v \in P_1$.
- $v \in P_2$.
- $v \in L_2 \cup L_3$.

By the discussion and definition of P_1, P_2 and P_3 above, if $v \in P_1$, $F_p(v)$ points inside $\{x > 0\}$ - and if $v \in P_2$, $F_p(v)$ points inside $\{\dot{y} > 0\}$. By the definition of Q as the intersection $\{\dot{x} \geq 0\} \cap \{\dot{y} \leq 0\} \cap \{x \leq 0\}$ we conclude that if $v \in P_1 \cup P_2$, $F_p(v)$ points outside of Q . Therefore, to conclude the proof of the Lemma 2.7, it would suffice to prove that on $v \in L_2 \cup L_3$, $F_p(v)$ points outside of Q .

We first prove it for L_2 . To this end, recall we parameterize L_2 by $L_2(x) = (x, -\frac{x}{a}, \frac{x}{a})$, $x \leq 0$, and that $P_{In} = (0, 0, 0) = L_2(x)$ - in particular, since the fixed point $P_{Out} \notin Q$, we have $P_{Out} \notin Q$. Therefore, by this discussion, it would suffice to prove that for any $x < 0$, $F_p(L_2(x))$ points outside Q . To do so, recall that by the definition of L_2 , we have $L_2 \subseteq \{\dot{x} = 0\}$. Further recall the normal vector to $\{\dot{x} = 0\}$ is $(0, 1, 1)$ - which, by direct computation, implies $F_p(x, -\frac{x}{a}, \frac{x}{a}) \bullet (0, 1, 1) = \frac{x^2 - cx + abx}{a}$. The polynomial $\frac{x^2 - cx + abx}{a}$ vanishes precisely for $x = 0, c - ab$ - therefore recalling we assume w.r.t. $p = (a, b, c)$ that $a, b \in (0, 1)$ and $c > 1$ (see the discussion in page 3), we conclude $c - ab > 0$. Therefore, $\frac{x^2 - cx + abx}{a}$ is positive for $x < 0$, and it follows that whenever $x < 0$, $F_p(x, -\frac{x}{a}, \frac{x}{a}) \bullet (0, 1, 1) > 0$. Additionally, recalling the set A_3 (see the proof of Lemma 2.3 for a definition), this entire discussion proves that for every $x < 0$, $(x, -\frac{x}{a}, \frac{x}{a}) \in A_3$. Since on A_3 the vector field F_p points into $\{\dot{x} < 0\}$,

by $Q \subseteq \{\dot{x} \leq 0\}$ we finally conclude that given $x < 0$, $F_p(L_2(x))$ points outside of Q .

Recalling $L_3 \subseteq \{\dot{y} = 0\}$ and that the normal vector to $\{\dot{y} = 0\}$ is $(1, a, 0)$, a similar argument establishes $L_3 \subseteq H_p^-$ - hence, by the results of Stage I, for $v \in L_3 \setminus \{P_{In}\}$, $F_p(v)$ points inside $\{\dot{y} > 0\}$, that is, outside of Q . The proof of Lemma 2.7 is now complete. \square

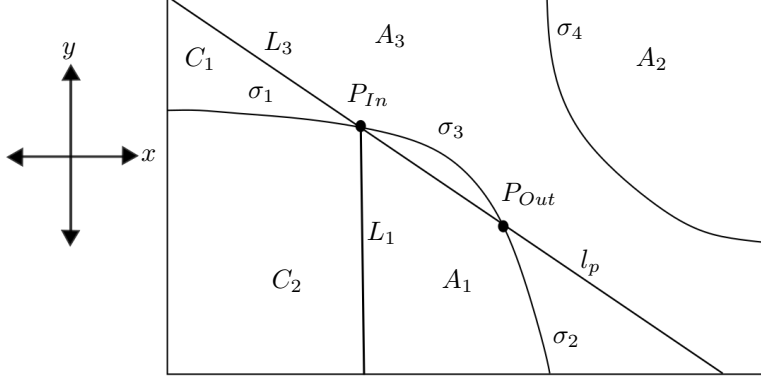


FIGURE 7. The lines L_1, L_3 and the regions C_1, C_2 on $\{\dot{x} = 0\}$.

Having proven Lemma 2.7, we now study the dynamics of F_p on P_3 - as we will discover, it is the only subset of ∂Q through which trajectories can enter Q . To this end, let us recall the curve σ , parameterized by $\sigma(x) = (x, -\frac{x(b+1)}{a+c-x}, \frac{x(b+1)}{a+c-x})$, $x \neq c+a$, is the tangency curve of F_p to $\{\dot{x} = 0\}$ - moreover, recall we denote by $\sigma_1 = \{\sigma(x) | x \leq 0\}$ the a component of $\sigma \setminus \{P_{In}, P_{Out}\}$ which connects P_{In}, ∞ in S^3 (see the discussion in Lemma 2.3 and Lemma 2.4, and the illustration in Fig.3). By Lemma 2.4 we conclude $\sigma_1 = Q \cap \sigma$ (see the illustration in Fig.6). Since σ_1 , by definition, is a curve on $\{\dot{x} = 0\}$ and since $Q \subseteq \{\dot{x} \geq 0\}$, we conclude $\sigma_1 \subseteq \partial Q \cap \{\dot{x} = 0\}$ - which implies $\sigma_1 \subseteq \overline{P_3}$ (see the illustration in Fig.7). We now prove:

Lemma 2.8. $P_3 \setminus \sigma_1$ consists of two components, C_1, C_2 s.t.:

- C_1 is the region trapped between L_3 and σ_1 . Moreover, F_p points on C_1 inside $\{\dot{x} < 0\}$, that is, outside of Q .
- C_2 is the region trapped between L_1 and σ_1 . Moreover, F_p points on C_2 inside $\{\dot{x} > 0\}$, that is, inside Q .

As a consequence, given $s \in \mathbf{R}^3$, its trajectory can enter Q **only** by hitting C_2 transversely.

Proof. First, recall $\overline{P_3} = P_3 \cup L_1 \cup L_3$ - therefore, by the parameterizations of L_1, L_3 and σ above, recalling $\sigma_1 = \{\sigma(x) | x < 0\}$ we conclude $L_1 \cap \sigma_1 = \emptyset$ and $L_3 \cap \sigma_1 = \emptyset$ - since P_3 , by its definition, is the region in $\{\dot{x} = 0\}$ trapped between L_1, L_2 this immediately proves $P_3 \setminus \sigma_1$ consists of two components, C_1, C_2 , defined as follows: C_1 is trapped between σ_1, L_3 , and C_2 is trapped between σ_1, L_1 . See the illustration in Fig.6 and 7.

Now, recall that by its definition σ is the tangency curve of F_p to the cross-section $\{\dot{x} = 0\}$ (w.r.t. the normal vector $(0, 1, 1)$). Therefore, since $\sigma_1 = Q \cap \sigma$ by the discussion above, we conclude that given $v \in P_3$, $F_p(v) \bullet (0, 1, 1) = 0$ precisely when $v \in \sigma_1$ - in other words, we have proven that the sign of $F_p(v) \bullet (0, 1, 1)$ is constant on both C_1, C_2 . Now, choose some $v \in L_3$ - as shown during the proof of Lemma 2.7, for $v \in L_3$, $F_p(v) \bullet (0, 1, 1) > 0$, which proves that for $v \in C_1$, $F_p(v) \bullet (0, 1, 1) > 0$. As a consequence, we conclude F_p points inside $\{\dot{x} < 0\}$ on C_1 - that is, on C_1 the vector field F_p points outside of Q (see the illustration in Fig.6). A similar argument (applied to L_1, C_2) proves that for $v \in C_2$, $F_p(v) \bullet (0, 1, 1) < 0$ - hence F_p points on C_2 inside Q .

Therefore, given any $s \in \mathbf{R}^3$ whose trajectory eventually enters Q , by Lemma 2.7 and the paragraph above it **cannot** enter Q by hitting transversely $\partial Q \setminus (C_2 \cup \sigma_1)$ - i.e., it can only enter Q by hitting $C_2 \cup L_1$. However, by the discussion preceding Cor.2.6, $L_1 = \{\dot{x} = 0\} \cup \{x = 0\}$ is the tangency curve of F_p to the plane $\{x = 0\}$, parameterized by $\{(0, y, -y) | y \leq 0\}$. Recalling the normal vector to $\{\dot{x}\}$ is $(0, 1, 1)$, we conclude $F_p(v) \bullet (0, 1, 1) < 0$ on $v \in L_1$ - and recalling the discussion in the proof of Lemma 2.3, we conclude $F_p(v)$ points inside $\{\dot{x} \geq 0\}$ at v . Therefore, since on L_1 the vector field F_p is tangent to $\{x = 0\}$, we conclude that given $v \in L_1$, its trajectory arrives at v from $\{x > 0\}$, hits v , and then bounce back to $\{x > 0\}$ - see the illustration in Fig.6. Therefore, we conclude the trajectories of initial conditions $s \in Q$ cannot escape Q by hitting L_1 , and Lemma 2.8 follows. \square

Having completed the proof of Lemma 2.8 we can almost begin constructing C_{In} , thus concluding the proof of Prop.2.1. As stated earlier, we will construct C_{In} out of flow lines in which connect regions in ∂Q - therefore,

to do so we need more information about how trajectories for the flow can escape Q . To this end, consider the curve σ_1 , and choose some initial conditions $s \in \sigma_1$. Recall $\sigma_1 \subseteq Q$ and that we denote the trajectory of $s \in \sigma_1$ by $\gamma_s(t), t \in \mathbf{R}, \gamma_s(0) = s$. Further recall we denote by $W_{I_n}^s$ the stable, one-dimensional manifold of P_{I_n} - we now prove:

Lemma 2.9. *For every $s \in \sigma_1 \setminus W_{I_n}^s$, there exists some **minimal** $t > 0$ s.t. $\gamma_s(t) \notin Q$ - that is, every initial condition in $\sigma_1 \setminus W_{I_n}^s$ eventually escapes Q in some positive time.*

Proof. Recall $Q = \{\dot{x} \geq 0\} \cap \{\dot{y} \leq 0\} \cap \{x \leq 0\}$, and that we parameterize σ_1 by $\{(x, -\frac{x(b+1)}{a+c-x}, \frac{x(b+1)}{a+c-x}) | x < 0\}$. Therefore, given any $s \in \sigma_1$, its x -coordinate is strictly lesser than 0 - therefore, by Lemma 2.4, given every $s \in \sigma_1$, there exists some ϵ s.t. for every $r \in [0, \epsilon)$, $\gamma_s(r) \in Q$ - in particular, by Lemma 2.4, for every $r \in (0, \epsilon)$, $\gamma_s(r) \in \{\dot{x} \geq 0\}$. Therefore, since by its definition that are no fixed-points in σ_1 (see the discussion before Lemma 2.4), given $s \in \sigma_1 \setminus W_{I_n}^s$ there are precisely two possibilities to consider:

- There exists some $t_0 > 0$ s.t. $\gamma_s(t_0) \in \{\dot{x} < 0\}$.
- For every $t > 0$, $\gamma_s(t) \in \{\dot{x} \geq 0\}$.

In the first possibility, there is little to prove - since $Q \subseteq \{\dot{x} \geq 0\}$, by $\gamma_s(t_0) \in \{\dot{x} < 0\}$ we immediately conclude $\gamma_s(t_0) \notin Q$. Therefore, to conclude the proof we must show that even if for every $t > 0$, $\gamma_s(t) \in \{\dot{x} \geq 0\}$, the trajectory of s eventually escapes Q . To do so, recall that given $s \in \sigma_1$, its x -coordinate is strictly lesser than 0, i.e., $s \in \{x < 0\}$. Therefore, if for every $t > 0$ we have $\gamma_s(t) \in \{\dot{x} \geq 0\}$, provided $s \notin W_{I_n}^s$ (i.e. not attracted to $P_{I_n} = (0, 0, 0)$), the x -coordinate along γ_s must grow monotonically - which implies the existence of some t_0 s.t. $\gamma_s(t_0) \in \{x > 0\}$. Since by its definition $Q \subseteq \{x \leq 0\}$, this proves $\gamma_s(t_0) \notin Q$ and Lemma 2.9 follows. \square

Now, recall Lemmas 2.7 and 2.8. Together they imply that given $s \in \sigma_1$, its forward trajectory can escape Q **only** by hitting $\partial Q \setminus (C_2 \cup \sigma_1)$ transversely (see the illustration in Fig.6). Therefore, recalling that given an initial condition $s \in \mathbf{R}^3$ we denote its trajectory by $\gamma_s, \gamma_s(0) = s$, Lemma 2.9 motivates us to make the following definition (see Fig.6 for an illustration):

Definition 2.1. *Let $s \in \sigma_1$ be an initial condition, $s \neq P_{I_n}$. Then, denote by $0 < t_1(s) \leq \infty$ the first **positive** time s.t. $\gamma_s(t_1(s)) \in P_1 \cup P_2 \cup C_1 \cup L_1 \cup L_2 \cup L_3$. We say $t_1(s) = \infty$ **if and only if** the following two conditions apply to s :*

- $s \in W_{I_n}^s \cap \sigma_1$.
- For every $t > 0, \gamma_s(t) \in Q$ - that is, the trajectory of s tends to P_{I_n} **from within** Q .

If $t_1(s) = \infty$, we write $\gamma_s(t_1(s)) = P_{I_n}$.

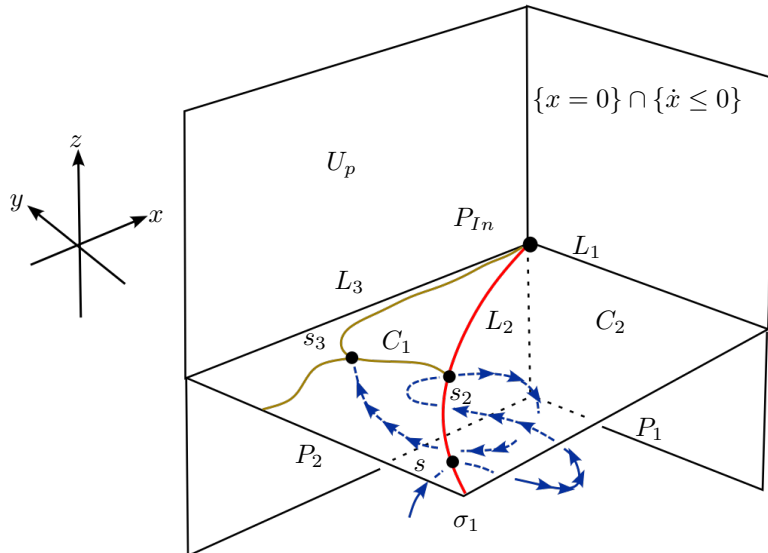


FIGURE 8. The curve γ is the brown line. The trajectory of s_1 hits σ_1 at s_2 before flowing to $\gamma_{s_1}(t_1(s)) = s_3$, which forces a branching in γ .

By Lemma 2.9, $t_1(s)$ is defined and finite for every $s \in \sigma_1 \setminus W_{I_n}^s$. And provided $s \in W_{I_n}^s \cap \sigma_1$ does not tend to P_{I_n} through Q , $t_1(s)$ is also defined and finite - otherwise, $t_1(s) = \infty$. Using the definition of t_1 , we can now finally construct the body C_{I_n} , thus concluding the proof of Prop.2.1. To begin, denote by $T = P_1 \cup P_2 \cup C_1 \cup L_1 \cup L_2 \cup L_3$, and consider the set $\gamma = \cup_{s \in \sigma_1} \gamma_s(t_1(s))$ - by the discussion above, we immediately conclude $\gamma \subseteq T$. Now, let Γ

denote the set of flow-lines connecting σ_1, γ (see the illustration in fig.8) - by definition, $\Gamma \subseteq Q$. Since by Lemma 2.8 $\gamma_s(t_1(s)) \notin C_2$ for every $s \in \sigma_1$, we conclude $\Gamma \cap C_2 = \emptyset$. Now, consider $Q \setminus \Gamma$ - by this discussion $Q \setminus \Gamma$ includes precisely two components - we therefore define C_{In} as the component of $Q \setminus \Gamma$ s.t. $C_{In} \cap C_2 = \emptyset$. Since $P_{In} \in \sigma_1$ and since $P_{Out} \notin Q$, by the definition of C_{In} we immediately conclude:

Corollary 2.1.2. $P_{In} \in \partial C_{In}$, and $P_{Out} \notin \overline{C_{In}}$. Moreover, $C_{In} \subseteq \{\dot{y} \geq 0\} \cap \{\dot{x} \geq 0\}$.

Proof. First, by definition, $P_{In} \in \sigma_1$ - which, by the definition of C_{In} immediately proves $P_{In} \in \partial C_{In}$. Moreover, recall $P_{Out} = (c - ab, \frac{ab-c}{a}, \frac{c-ab}{a})$, and that per our assumptions on the constants a, b, c , we have $a, b \in (0, 1)$, $c > 1$ (see the discussion at page 3). This proves $c - ab > 0$ - and since $Q = \{\dot{x} \geq 0\} \cap \{\dot{y} \leq 0\} \cap \{x \leq 0\}$, we conclude both $P_{Out} \notin \overline{Q}$, $Q \subseteq \{\dot{x} \geq 0\} \cap \{\dot{y} = 0\}$. Therefore, since by definition $C_{In} \subseteq Q$, this discussion proves both $P_{Out} \notin \overline{C_{In}}$ and $C_{In} \subseteq \{\dot{x} \geq 0\} \cap \{\dot{y} \leq 0\}$, and Cor.2.1.2 follows. \square

Therefore, having proven Cor.2.1.2, in order to conclude the proof of Prop.2.1 it remains to prove that given every $s \in \mathbf{R}^3$, its forward trajectory under F_p can never enter C_{In} . We do so in the following Lemma:

Lemma 2.10. *At every $v \in \partial C_{In}$, either $F_p(v)$ is tangent to ∂C_{In} , or F_p points outside of C_{In} - that is, given any $s \in \mathbf{R}^3 \setminus C_{In}$, its forward trajectory never enters C_{In} under the flow.*

Proof. By definition, ∂C_{In} is composed of flow-lines in Γ and regions on T . Recalling $T = P_1 \cup P_2 \cup C_1 \cup L_1 \cup L_2 \cup L_3$, by Lemmas 2.8 and 2.9 we know F_p points outside of Q throughout $T \cap \partial C_{In}$ - since $C_{In} \subseteq Q$, we conclude F_p also points outside C_{In} throughout $T \cap \partial C_{In}$. As such, since by definition F_p is tangent to Γ , Lemma 2.10 now follows. \square

Having proven Cor.2.1.2 and Lemma 2.10, we can summarize our findings as follows. We have proven the existence of a three-dimensional body C_{In} s.t.:

- $P_{In} \in \partial C_{In}$, and $P_{Out} \notin \overline{C_{In}}$.
- $C_{In} \subseteq \{\dot{x} \geq 0\} \cap \{\dot{y} \leq 0\}$.
- F_p is either tangent or points outside of C_{In} on ∂C_{In} .

In other words, we have completed the proof of Prop.2.1. \square

Having proven Prop.2.1, we can now conclude Stage II - namely, we are now ready to prove the existence of an invariant, unbounded, one dimensional manifold $\Gamma_{In} \subseteq C_{In}$. To this end, given $t \in \mathbf{R}$, we denote the flow generated by F_p at time t by ϕ_t^p . Furthermore, we denote by ψ_t^p the flow generated by the vector field $J_p(P_{In})$ - i.e., the linearization of F_p at P_{In} . By the Hartman-Grobman Theorem there exists some $r > 0$ s.t the flow ϕ_t^p in $B_r(P_{In})$ is orbitally equivalent to ψ_t^p in $B_d(P_{In})$, $d > 0$. Namely, there exists a homeomorphism $H : B_r(P_{In}) \rightarrow B_d(P_{In})$ s.t. $H(\phi_t^p(x)) = \psi_t^p(H(x))$.

Now, since F_p is either tangent or points outside C_{In} on ∂C_{In} , we conclude that given $v \in \partial C_{In}$, $-F_p(v)$ is either tangent or points inside C_{In} - in other words, no trajectories escape C_{In} under the inverse flow. As such, it immediately follows that no trajectory escapes $C_{In} \cap B_r(P_{In})$ under the inverse flow by hitting $C_{In} \cap \partial B_r(P_{In})$. Setting $K = H(C_{In} \cap B_r(P_{In}))$, we conclude the same is true for the dynamics of $-J_p(P_{In})$ on ∂K - that is, no trajectories for the linearization of $-F_p$ at P_{In} can escape K through ∂K . Therefore, there exists some eigenvector for $J_p(P_{In})$ in K - which, in turn, proves the existence of Γ_{In} , an invariant manifold for P_{In} , s.t. $\Gamma_{In} \cap C_{In} \cap B_r(P_{In}) \neq \emptyset$. Therefore, since no trajectories can escape C_{In} under the inverse flow, given any $x \in \Gamma_{In} \cap C_{In} \cap B_r(P_{In})$, for every $t < 0$ we have $\phi_t^p(x) \in C_{In}$ - which proves $\Gamma_{In} \subseteq C_{In}$.

Now, recall P_{In} is a saddle-focus with a 2-dimensional unstable manifold, W_{In}^u , transverse to P_{In} at $\{\dot{x} = 0\}$ (see Lemma 2.3 and the illustration in Fig.4). As such, the backwards trajectory of initial conditions in W_{In}^u must intersect **both** $\{\dot{x} > 0\}$ and $\{\dot{x} < 0\}$ infinitely many times. Now, by the construction of C_{In} in Prop.2.1, $C_{In} \cap \{\dot{x} < 0\} = \emptyset$ - therefore, since no trajectories can escape C_{In} under the inverse flow, this implies Γ_{In} cannot intersect $\{\dot{x} < 0\}$ - hence Γ_{In} is **not** a flow line in W_{In}^u . This proves Γ_{In} is a component of W_{In}^s , the unstable, one-dimensional manifold of P_{In} - and since $\Gamma_{In} \cap W_{In}^u = \emptyset$, it cannot be a homoclinic trajectory to P_{In} . Additionally, since $P_{Out} \notin \overline{C_{In}}$ (see Prop.2.1), because $\Gamma_{In} \subseteq C_{In}$ we also conclude $P_{Out} \notin \overline{\Gamma_{In}}$.

As such, all that remains is to conclude Stage II is to prove Γ_{In} is unbounded. However, since $C_{In} \subseteq \{\dot{x}\} \cap \{\dot{y} = 0\}$ we conclude **both** $-\dot{x}$, $-\dot{y}$ never change their sign on Γ_{In} . Therefore, since by previous paragraph Γ_{In} is **not** a homoclinic trajectory to P_{In} or a heteroclinic trajectory to P_{Out} , we conclude that given any $x \in \Gamma_{In}$, $\lim_{t \rightarrow -\infty} \phi_t^p(x) = \infty$. Therefore, we have proven:

Corollary 2.1.3. *There exists a component $\Gamma_{In} \subseteq W_{In}^s$, s.t. Γ_{In} is a heteroclinic trajectory for F_p in S^3 , connecting the fixed-points P_{In} and ∞ .*

That is, there exists an unbounded heteroclinic trajectory connecting the fixed points P_{In} and ∞ - and Stage II of the proof of Th.2.1 is now complete.

2.1.3. Stage III - the existence of Γ_{Out} . Having proven the existence of Γ_{In} , we will prove the analogous result for P_{Out} - namely, we will now prove the existence of a heteroclinic connection Γ_{Out} , a subset of the one-dimensional W_{Out}^u , which connects P_{Out}, ∞ . Similarly to Stage II, we will do so by constructing C_{Out} , a trapping set for Γ_{Out} . Despite slight differences in the proof which will arise due to F_p , in practice the proof will be almost symmetric to the one in Stage II. This section is organized as follows - similarly to Stage II, we begin by studying the local dynamics of F_p on some plane, which passes through the saddle-focus P_{Out} . After that, we prove Prop.2.2, in which we construct the three-dimensional body C_{Out} by hand - as we will prove, again we have $C_{Out} \subseteq \{\dot{x} \geq 0\} \cap \{\dot{y} \geq 0\}$. Following that, similar arguments to those used in Stage II will imply C_{Out} contains Γ_{Out} , a component of W_{Out}^u which connects P_{Out}, ∞ (see Cor.2.1.4).

To begin, recall $P_{Out} = (c - ab, \frac{ab-c}{a}, \frac{c-ab}{a})$, and consider the plane $\{x = c - ab\} = \{(c - ab, y, z) | y, z \in \mathbf{R}\}$ - further recall that by the discussion in page 3, $c - ab > 0$. A similar argument to that used to prove Lemma 2.6 now implies:

Lemma 2.11. *For every $v \in \{x = c - ab\}$, $F_p(v) \bullet (1, 0, 0) \geq 0$ if and only if $v \in \{\dot{x} \geq 0\} \cap \{x = c - ab\}$. In particular, on $\{x = c - ab\} \cap \{\dot{x} > 0\}$ the vector field F_p points inside $\{x > c - ab\}$ - and on $\{x = c - ab\} \cap \{\dot{x} < 0\}$, F_p points inside $\{x < c - ab\}$ (see the illustration in Fig.10).*

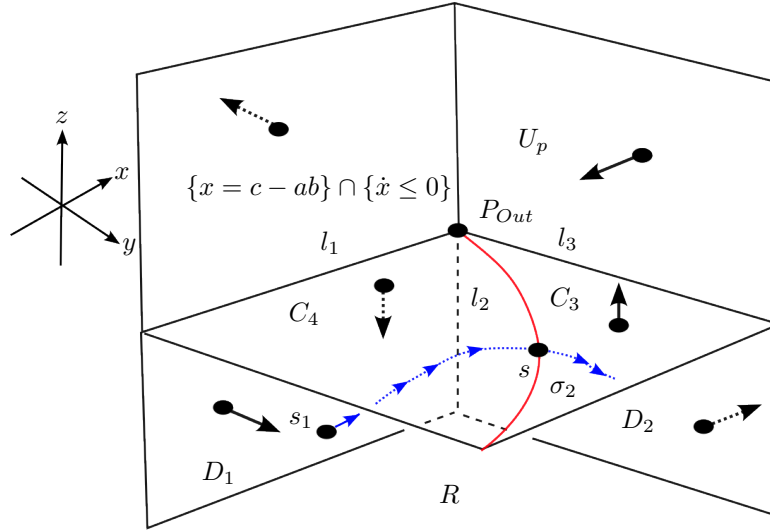


FIGURE 9. The region R , trapped between D_1, D_2 and $D_3 = C_3 \cup C_4$, along with the directions of F_p on ∂R . The blue curve denotes the forward-trajectory of $s_1 = \gamma_s(t_2(s))$ to $s \in \sigma_2$.

Now, similarly to the definition of Q in Stage II, consider the quadrant $R = \{\dot{x} \geq 0\} \cap \{\dot{y} \leq 0\} \cap \{x \geq c - ab\}$, trapped between the three planes $\{\dot{x} = 0\}$, $\{\dot{y} = 0\}$ and $\{x = c - ab\}$ (see the illustration in Fig.9). Analogously to Prop.2.1, we now prove:

Proposition 2.2. *There exists a three-dimensional, connected set C_{Out} , s.t.:*

- $P_{Out} \in \partial C_{Out}$, $P_{In} \notin \partial C_{Out}$.
- $C_{Out} \subseteq \{\dot{y} \leq 0\} \cap \{\dot{x} \geq 0\}$.
- For every $v \in \partial C_{Out}$, $F_p(v)$ is either tangent or points inside C_{Out} - that is, given any initial condition $s \in C_{Out}$, its forward trajectory never escapes C_{Out} .

Proof. Similarly to the proof of Prop.2.1, we will prove Prop.2.2 as a sequence of interconnected Lemmas and their Corollaries. The idea behind the proof is also similar - recall the curve σ_2 introduced at Stage I (see the discussion after Lemma 2.3, and Fig.3 for an illustration). By studying the behaviour of F_p on ∂R we will infer that given any $s \in \sigma_2$, the **backwards** trajectory of s eventually hits ∂R transversely (see Lemma 2.13). This will allow us to define the region C_{Out} , trapped between the said flow lines and ∂R - then, similarly to the proof in Stage II, it would follow that given any $v \in \partial C_{Out}$, $F_p(v)$ is either tangent to ∂C_{Out} at v or points inside of C_{Out} , thus completing the proof.

Therefore, similarly to the proof of Prop.2.1, we begin by studying the behaviour of F_p on ∂R . By its definition above, let us recall R is a quadrant trapped by three planes, given by the following parameterizations:

- $\{\dot{x} = 0\} = \{(x, y, -y) | x, y \in \mathbf{R}\}$.
- $\{\dot{y} = 0\} = \{(x, -\frac{x}{a}, z) | x, z \in \mathbf{N}\}$.
- $\{x = c - ab\} = \{(c - ab, y, z) | y, z \in \mathbf{R}\}$.

In order to study the behaviour of F_p on ∂R , we again define three curves, all of which lie in ∂R (see the illustration in Fig.10):

- $l_1 = \{x = c - ab\} \cap \{\dot{x} = 0\} \cap \{\dot{y} \leq 0\}$, which is parameterized by $\{(c - ab, y, -y) | y \leq 0\}$.
- $l_2 = \{x = c - ab\} \cap \{\dot{y} = 0\} \cap \{\dot{x} \geq 0\}$, which is parameterized by $\{(c - ab, 0, z) | z \leq 0\}$.
- $l_3 = \{\dot{y} = 0\} \cap \{\dot{x} = 0\} \cap \{x \geq c - ab\}$, parameterized by $\{(x, -\frac{x}{a}, \frac{x}{a}) | x \leq 0\}$. In particular, recalling the curve l_p from Stage I and its parameterization (the tangency curve to $\{\dot{y} = 0\}$ - see Lemma 2.5), we conclude $l_3 = \{l_p(x) | x \geq c - ab\}$.

By definition, the curves l_1, l_2, l_3 all connect the fixed point $P_{Out} = (c - ab, \frac{ab-c}{a}, \frac{c-ab}{a})$ to ∞ . Moreover, $\partial R \setminus (l_1 \cup l_2 \cup l_3)$ is composed of three disjoint planar sets, D_1, D_2, D_3 , defined as follows (see the illustration in Fig.6):

- D_1 is the interior of the convex hull of l_1 and l_2 - by definition, P_1 is a subset of $\{x = c - ab\} \cap \{\dot{x} \geq 0\}$. By Cor.2.6, F_p points inside $\{x > c - ab\}$ on D_1 - that is, that is, by the definition of R , on D_2 F_p points **inside** R .
- D_2 is the interior of convex hull of l_2 and l_3 - as such, it is a subset of $H_p^- = \{\dot{y} = 0\} \cap \{\dot{x} > 0\}$ (see the discussion before Lemma 2.1). By the discussion preceding Cor.2.1.1, on D_2 the vector field F_p points into $\{\dot{y} > 0\}$ - that is, by the definition of R , on D_2 F_p points **outside** R .
- D_3 is the convex hull of l_1 and l_3 - as such, it is a subset of $\{\dot{x} = 0\}$.

To continue, similarly to what we did in Stage II, we now study the dynamics of F_p on D_3 . To this end, let us recall the curve σ , parameterized by $\sigma(x) = (x, -\frac{x(b+1)}{a+c-x}, \frac{x(b+1)}{a+c-x})$, $x \neq c + a$, is the tangency curve of F_p to $\{\dot{x} = 0\}$ - moreover, recall we denote by $\sigma_2 = \{\sigma(x) | c - ab < x < a + c\}$ the a component of $\sigma \setminus \{P_{In}, P_{Out}\}$ which connects P_{Out}, ∞ in S^3 (see the discussion in Lemma 2.3 and Lemma 2.4, and the illustration in Fig.3). By Lemma 2.4 we conclude $\sigma_2 = R \cap \sigma$ (see the illustration in Fig.10). Since σ_2 is a curve on $\{\dot{x} = 0\}$, and because $R \subseteq \{\dot{x} \geq 0\}$, we again conclude $\sigma_2 \subseteq \partial R \cap \{\dot{x} = 0\}$ - that is, $\sigma_2 \subseteq \overline{D_3}$ (see the illustration in Fig.7). Therefore, similar arguments to those used to prove Lemma 2.8 now imply:

Lemma 2.12. $D_3 \setminus \sigma_2$ consists of two components, C_3, C_4 s.t.:

- C_3 is the region trapped between l_3 and σ_2 . Moreover, F_p points on C_3 inside $\{\dot{x} < 0\}$, that is, outside of R .
- C_4 is the region trapped between l_1 and σ_2 . Moreover, F_p points on C_4 inside $\{\dot{x} > 0\}$, that is, inside R .

As a consequence, given $s \in \mathbf{R}^3$, its forwards-trajectory can enter R **only** by hitting $C_4 \cup D_1 \cup l_1$ transversely.

We can almost begin constructing C_{Out} . Much like we did in Stage II, we will construct C_{Out} out of flow lines which emanate from σ_2 - however, this time we will do so using the inverse flow. To this end, recall the curve σ_2 , and choose some initial conditions $s \in \sigma_2$. Recall $\sigma_2 \subseteq R$ and that we denote the trajectory of $s \in \sigma_2$ by $\gamma_s(t), t \in \mathbf{R}$, $\gamma_s(0) = s$. Further recall we denote by W_{Out}^u the unstable, one-dimensional manifold of P_{Out} - we now prove an analogue of Lemma 2.9:

Lemma 2.13. For every $s \in \sigma_2 \setminus W_{Out}^u$, there exists some **maximal** $t < 0$ s.t. $\gamma_s(t) \notin R$ - that is, every initial condition in $\sigma_2 \setminus W_{In}^s$ eventually escapes R under the inverse flow.

Proof. Recall $R = \{\dot{x} \geq 0\} \cap \{\dot{y} \leq 0\} \cap \{x \geq c - ab\}$, and that we parameterize σ_2 by $\{(x, -\frac{x(b+1)}{a+c-x}, \frac{x(b+1)}{a+c-x}) | a + c < x < c - ab\}$. Therefore, given any $s \in \sigma_2$, its x -coordinate is strictly greater then $c - ab$ - therefore, by Lemma 2.4, given every $s \in \sigma_1$, there exists some ϵ s.t. for every $r \in (-\epsilon, 0]$, $\gamma_s(r) \in R$ - in particular, by Lemma 2.4, for every $r \in (-\epsilon, 0)$, $\gamma_s(r) \in \{\dot{x} \geq 0\}$. Therefore, similarly to the proof of Lemma 2.9, given $s \in \sigma_2 \setminus W_{Out}^u$ there are, again, precisely two possibilities to consider:

- There exists some $-\infty < t_0 < 0$ s.t. $\gamma_s(t_0) \in \{\dot{x} < 0\}$.
- For every $t < 0$, $\gamma_s(t) \in \{\dot{x} \leq 0\}$.

In the first possibility, there is little to prove - since $R \subseteq \{\dot{x} \geq 0\}$, by $\gamma_s(t_0) \in \{\dot{x} < 0\}$ we immediately conclude $\gamma_s(t_0) \notin R$. Therefore, to conclude the proof we must show that even if for every $t < 0$, $\gamma_s(t) \in \{\dot{x} \geq 0\}$, the trajectory of s eventually escapes R . To do so, recall we proved that given $s \in \sigma_2$ its x -coordinate is strictly greater than $c - ab$ - i.e., $s \in \{x > c - ab\}$. Therefore, if for every $t < 0$ we have $\gamma_s(t) \in \{\dot{x} \geq 0\}$, provided $s \notin W_{Out}^u$ (that is, the trajectory of s is **not** attracted to $P_{Out} = (c - ab, \frac{ab-c}{a}, \frac{c-ab}{a})$ under the inverse flow), the x -coordinate along γ_s must decrease - and since by assumption $\lim_{t \rightarrow -\infty} \gamma_s(t) \neq P_{Out}$, there exists some $t_0 < 0$

Proof. Recall that P_{Out} is a saddle-focus with a two-dimensional stable manifold W_{Out}^s and a one-dimensional unstable manifold W_{Out}^u . Moreover, recall that given $t \in \mathbf{R}$ we denote the flow generated by F_p at time t by ϕ_t^p . Additionally, similarly to Stage II, denote by ψ_t^p the flow generated by the vector field $J_p(P_{Out})$ - i.e., the linearization of F_p at P_{Out} . By the Hartman-Grobman Theorem there exists some $r > 0$ s.t. the flow ϕ_t^p in $B_r(P_{Out})$ is orbitally equivalent to ψ_t^p in $B_d(P_{Out})$, $d > 0$. Namely, there exists a homeomorphism $H : B_r(P_{Out}) \rightarrow B_d(P_{Out})$ s.t. $H(\phi_t^p(x)) = \psi_t^p(H(x))$.

By our construction of C_{Out} , $\forall s \in C_{Out}$ the trajectory of s under the flow is trapped in C_{Out} - as such, the trajectories of initial conditions in $C_{Out} \cap B_r(P_{Out})$ cannot escape it through $\partial C_{Out} \cap B_r(P_{Out})$. Therefore, similarly to the argument used to prove Cor.2.1.3, we conclude there exists some eigenvector for $J_p(P_{Out})$ in $K = H(C_{Out} \cap B_r(P_{Out}))$ - which, again, implies the existence of some invariant manifold for P_{Out} , Γ_{Out} , in C_{Out} . Now, recall Cor.2.1.1 proves the two-dimensional stable manifold for P_{Out} , W_{Out}^s , is transverse to $\{\dot{y} = 0\}$ at P_{Out} - that is, given $x \in W_{Out}^s$, its forwards-trajectory intersects **both** components of $\{\dot{y} \neq 0\}$ infinitely many times. As a consequence, from $C_{Out} \subseteq \{\dot{y} \leq 0\}$ we conclude Γ_{Out} is not a flow line in W_{Out}^s - which proves Γ_{Out} is a component of W_{Out}^u , and in particular, that Γ_{Out} is not a homoclinic trajectory to P_{Out} . Moreover, since by construction $P_{In} \notin \overline{C_{Out}}$, from $\Gamma_{Out} \subseteq \overline{C_{Out}}$ we conclude that Γ_{Out} cannot be a heteroclinic trajectory which connects P_{In} , P_{Out} .

Now, by $\Gamma_{Out} \cap C_{Out} \subseteq \{\dot{y} \leq 0\} \cap \{\dot{x} \geq 0\}$ we conclude both \dot{y}, \dot{x} do not change their sign along Γ_{Out} . Since by previous paragraph Γ_{Out} is not a homoclinic trajectory or a bounded heteroclinic trajectory, we conclude that given any $x \in \Gamma_{Out}$, $\lim_{n \rightarrow \infty} \phi_t^p(x) = \infty$. In other words, we have just proven Γ_{Out} is an unbounded heteroclinic trajectory in W_{Out}^u which connects P_{Out} and ∞ - hence Cor.2.1.4 follows. \square

2.1.4. Stage IV - constructing R_p and concluding the proof of Th.2.1. Having proven the existence of $\Gamma_{In}, \Gamma_{Out}$, invariant, unbounded one-dimensional manifolds in W_{In}^s, W_{Out}^u , respectively, we can now conclude the proof of Th.2.1. Namely, we will now use the fact $\overline{\Gamma_{Out}}, \overline{\Gamma_{In}}$ connect at ∞ to prove the existence of a smooth vector field on S^3 , s.t. the following conditions are satisfied:

- For every sufficiently large $r > 0$, we can construct R_p s.t. it coincides on $\{(x, y, z) | x^2 + y^2 + z^2 < r\}$ with F_p , the original vector field given by Eq.2.
- R_p has precisely two fixed points in S^3 - P_{In}, P_{Out} .
- R_p generates an unbounded heteroclinic trajectory, connecting P_{In}, P_{Out} .

To begin, recall $l_p = \{\dot{x} = 0\} \cap \{\dot{y} = 0\}$ (see Lemma 2.5). Now, given $r > 0$ consider $S_r = \{|w| = r, w \in \mathbf{R}^3\}$ - F_p can point on S_r at the $(0, 0, -d)$, $d > 0$ direction **only** at $S_r \cap l_p$. Further recall we earlier parameterized l_p by $\{(x, -\frac{x}{a}, \frac{x}{a}), x \in \mathbf{R}\}$, and that $F_p(l_p(x)) = (0, 0, bx + \frac{x^2 - xc}{a})$ (see Lemma 2.5). Therefore, for any sufficiently large $r > 0$, F_p **cannot** point at the $(0, 0, -d)$, $d > 0$ direction on S_r . This proves the index of F_p at the fixed point at ∞ is 0 - that is, the fixed point at ∞ can **only** be some degenerate fixed point for F_p .

Hence, by Hopf's Theorem (see pg. 51 in [17]), for every sufficiently large r , F_p is homotopic on the set $D_r = \{w \in \mathbf{R}^3 | |w| \geq r\}$ to a vector field which generates a tubular flow. Hence, applying Hopf's Theorem, we conclude that for a sufficiently large r we can smoothly deform F_p at D_r by some smooth homotopy which removes the fixed point at ∞ . As the index is 0, we do so s.t. no new fixed points are generated in D_r - in particular, we do so s.t. ∞ becomes a regular initial condition for the flow, with non-zero \dot{y} velocity (in other words, we take ∞ out of H_p - see the discussion preceding Lemma 2.1). More importantly, because $\infty \in \overline{\Gamma_{In}} \cup \overline{\Gamma_{Out}}$, we construct this perturbation s.t. $\Gamma_{In}, \Gamma_{Out}$ connect to a heteroclinic connection passing through ∞ - Γ .

Now, denote the vector field constructed above by R_p - by construction it is a smooth vector S^3 - and by the process described above, given a sufficiently large $r > 0$ we can construct R_p s.t. it coincides with F_p on $\{(x, y, z) | x^2 + y^2 + z^2 > r\}$. As a consequence, the construction above also proves R_p has precisely two fixed points in S^3 - P_{In}, P_{Out} , connected by an unbounded heteroclinic trajectory, Γ . Theorem 2.1 is now proven. \square

Remark 2.1. In [27] it was observed a component of W_{Out}^u always tends to infinity. As such, Th.2.1 (and in particular, Cor.2.1.4) is an analytic proof of this numerical observation.

It is time to introduce our last standing assumption. One recurring observation in the numerical studies of the Rössler System is that at many parameters, trajectories which are repelled from P_{In} are shielded from escaping to ∞ by the two-dimensional W_{Out}^s (see, for example, Section V in [27]). Motivated by these observations (and by Fig.5.C1 in [27]), we now add the following to our four standing assumptions on our parameter space P (see the discussion at page 3):

- **Assumption 5** - from now on, we will **always** assume that for every parameter $p \in P$, the two-dimensional invariant manifolds W_{Out}^s and W_{In}^u (see the discussion in page 3) intersect transversely. We will denote the said intersection by $W_{In}^u \pitchfork W_{Out}^s$.

Now, recall the set of parameters which satisfy Assumptions 1 – 4 are open in the parameter space of the Rössler system (see the discussion in page 3). The condition $W_{In}^u \pitchfork W_{Out}^s$ is also stable in the parameter space - hence, P remains an open set in the region $\{c > ab\}$ once we add the assumption that $\forall p \in P, W_{In}^u \pitchfork W_{Out}^s$. The proof of Th.2.1, as must be stated, is independent of the assumption $W_{In}^u \pitchfork W_{Out}^s$. Plugging it in and recalling we assume $(\nu_{In} < 1) \vee (\nu_{Out} < 1)$ holds throughout the parameter space P (see the discussion in page 3), we derive the following corollary:

Corollary 2.1.5. *$\forall p \in P, R_p$ can be approximated by smooth vector fields of S^3 which satisfy Shilnikov's chaotic homoclinic scenario.*

Proof. Choose some $p \in P$. By Th.2.1, we can always perturb F_p into a smooth vector field on S^3, R_p . Per Th.2.1, R_p generates a heteroclinic connection Γ through ∞ , which flows from P_{Out} towards P_{In} (in infinite time).

Assume first that $\nu_{Out} < 1$. Now, perturb R_p around the fixed point P_{In} by connecting Γ and $W_{In}^u \pitchfork W_{Out}^s$ to ζ , a homoclinic trajectory to P_{Out} (as must be remarked, this perturbation of R_p can be taken to be arbitrarily small in the C^∞ metric on \mathbf{R}^3). As $\nu_{Out} < 1$, from Shilnikov's Theorem (see [3]) the dynamics around the homoclinic trajectory are chaotic. When $\nu_{In} < 1$, similar arguments (when applied to $-R_p$) allow us to infer the same result. \square

Corollary 2.1.5 may appear surprising at first - especially since most numerical studies observed the existence of open regions in the parameter space, intersecting with the chaotic Shilnikov homoclinic curves, **at which no chaotic dynamics were detected** (see, for example, [22],[20],[27]). Even though such numerical evidence appears to contradict Cor.2.1.5 in practice it is not so: for even if $\forall p \in P$ the vector field F_p generates some chaotic dynamics around ∞ , those dynamics are possibly restricted to meagre or null sets - as such, they may be hard to observe. In fact, it should also be stated that Cor.2.1.5 correlates with the results of some numerical studies. As observed in [22], the dynamics at non-chaotic parameters of initial conditions close to ∞ behaved a-periodically for a long duration of time - until they finally settled to some periodic behavior. As such, Cor.2.1.5 is a possible analytic explanation for this phenomenon, termed **Transient Chaos** in [22].

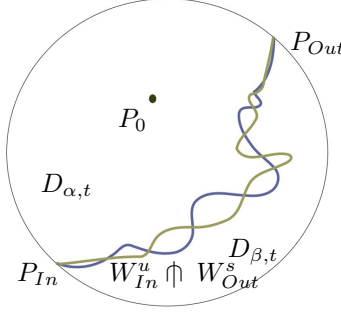
2.2. The global dynamics of F_p . To continue, from now on and throughout the remainder of this section, let us denote by $R_{p,t}, 1 > t > 0$ a vector field given by Th.2.1, which coincides with F_p on $B_{\frac{1}{t}}(P_{In})$. Moreover, recall we denote by W_{In}^s the one-dimensional stable manifold of the saddle-focus P_{In} . In this section we prove the existence of a cross-section $D_\alpha \subseteq \mathbf{R}^3$, on which the first-return map for the vector field F_p is well-defined (see Th.2.2). We begin with the following Corollary of Th.2.1, where we prove we can meaningfully define the first-return map for the vector field $R_{p,t}$:

Corollary 2.1.6. *Given any $p \in P$ and every sufficiently small $t > 0$, $R_{p,t}$ generates a cross-section $U_{p,t}$, satisfying the following:*

- W_{In}^u, W_{Out}^s are transverse to $U_{p,t}$ at P_{In}, P_{Out} . Moreover, $H_{p,t}$ is a topological disc.
- Given any initial condition $s \in \mathbf{R}^3 \setminus W_{In}^s$ which is **not** a fixed point, the trajectory of s eventually hits $U_{p,t}$ transversely.
- The first return map, $f_{p,t} : \overline{U_{p,t}} \rightarrow \overline{U_{p,t}}$, is well-defined at every initial condition $s \in \overline{U_{p,t}} \setminus W_{In}^s$.

Proof. Consider $R_{p,t}$. From Th.2.1, for $t > 0$ sufficiently small $R_{p,t}$ is a smooth vector field defined throughout S^3 , with precisely two fixed points - P_{In}, P_{Out} . By Th.2.1, P_{In}, P_{Out} are connected by a heteroclinic trajectory Γ , which passes through ∞ . Let us denote by T the tangency curve of $R_{p,t}$ in $\{\dot{y} = 0\}$, and let us choose $t > 0$ sufficiently small s.t. $\{\dot{y} = 0\} \setminus T$ (with \dot{y} taken w.r.t. $R_{p,t}$) is homeomorphic to two half planes (by definition, $P_{In}, P_{Out} \in T$). Furthermore, let us denote by $U_{p,t}$ one of the components of $\{\dot{y} = 0\} \setminus T$ which satisfies $U_{p,t} \cap B_{\frac{1}{t}}(0) = U_p \cap B_{\frac{1}{t}}(0)$ - with U_p as in Lemma 2.1. As such, given $s \in \{\dot{y} \neq 0\}$ and denoting by γ_s the trajectory of $s, \gamma_s(0) = s$, if \dot{y} changes sign along γ_s at least twice, then γ_s must intersect $U_{p,t}$ transversely. Moreover, by the definition of $U_{p,t}$ and Cor.??, provided $t > 0$ is sufficiently small, the two-dimensional invariant manifolds W_{Out}^s, W_{In}^u are transverse to $U_{p,t}$ at P_{Out}, P_{In} , respectively.

To conclude the proof, by the definition of the first-return map it would suffice to prove that given $s \in \mathbf{R}^3 \setminus W_{In}^s$ which is **not** a fixed point, its forward trajectory hits $U_{p,t}$ transversely infinitely many times. Denoting by $\gamma_s, \gamma_s(0) = s$ the trajectory of s , we conclude it would suffice to prove the sign of \dot{y} changes infinitely many times along γ_s . To begin, recall $R_{p,t}$ generates a heteroclinic trajectory Γ , connecting P_{In}, P_{Out} in S^3 , s.t. $\infty \in \Gamma$ (see Th.2.1). Therefore, since $\Gamma \subseteq W_{In}^s$ we conclude the forward trajectory of s **cannot** blow up to ∞ (in S^3) - that is, provided γ_s does not limit to a fixed point in forward time, γ_s must intersect transversely with $U_{p,t}$ infinitely many times. Recalling the stable manifolds for the saddle-foci P_{In}, P_{Out} are the one-dimensional W_{In}^s and the two-dimensional W_{Out}^s , we have just proven that if $s \in \mathbf{R}^3 \setminus W_{In}^s \cup W_{Out}^s$, its forward trajectory hits $U_{p,t}$ transversely infinitely many times. However, since P_{Out} is a saddle-focus and since we have already proven

FIGURE 11. the partition of $H_{p,t}$ to $D_{\alpha,t}$ and $D_{\beta,t}$.

W_{Out}^s is transverse to $U_{p,t}$ at P_{Out} (see Fig.4), if $s \in W_{Out}^s$, its trajectory still must hit $U_{p,t}$ infinitely many times. Therefore, $\forall s \in \mathbf{R}^3 \setminus W_{In}^s$ which is not a fixed point, its trajectory hits $U_{p,t}$ transversely infinitely many times.

All in all, we conclude that $\forall s \in \mathbf{R}^3 \setminus W_{In}^s$, the trajectory of s must hit $U_{p,t}$ transversely infinitely many times. As such, by the definition of the first-return map $f_{p,t} : \overline{U_{p,t}} \rightarrow \overline{U_{p,t}}$ we conclude $f_{p,t}$ is well-defined on $\overline{U_{p,t}} \setminus W_{In}^s$ and Cor.?? follows. \square

Having proven the existence of a well-defined first-return map $f_{p,t} : \overline{U_{p,t}} \rightarrow \overline{U_{p,t}}$, we now study its global dynamics. We do so in the following Lemma, where we study the dynamical structure of the cross-section $U_{p,t}$ w.r.t. $f_{p,t}$:

Lemma 2.14. *Let $p \in P$ be some parameter. For a sufficiently small $t > 0$, there exists a partition of the cross-section $\overline{U_{p,t}}$ into two sets, $D_{\alpha,t}, D_{\beta,t}$, s.t. both fixed points satisfy $P_{In}, P_{Out} \in \partial D_{\alpha,t}$, and $f_{p,t}(\overline{D_{\alpha,t}}) \subseteq \overline{D_{\alpha,t}}, f_{p,t}(\overline{D_{\beta,t}}) \subseteq \overline{D_{\beta,t}}$. Moreover, $D_{\alpha,t}$ is bounded, and both $D_{\alpha,t}, D_{\beta,t}$ are non-empty.*

Proof. To begin, recall we always assume $W_{In}^u \cap W_{Out}^s$ (w.r.t. F_p). Therefore, by Th.2.1 and Cor.??, when $t > 0$ is sufficiently small, $W_{In}^u \cap W_{Out}^s$ persists when we deform F_p to $R_{p,t}$. Now, let Γ denote the unbounded heteroclinic connection for $R_{p,t}$, connecting P_{In}, P_{Out} (see Th.2.1) - by its existence, there exists some neighborhood V of Γ s.t. $R_{p,t}$ points on ∂V into $S^3 \setminus V$. This immediately proves that given any initial condition $x \in W_{In}^u$, its trajectory cannot enter V - hence it follows that $W_{In}^u \cap V = \emptyset$. Moreover, a similar argument applied to the inverse flow proves there exists W , a neighborhood of Γ (in S^3) s.t. $W_{Out}^s \cap W = \emptyset$. All in all, we conclude there exists a neighborhood N of Γ in S^3 s.t. $N \cap (\overline{W_{Out}^s} \cup \overline{W_{In}^u}) = \emptyset$. By this discussion we conclude there exists a component B_β of $S^3 \setminus (W_{In}^u \cup W_{Out}^s)$ s.t. $\Gamma \subseteq N \subseteq B_\beta$ - and in particular, B_β is non-empty.

Now, denote by $B_\alpha = S^3 \setminus \overline{B_\beta}$ - by their definition, both B_β, B_α are invariant under $R_{p,t}$. Since $\infty \in \Gamma$, by $\Gamma \subseteq N \subseteq B_\beta$ we conclude B_α is bounded - additionally, by the transverse intersection of W_{Out}^s, W_{In}^u we conclude B_α is non-empty. Now, set $D_\alpha = B_\alpha \cap U_{p,t}$, $D_\beta = B_\beta \cap U_{p,t}$ (see the illustration in Fig.11)- therefore, all that remains to conclude the proof of Lemma 2.14 is to show both are non-empty. We first prove $D_{\beta,t} \neq \emptyset$ - to do so, recall Γ is a curve in W_{In}^s , i.e., the trajectory of every initial condition on Γ flows to P_{In} (in infinite time). Therefore, given $x \in N \setminus \Gamma$ sufficiently close to Γ , by Cor.2.1.6 its trajectory must hit $U_{p,t}$ transversely - by the definition of $D_{\beta,t}$ and the invariance of B_β this can only occur at $D_{\beta,t}$, hence $D_{\beta,t} \neq \emptyset$. Additionally, since we have already proven $W_{In}^u \cap B_\beta = \emptyset$, by the transverse intersection of $W_{In}^u, U_{p,t}$ a similar argument proves $D_{\alpha,t} \neq \emptyset$ and Lemma 2.14 follows. \square

Remark 2.2. *Despite the illustration in Fig.11, in practice, $W_{In}^u \cup W_{Out}^s$ intersects $\overline{U_{p,t}}$ in a much, much more complicated set than the two curves sketched in Fig.11. However, as we will see, this incorrect (yet convenient) illustration will not affect our reasoning whatsoever.*

Remark 2.3. *By construction, $\partial D_{\alpha,t} \cap \partial H_{p,t}$ includes precisely one component, Γ , which is an arc connecting P_{In}, P_{Out} .*

We now generalize Lemma 2.14 to the original vector field, F_p . To do so, let U_p be the cross-section introduced in Lemma 2.1, and recall we denote by $f_p : \overline{U_p} \rightarrow \overline{U_p}$ the first-return map of F_p , the original vector field given by Eq.2 (wherever defined in U_p). We now prove:

Lemma 2.15. *Let $p \in P$ be a trefoil parameter. Then, there exists a partition of $\overline{U_p}$ to two sets, D_α, D_β s.t. D_α, D_β are separated in $\overline{U_p}$ by $W_{Out}^s \cup W_{In}^u$. In addition, $f_p(\overline{D_\alpha}) \subseteq \overline{D_\alpha}, f_p(\overline{D_\beta}) \subseteq \overline{D_\beta}$.*

Proof. Consider $R_{p,s}$, with $s \in (0, t]$ s.t. $\forall s > 0$, $R_{p,s}$ satisfies the conditions of Lemma 2.14 - by the definition of $R_{p,s}$ (see the discussion preceding Cor.2.1.6), $R_{p,s}$ coincides with F_p in $B_{\frac{1}{s}}(0)$. By Cor.2.1.6 each $R_{p,s}$ induces a first-return map $f_{p,s} : \overline{U_{p,s}} \rightarrow \overline{U_{p,s}}$, $s > 0$ - and by Lemma 2.14, for every $s > 0$ $g_{p,s}$ induces a partition of $\overline{U_{p,s}}$ to two $f_{p,s}$ -invariant sets, $D_{\alpha,s}, D_{\beta,s}$, separated by a set $C_s \subseteq (\overline{W_{Out}^s} \cup \overline{W_{In}^u})$. Now, denote by D_α, D_β the respective limits in $\overline{U_p}$ of points in $\overline{D_{\alpha,s}}, \overline{D_{\beta,s}}$ when $s \rightarrow 0$. Because $R_{p,s}, F_p$ coincide on $B_{\frac{1}{s}}(P_{In})$, we immediately conclude $f_p(\overline{D_\alpha}) \subseteq \overline{D_\alpha}, f_p(\overline{D_\beta}) \subseteq \overline{D_\beta}$. Lemma 2.15 is therefore proven. \square

Having proven Cor.2.1.6, Lemma 2.14 and Lemma 2.15, we are now ready to prove Th.2.2 where we prove the dynamics of F_p on D_α are bounded - that is, we now prove that given any $x \in \overline{D_\alpha}$, its trajectory is uniformly bounded in $B_r(P_{In})$, for some $r > 0$ independent of x . In other words, recalling the definition of $R_{p,t}, t > 0$ given in the beginning of this section, Th.2.2 proves that provided $t > 0$ is sufficiently small we have $D_\alpha = D_{\alpha,t}$, and that the dynamics of the vector fields $R_{p,t}, F_p$ on initial conditions in D_α coincide.

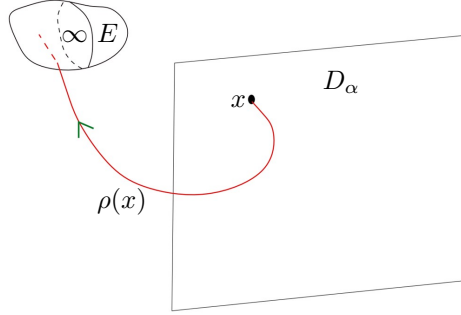


FIGURE 12. an initial condition $x \in D_\alpha$ s.t. $\Gamma(x)$ enters E - as we will prove, this scenario forces a contradiction.

Theorem 2.2. *Let $p \in P$ be a trefoil parameter. With previous notations, for every sufficiently small $t > 0$, $D_\alpha = D_{\alpha,t}$ and $R_{p,t}, F_p$ coincide on the trajectories of initial conditions in $\overline{D_\alpha}$. In particular, $f_{p,t}|_{\overline{D_{\alpha,t}}} = f_p|_{\overline{D_\alpha}}$. In particular, D_α is bounded.*

Proof. To prove Th.2.2, it would suffice to prove the existence of some $\delta > 0$, independent of t , s.t. the trajectories under F_p of initial conditions in D_α are all trapped in $B_\delta(P_{In})$. To see why this would suffice, first recall that by definition $R_{p,t}$ and F_p coincide in $B_{\frac{1}{t}}(P_{In})$. Now, choose $t > 0$ s.t. both $\delta < \frac{1}{t}$ and Lemmas 2.14 and Lemma 2.15 hold. If the trajectories under F_p of initial conditions in D_α never escape $B_\delta(P_{In})$, by definition we have $\overline{D_{\alpha,t}} = \overline{D_\alpha}$, $f_{p,t}|_{\overline{D_{\alpha,t}}} = f_p|_{\overline{D_\alpha}}$. Let us therefore prove the existence of such $\delta > 0$. We do so by contradiction - namely, we will prove the non-existence of such a δ generates a contradiction to Lemma 2.14.

To do so, assume there is no $\delta > 0$ as described above. That is, assume that for any small $d > 0$ there exists some initial condition $x \in D_\alpha$, with a forward trajectory $\rho(x)$ (under F_p), s.t. $\Gamma(x) \cap B_d(\infty) \neq \emptyset$ (with $B_d(\infty)$ considered as an open ball in S^3). Now, consider $d > 0$ s.t. Lemma 2.14 holds, an $x \in D_\alpha$ and an ellipsoid $E \subseteq B_d(\infty)$ s.t. $\infty \in E$, $x \notin \overline{E}$ and $\rho(x) \cap E \neq \emptyset$ (see Fig.12 for an illustration of the situation). In line with Th.2.1, construct a C^∞ perturbation R'_p of F_p in S^3 , which coincides with F_p on $S^3 \setminus E$ and generates an unbounded heteroclinic, connection passing through E and connecting P_{In}, P_{Out} . That is, the one-dimensional, stable manifold of the fixed-point P_{In} , W_{In}^s , has two components under R'_p : a bounded one, Θ , and an unbounded one, Γ , which is a heteroclinic trajectory connecting P_{In}, P_{Out} through E .

Now, recall we originally choose d sufficiently small s.t. R'_p satisfies the conditions of Lemma 2.14. Therefore, denoting by $f'_p : \overline{U'_p} \rightarrow \overline{U'_p}$ the first-return map for R'_p (with U'_p constructed similarly to Cor.2.1.6), there exists a partition of $\overline{U'_p}$ to two g'_p -invariant sets, D'_α, D'_β s.t. $f'_p(\overline{D'_\alpha}) \subseteq \overline{D'_\alpha}$, $f'_p(\overline{D'_\beta}) \subseteq \overline{D'_\beta}$ (by Lemma 2.14, both D'_α, D'_β are non-empty) - moreover, by definition, $D_\alpha \setminus \overline{E} = D'_\alpha \setminus \overline{E}$, $D_\beta \setminus \overline{E} = D'_\beta \setminus \overline{E}$. Additionally, recall that as shown at the end of the proof of Lemma 2.14, the trajectories of initial conditions sufficiently close to Γ eventually hit D'_β transversely. We now use these facts to generate a contradiction and conclude the proof of Th.2.2.

To do so, recall we originally chose $x \in D_\alpha \setminus \overline{E}$ s.t. its trajectory under F_p , $\rho(x)$, flows into E in some finite time. Moreover, recall F_p, R'_p coincide in $S^3 \setminus E$ - therefore, by $\rho(x) \cap E \neq \emptyset$ and the discussion in the previous paragraph, we can choose R'_p in E s.t. the trajectory of x w.r.t. R'_p passes arbitrarily close to ∞ . However, by previous paragraph this implies we can choose the said trajectory s.t. after escaping E along Γ it eventually intersects transversely with D'_β . Since $x \in D_\alpha \setminus \overline{E}$, by $D_\alpha \setminus \overline{E} = D'_\alpha \setminus \overline{E}$ we conclude $f'_p(\overline{D'_\alpha}) \cap D'_\beta \neq \emptyset$. This is a

contradiction to $f_p'(\overline{D'_\alpha}) \subseteq \overline{D'_\alpha}$ - hence, all in all, we conclude there exists a $\delta > 0$ s.t. the trajectories under F_p of initial conditions in D_α never escape $B_\delta(P_{In})$, and Th.2.2 follows. \square

Remark 2.4. We have, in fact, proven something stronger - we proved that provided $t > 0$ is sufficiently small, B_α does not depend on $R_{p,t}$ (see the proof of Lemma 2.14 for the definition). Or, put simply, we have just proven $W_{Out}^s \cup W_{In}^u$ is bounded for every vector field F_p , $p \in P$. In particular, Th.2.2 implies that provided $t > 0$ is sufficiently small, the set B_α introduced in the proof of Lemma 2.14 is independent of t .

Now, recall that given $p \in P$ we denote by $f_p : \overline{U_p} \rightarrow \overline{U_p}$ the first-return map corresponding to F_p (wherever defined). By Lemma 2.1, Cor.2.1.6 and Th.2.2 we immediately conclude:

Corollary 2.2.1. Let $p = (a, b, c) \in P$ be some parameter - then, $f_p : \overline{D_\alpha} \rightarrow \overline{D_\alpha}$ is well-defined (at least away from W_{In}^s) as a first return map for the vector field F_p . Additionally, $f_p(\overline{D_\alpha}) = \overline{D_\alpha}$.

Th.2.2 and Cor.2.2.1 both suggest that in order to prove the existence of bounded, chaotic dynamics for F_p , it would be best to look for them in $\overline{D_\alpha}$ - as it corresponds to the bounded part of the dynamics for F_p . However, to do so we need more information about the flow dynamics for F_p - in the next Section we show that at a very specific type of parameters $p \in P$, the existence of chaotic dynamics for F_p in D_α can be proven rigorously. In the meantime, we conclude Section 2 with the following fact, which allows us to characterize the topology of D_α completely - namely, we will now prove that given any $p \in P$, it corresponding D_α is a bounded topological disc on the cross-section U_p (see the discussion before Lemma 2.1).

To begin, first recall the cross-section $\{\dot{x} = 0\} = \{(x, y, -y) | x, y \in \mathbf{R}\}$ analyzed in Stage I of the proof of Th.2.1 - as shown in the proof of Lemma 2.3, the tangency curve of F_p to the cross-section $\{\dot{x} = 0\}$, σ , is parameterized by $\sigma(x) = (x, -\frac{x(b+1)}{a+c-x}, \frac{x(b+1)}{a+c-x})$, $x \neq c+a$. Moreover, $\mathbf{R}^3 \setminus \{\dot{x} = 0\}$ consists of two components - $\{\dot{x} < 0\}$ which lies **above** $\{\dot{x} = 0\}$, and $\{\dot{x} > 0\}$ which lies **below** it. As proven in Lemma 2.3, $\{\dot{x} = 0\} \setminus \sigma$ consists of three-regions: A_1, A_2, A_3 (see Fig.3) s.t. F_p points inside $\{\dot{x} > 0\}$ on A_1, A_2 and inside $\{\dot{x} < 0\}$ on A_3 (see the illustration in Fig.13). Moreover, recall the cross-section $\{\dot{y} = 0\}$ is transverse to $\{\dot{x} = 0\}$, and that the intersection $\{\dot{y} = 0\} \cap \{\dot{x} = 0\}$ is a curve l_p , parameterized by $l_p(x) = (x, -\frac{x}{a}, \frac{x}{a})$, $x \in \mathbf{R}$ (see the illustration in Fig.5 and Fig.13). As proven in Stage I of the proof of Th.2.1, $\{\dot{y} = 0\} \setminus l_p$ is composed of two components - $U_p = \{\dot{y} = 0\} \cap \{\dot{x} < 0\}$, and $L_p = \{\dot{y} = 0\} \cap \{\dot{x} > 0\}$ (see the illustration in Fig.5 and Fig.13).

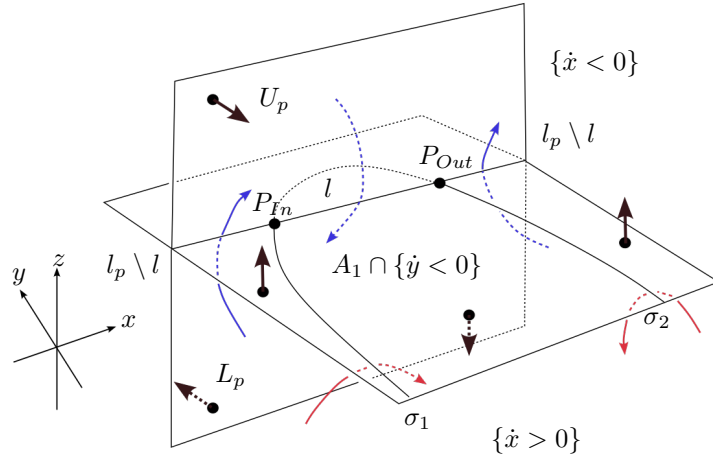


FIGURE 13. The directions of F_p on A_1, σ_1, σ_2 and A_1 , along with a sketch of some flow lines on σ_1, σ_2 and $l, l \setminus l$.

Now, recall we parameterize the components of $\{\dot{x} = 0\} \setminus \sigma$ by $A_1 = \{(x, -y, y) | x < a+c, y < -\frac{x(b+1)}{a+c-x}\}$, $A_2 = \{(x, -y, y) | x > a+c, y < -\frac{x(b+1)}{a+c-x}\}$, and $A_3 = \{(x, -y, y) | x \neq a+c, y > -\frac{x(b+1)}{a+c-x}\}$ (see the discussion immediately after the proof of Lemma 2.4). As a consequence from this discussion, by $P_{In} = (0, 0, 0)$, $P_{Out} = (c-ab, \frac{ab-c}{a}, \frac{c-ab}{a})$ we conclude $l_p \cap \sigma = \{P_{In}, P_{Out}\}$. As such, the region $A_1 \cap \{\dot{y} > 0\}$ is a half-disc $C_1 \subseteq A_1$ on $\{\dot{x} = 0\}$ bounded by $\sigma_3 = \{\sigma(x), 0 \leq x \leq c-ab\}$ and $l = \{l_p(x) | 0 \leq x \leq c-ab\}$ (see the illustration in Fig.13). As stated, we now conclude Section II with the technical (yet useful) Prop.2.3, which is a corollary of Th.2.2. As we will see in Section III, Prop.2.3 would form a major tool in the proof of Th.3.1, where we prove the existence of chaotic dynamics for the Rossler system.

Proposition 2.3. *Let $p = (a, b, c) \in P$ be a parameter, and let F_p denote the corresponding vector field, given by Eq.2. Then, the set $\overline{D_\alpha} \subseteq \overline{U_p}$ is a two-dimensional topological disc bounded by l and arcs on $(W_{Out}^s \cup W_{In}^u) \cap U_p$.*

Proof. To begin, let us first motivate the proof. Despite the many technical details below, the idea behind the proof is fairly simple. To motivate it, first recall that by the discussion above, since $\{\dot{y} = 0\}$ is transverse to $\{\dot{x} = 0\}$ at the curve l_p , by $U_p = \{\dot{x} < 0\} \cap \{\dot{y} = 0\}$, $L_p = \{\dot{x} > 0\} \cap \{\dot{y} = 0\}$ (see the illustration in Fig.13) the trajectories of initial conditions in U_p must first hit $\{\dot{x} = 0\}$ **before** hitting L_p - and vice versa (see the illustration in Fig.13). Or, in other words, given an initial condition $s \in U_p$, in order for its forward trajectory to hit L_p it must **first** hit $\{\dot{x} = 0\}$ transversely, and vice versa. Capitalizing on this observation, since by Lemma 2.3 and Cor.2.1.1 W_{In}^u, W_{Out}^s are transverse to **both** $\{\dot{y} = 0\}$, $\{\dot{x} = 0\}$, by studying the tangencies of the vector field F_p to both these sections it would follow that $W_{In}^u \cap U_p, W_{Out}^s \cap U_p$ are both connected curves on U_p . Therefore, by their transverse intersection (and the definition of D_α - see the discussion before Lemma 2.15) it would follow D_α is, in fact, a topological disc.

To begin, recall that given any $s \in \mathbf{R}^3$, we parameterize its trajectory by $\gamma_s(t)$, $t \in \mathbf{R}$, $\gamma_s(0) = s$. We first prove that given any $s \in \overline{A_2} \subseteq \{\dot{x} = 0\}$, $\lim_{t \rightarrow \infty} \gamma_s(t) = \infty$. To do so, choose some $s \in \overline{A_2}$, $s = (x_0, y_0, z_0)$, and consider the half-planes $P_0 = \{\dot{x} > 0\} \cap \{(x, y, z) | x = x_0, y \geq y_0\}$, $P_1 = \{\dot{x} > 0\} \cap \{(x, y, z) | y = y_0, x \geq x_0\}$. These planes intersect at the line $l_0 = \{(x_0, y_0, z) | z < z_0\}$ (see the illustration in Fig.14). In particular, P_0, P_1 and the region $P_3 = \{(x, y, z) \in A_2 | x \geq x_0, y \leq y_0\}$ together form the boundary of a closed quadrant Q , which lies strictly inside $\{\dot{x} \geq 0\}$ (see the illustration in Fig.14). Moreover, by our choice of P_3 (and the concavity of ∂A_2 , parameterized by $\sigma(x) = (x, -\frac{x(b+1)}{a+c-x}, \frac{x(b+1)}{a+c-x})$, $x > c + a$), we conclude $P_3 \subseteq \overline{A_2}$ - as such, $Q \cap \{\dot{x} = 0\} = P_3$. As proven in Lemma 2.3, on A_2 the vector field F_p points inside $\{\dot{x} > 0\}$, i.e., below the cross-section $\{\dot{x} = 0\}$. Additionally, because the normal vectors to P_0, P_1 are $(1, 0, 0)$, $(0, 1, 0)$ (respectively), by calculation it follows F_p points inside Q throughout ∂Q (see the illustration in Fig.14). Therefore, given any $\omega \in \overline{Q}$ and every $t > 0$, $\gamma_\omega(t) \in Q$. As a consequence, since by definition $Q \subseteq \{\dot{x} \geq 0\}$, because $s \in Q$, the x -component in γ_s blows up when $t \rightarrow \infty$, i.e. $\lim_{t \rightarrow \infty} \gamma_s(t) = \infty$. Since we chose $s \in \overline{A_2}$ arbitrarily, it follows that given any $s \in \overline{A_2}$, $\lim_{t \rightarrow \infty} \gamma_s(t) = \infty$.

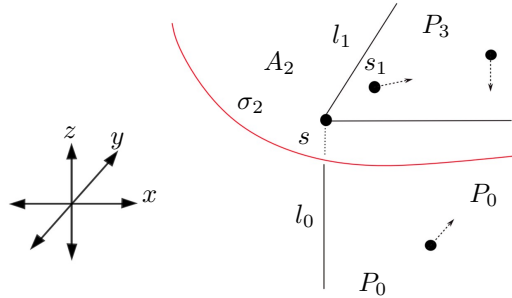


FIGURE 14. The directions of F_p on the body Q s.t. $s \in \partial Q$ (with $l_1 = P_1 \cap A_2$, and $s_1 \in P_1$). Since F_p points inside Q throughout ∂Q , no trajectory can escape Q in positive time/

Having proven the trajectory of every initial condition in $\overline{A_2}$ escapes to ∞ , we now prove the two-dimensional W_{Out}^s, W_{In}^u both intersect the region A_3 in two curves, which never hit ∂A_3 (see the illustration in Fig.15). To do so, recall that by Th.2.2, both W_{In}^u, W_{Out}^s are bounded - therefore, by previous paragraph we conclude $W_{In}^u \cap \overline{A_2}$, $W_{Out}^s \cap \overline{A_2}$ are both empty - therefore, since by the definition of the regions A_2, A_3 we have $\partial A_2 \subseteq \partial A_3$ (see the discussion after the proof of Lemma 2.3), we conclude $W_{In}^u \cap \overline{A_3}$, $W_{Out}^s \cap \overline{A_3}$ both lie away from $\overline{A_2}$. Now, recall that by Lemma 2.3 and Cor.2.1.1, W_{In}^s, W_{In}^u are both transverse to the cross-sections $\{\dot{x} = 0\}$ and $\{\dot{y} = 0\}$ at the fixed points P_{Out}, P_{In} , respectively. Additionally, recall A_3 is the (unique) region on $\{\dot{x} = 0\}$ on which F_p points into $\{\dot{x} > 0\}$ (i.e. above $\{\dot{x} = 0\}$) - therefore, by this discussion we conclude $W_{In}^u \cap A_3$ includes a curve, ρ_{In} , which begins at P_{In} and enters $\{\dot{y} > 0\} \cap A_3$ (see the illustration in Fig.15). Similarly, there exists a curve $\rho_{Out} \subseteq W_{Out}^s \cap A_3$ which begins at P_{Out} and enters $A_3 \cap \{\dot{y} > 0\}$.

With previous notations, further recall that as proven in Lemma 2.5, given $s \in l_p \setminus l$, for a sufficiently large $t < 0$, $\gamma_s(t) \in \{\dot{y} < 0\}$ - i.e., the flow line arrives at $s \in l_p \setminus l$ from $\{\dot{y} < 0\}$ (see the illustration in Fig.13 and Fig.5). Therefore, since the curve ρ_{In} begins at $A_3 \cap \{\dot{y} > 0\}$, by the definition of A_3 in the proof of Lemma 2.3 we conclude that given $s \in \rho_{In}$ for every sufficiently large $t < 0$ we have $\gamma_s(t) \in \{\dot{x} > 0\} \cap \{\dot{y} > 0\}$. Therefore, since the flow lines arrive at $l \setminus l_p$ from $\{\dot{y} < 0\}$, by this discussion the curve ρ_{In} can never hit $l \setminus l_p$, i.e., $\rho_{In} \cap l_p \setminus l = \emptyset$ - and as a consequence, $\rho_{In} \subseteq \{\dot{y} > 0\}$. Additionally, recall we denote by $\sigma_3 = \{\sigma(x) | x \in (0, a + c)\}$ - by a similar argument to the proof of Lemma 2.4, it follows that given $s \in \sigma_3$, for every sufficiently large $t > 0$ $\gamma_s(t) \in \{\dot{x} < 0\}$,

i.e. the flow lines w.r.t. F_p arrive at σ_3 from $\{\dot{x} < 0\}$ (that is, from above $\{\dot{x} = 0\}$ - see the illustration in Fig.15). Therefore, it also follows we also have $\rho_{In} \cap \sigma_3 = \emptyset$. In other words, we have proven ρ_{In} is a curve in $\overline{A_3 \cap \{\dot{y} > 0\}}$ s.t. $\rho_{In} \cap \partial A_2$, $\rho_{In} \cap l_p \setminus l$ and $\rho_{In} \cap \sigma_3$ are all empty - therefore, by $\partial A_3 \cap \{\dot{y} > 0\} = (l \setminus l_p) \cup \partial A_2 \cup \sigma_3 \cup \{P_{In}, P_{Out}\}$, we conclude ρ_{In} is a curve which begins at P_{In} , and after leaving P_{In} never hits $\partial(A_3 \cap \{\dot{y} > 0\})$ again. In particular, it immediately follows that $\rho_{In} = W_{In}^u \cap A_3$. A similar argument proves $\rho_{Out} = W_{Out}^s \cap A_3$ is a curve in $A_3 \cap \{\dot{y} > 0\}$ beginning at the fixed-point P_{Out} and never hitting $\partial(A_3 \cap \{\dot{y} > 0\})$ (see the illustration in Fig.15).

Therefore, by the transverse intersection of W_{Out}^s, W_{In}^u we conclude the union of all the bounded regions in $A_3 \setminus (W_{In}^u \cup W_{Out}^s)$ forms a topological disc V_α - see the illustration in Fig.15. In particular, there exists a first-return map $h : \rho_{In} \cup \rho_{Out} \rightarrow \rho_{In} \cup \rho_{Out}$ - and because $\rho_{In} \cup \rho_{Out}$ lies away from $\partial A_3 \cap \{\dot{y} = 0\}$ we conclude F_p is transverse to A_3 on $\rho_{In} \cup \rho_{Out}$, which implies h is continuous. In particular, by the definition of A_1, A_2, A_3 we know that given $s \in \rho_{In} \cup \rho_{Out}$, the flow-line connecting $s, h(s)$ enters $\{\dot{x} < 0\}$ immediately upon leaving s , then eventually hits $\{\dot{x} = 0\}$ transversely, after which it flows to $h(s)$. Since $\rho_{In} \cup \rho_{Out}$ is bounded by Th.2.2, by the discussion above the forward trajectory of s cannot hit A_2 , i.e., it only hits A_1 .

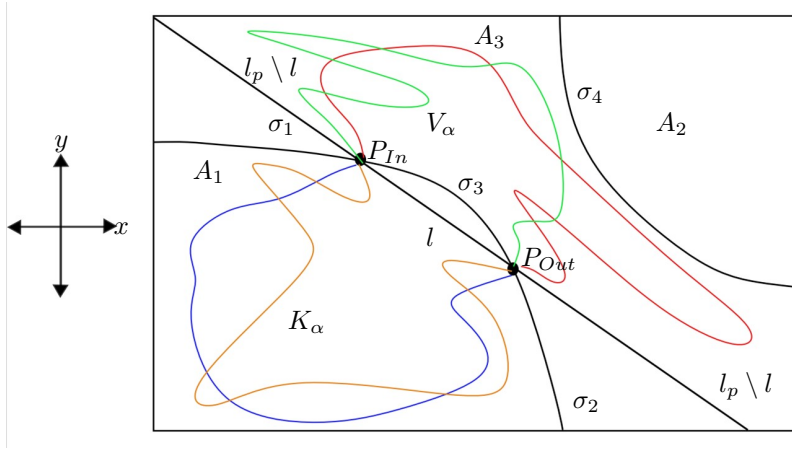


FIGURE 15. The sets V_α, K_α on the cross-section $\{\dot{x} = 0\}$. The green and blue lines arcs ρ_{In}, μ_{In} respectively, while the red and orange curves denote ρ_{Out}, μ_{Out} .

By this discussion we conclude that given $s \in \rho_{In} \cup \rho_{Out}$ there exists a minimal $t_1(s) > 0$ s.t. $\gamma_s(t_1(s)) \in \overline{A_1}$. Since we have already proven $(\rho_{In} \cup \rho_{Out}) \cap \sigma_3 = \emptyset$, by $\sigma_3 \subseteq \partial A_1 \cap \partial A_3$ and $h(\rho_{In} \cup \rho_{Out}) = \rho_{In} \cup \rho_{Out}$ we conclude that given $s \in \rho_{In} \cup \rho_{Out}$ we **cannot** have $\gamma_s(t_1(s)) \in \sigma_3$ - for this would imply, by definition, that such an s satisfies $h(s) \in \sigma_3$, i.e. $(\rho_{In} \cup \rho_{Out}) \cap \sigma_3 \neq \emptyset$. Now, let us recall that in Stage I of the proof of Th.2.1 we defined σ_1, σ_2 as the two components of $\partial A_1 \setminus \sigma_3$ (see the discussion after Lemma 2.3) - and as proven in Lemma 2.4, the trajectory of a given $s \in \sigma_1 \cup \sigma_2$ arrives at s from $\{\dot{x} > 0\}$. Therefore, given $s \in \rho_{In} \cup \rho_{Out}$ since γ_s arrives from s to $\gamma_s(t_1(s))$ from $\{\dot{x} < 0\}$ we conclude it **cannot** hit σ_1, σ_2 . Hence, by $\partial A_1 = \sigma_1 \cup \sigma_2 \cup \sigma_3$, similarly to previous arguments we conclude $\mu_{In} = W_{In}^u \cap A_1$, $\mu_{Out} = W_{Out}^s \cap A_1$ are both curves beginning at P_{In}, P_{Out} (respectively) and never hitting ∂A_1 . In particular, the union of all the bounded regions in $A_1 \setminus (\mu_{In} \cup \mu_{Out})$ includes a topological disc, K_α - see the illustration in Fig.15.

Now, set $P_\alpha = V_\alpha \cup K_\alpha \cup \{P_{In}, P_{Out}\}$ - by the arguments above, we conclude ∂P_α is a Jordan curve. We now conclude the proof of Prop.2.3 by proving $\partial P_\alpha \cap l = \emptyset$, and we do so by contradiction. To do so, let us first recall several facts. As mentioned earlier, the two-dimensional W_{In}^u, W_{Out}^s are both transverse to $\{\dot{y} = 0\}$ at P_{In}, P_{Out} (respectively) - and in particular, they are transverse to the cross-section U_p (see the illustration in Fig.4). Moreover, recall we defined D_α as the union of all the bounded components in $\mathbf{R}^3 \setminus (W_{In}^u \cup W_{Out}^s)$ (see the discussion before Lemma 2.15). Now, consider the set of flow lines connecting $\rho_{In} \cup \rho_{Out}$ to $\mu_{In} \cup \mu_{Out}$ - since $\rho_{In} \cup \rho_{Out}, \mu_{In} \cup \mu_{Out}$ are separated by U_p , if $l \not\subseteq D_\alpha$ it follows there must exist some $p_0 \in l$ s.t. $p_0 \in \partial P_\alpha$ - and since $l \subseteq A_1$ (see the discussion before Lemma 2.5) there exists a point $p_0 \in (\mu_{In} \cup \mu_{Out}) \cap l$.

Let us therefore denote by $p_1 = (x_1, y_1, z_1) \in (\mu_{In} \cup \mu_{Out}) \cap l$ be the point closest to P_{In} - since W_{In}^u, W_{Out}^s are both transverse to U_p at the respective fixed points, it follows $\partial D_\alpha \cap U_p$ includes a curve γ_1 which begins at P_{In} and terminates at p_1 . By the continuity of the flow, since the forward-trajectories of initial conditions in l enter $\{\dot{y} > 0\}$ immediately upon leaving l (see Lemma 2.5), the same argument implies $L_p \cap \partial D_\alpha$ also includes an arc γ_2 beginning at P_{In} and terminating at p_1 - see the illustration in Fig.16. In particular, every point $s \in \gamma_1$ is

connected by a flow-line to some $\omega \in \gamma_2$ and vice versa.

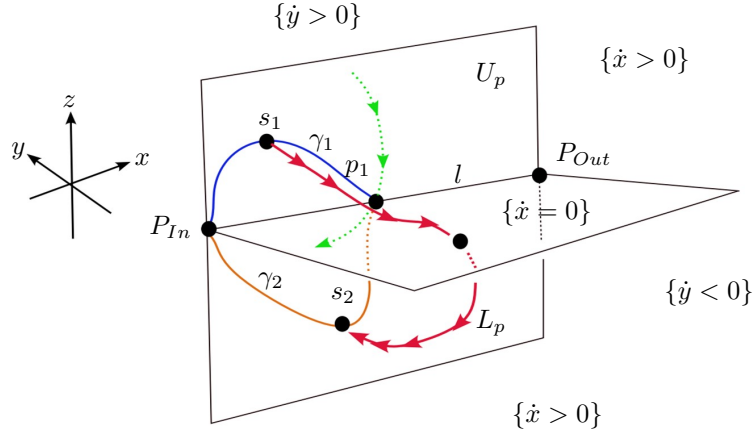


FIGURE 16. The curves γ_1, γ_2 and the point p_1 , along with some flow lines. In particular, the red flow line connects $s_1 \in \gamma_1$ with $s_2 \in \gamma_2$, while the green flow line is tangent to $\{y = 0\}$ at p_1 and lies wholly in $\{y > 0\}$.

Now, recall $p_1 = (x_1, y_1, z_1)$ and set P_1 as the half-plane $\{(x, y, z) | y = y_1, x \geq x_1\}$ (see the illustration in Fig.17), and consider the region R_1 bounded between P_1 and ∂P_α satisfying $P_{In} \in \partial R_1$ (see the illustration in Fig.17 - as must be mentioned, $\partial R_1 \cap \{y < 0\}$ consists of all the flow-lines connecting γ_1, γ_2). Because the normal vector to P_1 is $(0, 1, 0)$, it follows F_p points on P_1 inside R_1 - therefore, since F_p is tangent to $\partial R_1 \setminus P_1$, it follows no trajectory can escape R_1 in forward time.

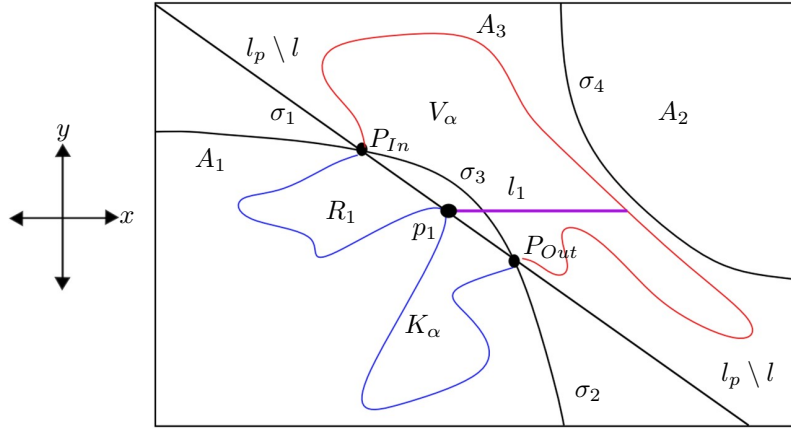


FIGURE 17. The magenta colored line l_1 corresponds to $P_1 \cap \{x = 0\}$, thus generating a body R_1 as described above. We prove this scenario is impossible.

However, because $P_{Out} \notin \overline{R_1}$ by the transverse intersection of W_{In}^u, W_{Out}^s it follows by the continuity of the flow that the trajectories of some initial conditions in R_1 **must** eventually flow inside $P_\alpha \setminus R_1$. This is a contradiction, hence it follows $l \subseteq D_\alpha$, and that $\partial P_\alpha \cap l = \emptyset$. In particular, because the trajectories of initial conditions in $\rho_{In} \cup \rho_{Out}$ must first hit U_p transversely **before** hitting $A_1 \cap \{y = 0\}$ it follows $\partial D_\alpha \cap \partial U_p = \{P_{In}, P_{Out}\}$ and Prop.2.3 follows - see the illustration in Fig.18.

□

3. CHAOTIC DYNAMICS AND TREFOIL KNOTS

From now on, let $(a, b, c) = p \in P$ be some parameter, let F_p denote its corresponding vector field (see Eq.2) - that is, F_p is the vector field generating the Rössler system corresponding to p . Moreover, recall we denote by U_p denote the cross-section analyzed in Section 2 (see the discussion before Lemma 2.1) - as shown, U_p is a half plane, i.e. a topological disc. Additionally, from now on we always denote by $D_\alpha \subseteq U_p$ the set introduced in the proof of Lemma 2.15 - as proven in Section 2 (see Prop.2.3), D_α is a topological disc, and the first-return

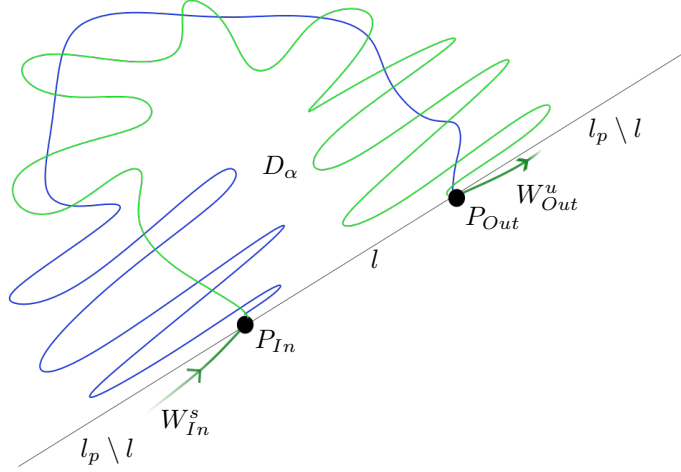


FIGURE 18. D_α sketched on the half-plane U_p . ∂D_α consists of the fixed points, the curve l , and arcs on the green and blue curves which denote $W_{In}^s \cap U_p$, $W_{Out}^s \cap U_p$ respectively.

map $f_p : \overline{D_\alpha} \rightarrow \overline{D_\alpha}$ is well-defined (see Prop.2.3, Th.2.2 and Remark 2.2.1). By definition, $P_{In}, P_{Out} \in \partial D_\alpha$. In particular, ∂D_α is composed of the closure of the arc $l = \{(x, -\frac{x}{a}, \frac{x}{a}) | x \in (0, c - ab)\}$, along with arcs on $W_{In}^s \cap U_p$, $W_{Out}^s \cap U_p$ connecting at the points of $W_{In}^s \cap W_{Out}^s$, (see the discussion at page 16) - see the illustration in Fig.18.

To continue, recall our definition of chaotic dynamics in Def.1.1 - our main objective in this section is to prove the chaoticity of the dynamics generated by the Rössler system at some specific parameter values $p \in P$. Using the results obtained in Section 2, we prove this is the case in Th.3.1 (that is, Th.2 from the introduction) - however, to do so we must first introduce two definitions. Recall we denote by W_{In}^s the stable, invariant one-dimensional manifold of the saddle-focus P_{In} , and by W_{Out}^u the unstable, invariant one-dimensional manifold of the saddle focus P_{Out} (see the discussion in page 3 and the illustration in Fig.4). We begin with the following definition:

Definition 3.1. Let $p \in P$ be s.t. there exists a **bounded** heteroclinic trajectory for F_p in $W_{In}^s \cap W_{Out}^u$, connecting P_{In}, P_{Out} . In that case we say p is a **heteroclinic parameter**.

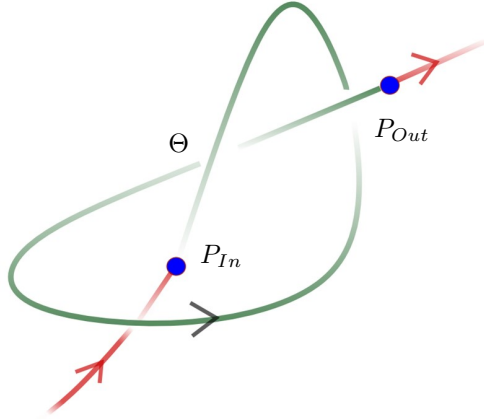


FIGURE 19. a heteroclinic trefoil knot (see Def.3.2). Θ denotes the bounded heteroclinic connection.

From now on throughout the remainder of this paper we will be interested in a specific type of heteroclinic parameters. Before introducing them, consider Fig.19 where the green line Θ denotes the bounded heteroclinic connection between P_{In}, P_{Out} - and the red lines denote the components of W_{In}^s, W_{Out}^u (which, by Th.2.1, are unbounded heteroclinic trajectories). Now, let $p \in P$ be a heteroclinic parameter, and denote by $\Lambda = \{P_{In}, P_{Out}, \infty\} \cup W_{In}^s \cup W_{Out}^u$. Clearly, Λ forms a knot in S^3 , composed of the union of the separatrices in W_{In}^s, W_{Out}^u and the fixed points for F_p (in S^3). This discussion motivates the following definition:

Definition 3.2. Let $p \in P$ be a heteroclinic parameter and Λ be as above. Let Θ denote the bounded heteroclinic connection - that is, the bounded component of $\Lambda \setminus \{P_{Out}, P_{In}\}$. We say p is a **trefoil parameter** provided the following two conditions are satisfied:

- $\Theta \cup (W_{In}^u \cap W_{Out}^s) \cup \{P_{In}, P_{Out}\}$ forms a trefoil knot.
- $\Theta \cap \overline{U_p} = \{P_0\}$ is a point of transverse intersection.

See Fig.19 and Fig.20 for illustrations.

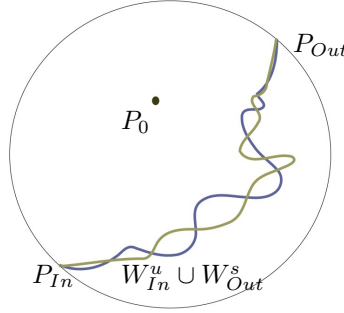


FIGURE 20. The geography of the cross-section U_p .

The existence of a trefoil parameter $p \in P$ for the Rössler system at approximate parameter values $(a, b, c) \approx (0.468, 0.3, 4.615)$ was observed numerically (see Fig.5.B1 and Fig.5.C1 in [27]). Recalling the definitions of B_α and D_α from Lemmas 2.14 and 2.15, as an immediate consequence of Def.3.2, Th.2.2 and Prop.2.3 we now derive the following:

Proposition 3.1. *Let $p \in P$ be a trefoil parameter. Then, with the notations above, P_0 is an interior point to D_α . Moreover, with previous notations, Λ forms a trefoil knot in S^3 .*

Proof. Let us recall we saw in the proof of Th.2.2 that the union of the two-dimensional invariant manifolds $W_{In}^u \cup W_{Out}^s$ is bounded, and that we assume $W_{In}^u \cap W_{Out}^s$ holds throughout our parameter space P (i.e., we assume W_{In}^u, W_{Out}^s intersect transversely throughout P - see the discussion at page 16). Moreover, recall we defined B_α as the closure of the union of all the bounded components of $\mathbf{R}^3 \setminus W_{In}^u \cup W_{Out}^s$, and that $\overline{D_\alpha}$ was defined as $B_\alpha \cap \overline{U_p}$ (see Lemma 2.14, Lemma 2.15 and Remark 2.4). As proven in Th.2.2 B_α is bounded, and invariant under the flow generated by F_p . Now, recall we denote by Γ_{Out} the component of the one-dimensional invariant manifold W_{Out}^u which forms an unbounded heteroclinic connection between P_{Out} and ∞ (see Th.2.1) - by this discussion, $\Gamma_{Out} \cap B_\alpha = \emptyset$. Additionally, recall we denote by $J_p(P_{Out})$ the linearization of the vector field F_p at P_{Out} , and that by the definition of B_α , we have $P_{Out} \in \partial B_\alpha$. Now, denote by V_{Out} the eigenvalue of $J_p(P_{Out})$ which is tangent to Γ_{Out} - by this discussion, V_{Out} points **outside** of B_α (see the illustration in Fig.21).

As a consequence, $-V_{Out}$ points inside B_α , i.e., there exists a component of W_{Out}^s which intersects B_α (see the illustration in Fig.21). By the invariance of B_α under the flow, that component is trapped in B_α - and since we assume p is a trefoil parameter, that component can only be Θ from Def.3.2, i.e., the bounded heteroclinic connection. Therefore, we conclude Θ is trapped in B_α . Now, since p is a trefoil parameter, by Def.3.2 there exists some P_0 s.t. $\{P_0\} = \Theta \cap U_p$, and moreover, P_0 is interior to U_p . As we defined $\overline{D_\alpha} = \overline{U_p} \cap B_\alpha$, by the discussion above $P_0 \in \overline{D_\alpha}$. Now, let us recall Θ is a heteroclinic connection in **both** the one-dimensional W_{In}^u, W_{Out}^u - as such, it is not a homoclinic trajectory to either fixed point, i.e., $\Theta \cap (W_{In}^u \cup W_{Out}^u) = \emptyset$. Finally, recall ∂D_α is composed of two sets - the arc $l \subseteq \partial U_p$ and arcs on $W_{Out}^s \cap U_p, W_{In}^u \cap U_p$ (see the proof of Prop.2.3). Therefore, since P_0 is interior to U_p , by this discussion and by $l \subseteq \partial U_p$ it follows P_0 is strictly interior to D_α .

Therefore, to conclude the proof of Cor.3.1, it remains to prove that given a trefoil parameter $p \in P$, Λ forms a trefoil knot. To do so, let us recall that since $p \in P$, by Th.2.1 F_p generates two heteroclinic connections, connecting P_{In}, P_{Out} to $\infty - \Gamma_{In}, \Gamma_{Out}$, respectively. Moreover, by Stages II and III of the proof of Th.2.1, both $\Gamma_{In}, \Gamma_{Out}$ are trapped inside C_{In}, C_{Out} , three-dimensional bodies satisfying $C_{In} \subseteq \{(x, y, z) | x \leq 0\}$, and $C_{Out} \subseteq \{(x, y, z) | x \geq c - ab\}$. Since by our assumptions on the parameter space P $c - ab > 0$ (see the discussion at 3), as a consequence, $\Gamma_{In}, \Gamma_{Out}$ cannot be asymptotically linked with one another. And since both $\Gamma_{In}, \Gamma_{Out}$ are unbounded, we also have $(\Gamma_{In} \cup \Gamma_{Out}) \cap B_\alpha = \emptyset$, which, by $\Theta \subseteq B_\alpha$, immediately yields neither $\Gamma_{In}, \Gamma_{Out}$ are asymptotically linked with Θ (see the illustration in Fig.21). As a consequence, it now follows $\Lambda = \Gamma_{In} \cup \Gamma_{Out} \cup \Theta \cup \{P_{In}, P_{Out}, \infty\}$ is a trefoil knot in S^3 and Prop.3.1 now follows. \square

Having proven Cor.3.1, let us give a sketch of what lies ahead. As stated earlier, our objective in this section is to prove the dynamics of the Rössler system at trefoil parameters (i.e. of F_p) are chaotic and admit infinitely

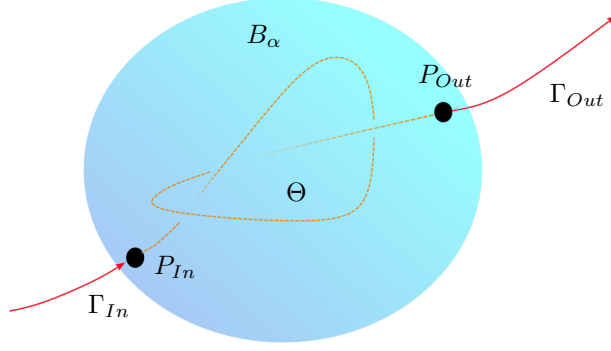


FIGURE 21. The separatrix Θ trapped inside B_α , the blue sphere.

many periodic trajectories - and we will do so in Th.3.1. Despite the relatively easy formulation, the proof of Th.3.1 is rather technical, depending on several Lemmas and Propositions which analyze and study the dynamics of F_p and its first-return map $f_p : \overline{D_\alpha} \rightarrow \overline{D_\alpha}$. The idea behind the proof for Th.3.1 is as follows - we first study the discontinuities of f_p in the topological disc D_α (see Prop.3.2 and Cor.3.0.1). Motivated by our findings, we then use our results to define symbolic dynamics for f_p on some invariant $Q \subseteq \overline{D_\alpha}$ - as will be made clear, Q includes periodic orbits of all minimal period for f_p thus Th.3.1 would follow. Later on in Section 4 we will provide several corollaries for Th.3.1, which study both the non-hyperbolic nature of the flow at trefoil parameters and the bifurcations of periodic trajectories in Q .

To begin, from now on unless stated otherwise, let $(a, b, c) = p \in P$ be a trefoil parameter as in Def.3.2, and let Θ denote the bounded component of W_{In}^s, W_{Out}^u - in other words, Θ is the bounded heteroclinic connection for the vector field F_p , given by Def.3.2. Additionally, recall we denote by $f_p : \overline{U_p} \rightarrow \overline{U_p}$ the first return map generated by the vector field F_p (wherever defined - see Lemma 2.1). As stated above, we begin this section by studying the discontinuities of $f_p : \overline{D_\alpha} \rightarrow \overline{D_\alpha}$. To motivate our results, let us first recall P_0 is the **unique** point of intersection between Θ and the cross-section D_α (see Def.3.2), and that P_0 is interior to D_α (see Cor.3.1) - which implies $D_\alpha \setminus \{P_0\}$ contains a topological annulus centered at P_0 . Since P_0 flows to P_{In} in infinite time, as P_0 is interior to U_p and because $P_{In} \in \partial U_p$, we would expect f_p to be discontinuous at P_0 - if only because the said annulus has to be torn by f_p . This motivates us to prove the following Proposition, characterizing the discontinuities of f_p in the topological disc D_α :

Proposition 3.2. *Let $p \in P$ be a trefoil parameter. Then, the discontinuities of f_p in D_α are given by $f_p^{-1}(l) \cap D_\alpha$ (with l as in Prop.2.3). In addition, there exists an arc of discontinuity points for f_p , $\delta \subseteq \overline{D_\alpha}$ s.t.:*

- δ connects $P_0 \in D_\alpha$ and a point $\delta_0 \in \partial D_\alpha \setminus \{P_{In}, P_{Out}\}$.
- $f_p(\delta) \subseteq l$.
- δ is the **only** curve of discontinuity points for f_p with an endpoint interior to D_α .

Proof. First, recall D_α is a topological disc (see Prop.2.3) and invariant under the first-return map $f_p : \overline{D_\alpha} \rightarrow \overline{D_\alpha}$ (see Lemma 2.15) - as such, we immediately conclude f_p is discontinuous at some interior $x \in D_\alpha$ **if and only if** the trajectory of x hits ∂D_α , i.e. $f_p(x) \in \partial D_\alpha$. Let us now recall ∂D_α is composed of either the arc l or arcs on $W_{In}^u \cap U_p, W_{Out}^s \cap U_p$ (see the proof of Prop.2.3) - because $W_{In}^u \cap U_p, W_{Out}^s \cap U_p$ are both invariant under f_p , we conclude that if $f_p(x) \in \partial D_\alpha$ it must lie in l . Therefore, by the discussion above we conclude the discontinuities of f_p in D_α are given precisely by the set $f_p^{-1}(l) \cap D_\alpha$.

To continue, in order to define and analyze the curve δ , we first prove f_p is continuous around P_{In} (in $\overline{D_\alpha}$) - to do so, recall that by Cor.2.1.1 the two-dimensional unstable manifold of P_{In} , W_{In}^u , is transverse to ∂U_p at P_{In} . Since P_{In} is a saddle-focus, initial conditions on the arc l sufficiently close to P_{In} must be mapped inside U_p by f_p - which proves f_p is continuous on some neighborhood of P_{In} in $\overline{U_p}$. Because $\overline{D_\alpha} \subseteq \overline{U_p}$ (see the illustration in Fig.22), we conclude f_p is continuous on some neighborhood of f_p in $\overline{D_\alpha}$ as well. We can now prove the existence of the discontinuity curve δ , as posited above. To do so, consider some closed loop ζ in D_α , surrounding P_0 . Since p is a trefoil parameter, the trajectory of P_0 flows to P_{In} in infinite time, without ever hitting $\overline{D_\alpha}$ along the way (see Def.3.2) - hence, f_p cannot be continuous on ζ : for if it was continuous on ζ , $f_p(\zeta)$ would be a closed curve in D_α surrounding P_{In} . Because this is impossible, by the discussion above there must exist a discontinuity on $\zeta_0 \in \zeta$, $f_p(\zeta_0) \in l$. Varying the loop ζ continuously in D_α we construct a curve δ of discontinuity points, connecting

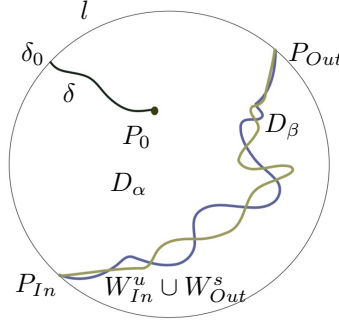


FIGURE 22. the curve δ , with endpoints P_0, δ_0 . l is the arc on ∂D_α connecting $P_{In}, P_{Out}, \delta_0$.

P_0 and some point δ_0 in ∂D_α , s.t. $\delta \setminus \{\delta_0\} \subseteq D_\alpha$ (see the illustration in Fig.22).

Having proven the existence of δ , our next objective is to prove the following two facts:

- $\delta_0 \neq P_{In}$.
- $\delta_0 \neq P_{Out}$.

The proof of $\delta_0 \neq P_{In}$ is immediate - to see why this is so, recall we already proved f_p is continuous around P_{In} , i.e., f_p maps points on $\overline{D_\alpha}$ sufficiently close to P_{In} away from l . Hence, since $f_p(\delta) \subseteq l$, we must have $\delta_0 \neq P_{In}$. The proof $\delta_0 \neq P_{Out}$ would require a different approach. To this end, we must first make several observations. First recall that D_α is an invariant subset (w.r.t. f_p) on the cross-section U_p , and that by Lemma 2.15, $U_p = \overline{D_\alpha} \cup \overline{D_\beta}$, and $f_p(\overline{D_\alpha}) \subseteq \overline{D_\alpha}$, $f_p(D_\beta) \subseteq \overline{D_\beta}$. Additionally, recall that given any initial condition $s \in \mathbf{R}^3$ whose trajectory is bounded and **does not** limit to a fixed point, the trajectory of s eventually hits U_p transversely (see Lemma 2.1). As a consequence, because D_α is bounded by Th.2.2, we conclude that given any $x \in \overline{D_\alpha} \setminus \{P_0\}$, $f_p^{-1}(x)$ is well-defined in $\overline{D_\alpha} \setminus \{P_0\}$. Now, by the arguments above it follows $f_p(\delta)$ is an arc on l , whose closure connects $f_p(\delta_0)$ and P_{In} .

We can now prove $\delta_0 \neq P_{Out}$. To do so, assume otherwise - if $\delta_0 = P_{Out}$, by $f_p(P_{Out}) = P_{Out}$ we conclude $f_p(\delta)$ is an arc on l whose closure connects P_{Out} and P_{In} , i.e., $\bar{l} = \overline{f_p(\delta)}$. Since the discontinuities of f_p are given by $f_p^{-1}(l) \cap D_\alpha$, this would imply f_p is continuous on $D_\alpha \setminus \delta$ - and by the continuity and injectivity of f_p (i.e. it is a homeomorphism of the topological disc $D_\alpha \setminus \delta$), it would follow $f_p(D_\alpha \setminus \delta) = D_\alpha$. Since P_0 is strictly interior to D_α this yields the existence of some $y \in D_\alpha$ s.t. $f_p(y) = P_0$ - however, since p is a trefoil parameter, by Def.3.2 and Cor.3.1, P_0 is the unique intersection point between the bounded heteroclinic trajectory and D_α . As a consequence, there **cannot** exist any $y \in D_\alpha$ s.t. $f_p(y) = P_0$ - this is a contradiction, hence it follows $\delta_0 \neq P_{Out}$.

Therefore, having proven $P_{Out}, P_{In} \notin \delta$, in order to conclude the proof of Lemma 3.2 it remains to show that given any discontinuity curve for f_p $\rho \subseteq D_\alpha$ s.t. ρ has an endpoint strictly **interior** to D_α , then $\rho = \delta$. Before doing so, let us first characterize topologically the components of the discontinuity set for f_p in D_α . Denote by $Dis(f_p) = f_p^{-1}(l) \cap D_\alpha$, the set of all the discontinuity points of f_p in D_α . We immediately conclude interior points in D_α which are **not** P_0 **cannot** form components in $Dis(f_p)$ - since given an interior point $x \in D_\alpha \setminus \{P_0\}$ s.t. $f_p(x) \in \partial D_\alpha$, by the continuity of the flow there exists an arc $\gamma \subseteq D_\alpha$, $x \in \gamma$, s.t. $f_p(\gamma)$ is an arc on ∂D_α . This proves all the components of $Dis(f_p)$ are arcs in D_α . The exact same argument also proves any component of $Dis(f_p)$ which is an arc must have at least one endpoint on the arc l .

We can now prove that given a component $\rho \subseteq Dis(f_p)$ with an endpoint interior to D_α , then $\rho = \delta$. To do so, assume $\rho \subseteq Dis(f_p)$ is a component with some endpoint strictly interior to D_α . Now, recall P_{Out} has a two-dimensional unstable manifold, transverse to the cross-section U_p at P_{Out} - which proves that given any $x \in U_p$ at which the first-return point $f_p(x)$ is defined, we must have $f_p(x) \neq P_{Out}$. A similar argument proves that provided $x \neq P_{In}$, we also have $f_p(x) \neq P_{In}$. Hence, because $D_\alpha \subseteq U_p$ it follows that given $x \in D_\alpha \setminus \{P_{In}, P_{Out}, P_0\}$, $f_p(x) \neq P_{Out}, P_{In}, P_0$. Now, parameterize ρ by $[0, 1]$ - we do so s.t. it has endpoints $\rho(0) \in l$, $\rho(1) \in D_\alpha$. If $\rho(1) \neq P_0$, since $f_p(\rho(1)) \neq P_{In}, P_{Out}$, by the continuity of the flow f_p^{-1} must be defined on a neighborhood of $f_p(\rho(1))$ in l . As this contradicts the maximality of ρ , hence the only possibility is that the trajectory of $\rho(1)$ tends to P_{In} , i.e. $\rho(1) = P_0$ - that is, we have just proven that if ρ is a component of $Dis(f_p)$ with an endpoint $\rho(1)$ strictly interior to D_α , that endpoint must be P_0 .

We now prove $\rho = \delta$, thus concluding the proof of Prop.3.2. By definition, we have $f_p(\rho), f_p(\delta) \subseteq l$. However, l is an arc on ∂D_α whose endpoints are P_{In}, P_{Out} - as such, since $P_0 \in \rho, \delta$ and because P_0 tends to P_{In} in infinite time, $P_{In} \in \overline{f_p(\delta)} \cap \overline{f_p(\rho)}$. Since both $f_p(\delta), f_p(\rho)$ are arcs on l with an endpoint at P_{In} , it follows $f_p(\rho \setminus \{P_0\}) \cap f_p(\delta \setminus \{P_0\}) \neq \emptyset$ - therefore, by the Existence and Uniqueness Theorem $\rho \cap \delta \neq \emptyset$. Since ρ, δ are both components of $Dis(f_p)$, it follows that $\rho = \delta$, and Prop.3.2 follows. See Fig.23 for an illustration. \square

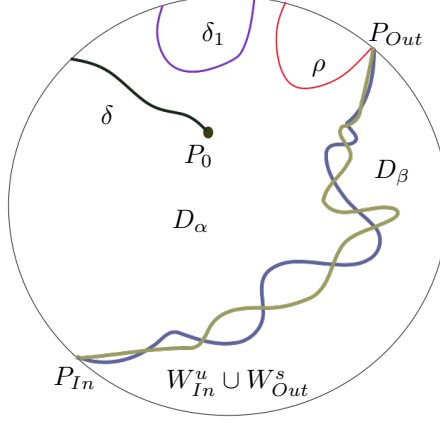


FIGURE 23. The discontinuity curves for f_p in D_α - δ, ρ , and δ_1 , another possible discontinuity curve.

In fact, we can say more. Extending the results of Prop.3.2 we now conclude:

Corollary 3.0.1. *Let $p \in P$ be a trefoil parameter. Then, there exists a component $\rho \subseteq Dis(f_p)$ s.t. $P_{Out} \in \bar{\rho}$ and $\delta \neq \rho$ (see Fig.23 for an illustration).*

Proof. Let us recall the two-dimensional stable manifold for P_{Out} , W_{Out}^s , is transverse to the cross-section U_p at P_{Out} (see Cor.2.1.1). This implies that the **backwards** trajectories of initial conditions on the arc $l = \partial D_\alpha \cap \partial U_p$ sufficiently close to P_{Out} all hit U_p transversely - or, in other words, there exists a curve $\rho \subseteq Dis(f_p)$, $P_{Out} \in \bar{\rho}$, s.t. $f_p(\rho)$ is an arc on l with an endpoint at P_{Out} . Since by Cor.2.3 $l \subseteq \overline{D_\alpha}$, by the forward and backwards invariance of $\overline{D_\alpha}$ under f_p (see Lemma 2.15) we conclude $\rho \subseteq \overline{D_\alpha}$ - and since $P_{Out} \in \bar{\rho}$, from $P_{Out} \notin \delta$ (see Prop.3.2) we immediately have $\rho \neq \delta$ and Cor.3.0.1 now follows (see the illustration in Fig.23). \square

We are now ready to state and prove Th.3.1 - that is, we are now ready to prove that given a trefoil parameter $p \in P$, the first-return map $f_p : \overline{D_\alpha} \rightarrow \overline{D_\alpha}$ is chaotic on some invariant set $Q \subseteq \overline{D_\alpha}$ (in the sense of Def.1.1). To motivate the proof, let us first introduce a heuristic which explains why we expect the dynamics of F_p to be chaotic. To begin, consider a scenario as in Fig.24. That is, given a trefoil parameter $p \in P$ and the corresponding bounded heteroclinic trajectory Θ (see Def.3.2), choose some curve $\gamma \subseteq \overline{D_\alpha}$ s.t. γ connects the fixed point P_{In} and P_0 in $\overline{D_\alpha}$ (with P_0 as in Def.3.2 - see the illustration in Fig.24).

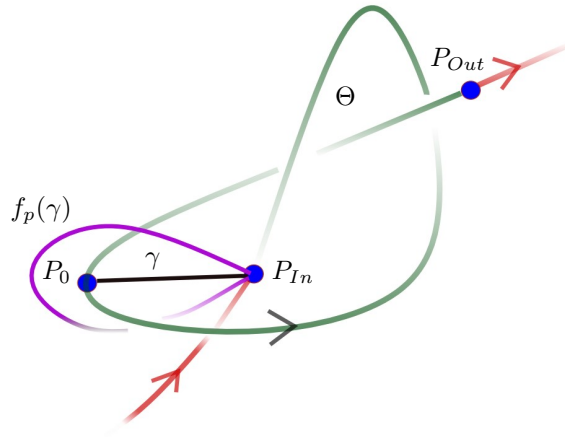


FIGURE 24. Flowing γ along the trefoil. Θ is the green separatrix.

Now, let us suspend the curve γ along Θ , the bounded component of the heteroclinic trefoil knot (see the illustration in Fig.24). By the topology of Θ , we conclude it constrain γ to return to D_α as in Fig.24 - that is, $f_p(\gamma)$ is a closed loop in the topological disc D_α , which begins and terminates at the fixed point P_{In} . Therefore, we can impose $f_p(\gamma)$ on the topological disc D_α roughly as in Fig.25 - which, heuristically, implies the existence of a Smale Horseshoe map for f_p in the cross-section D_α .

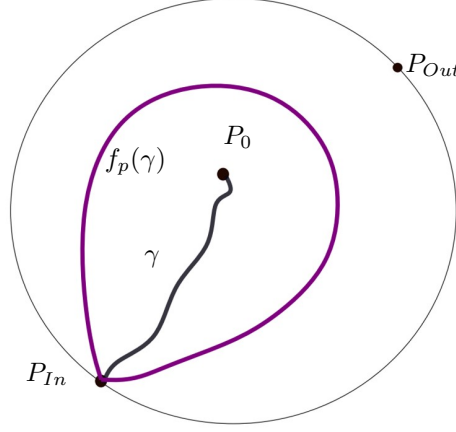


FIGURE 25. imposing $f_p(\gamma)$ on H_p .

In practice, due to Prop.3.2 and Cor.3.0.1 the heuristic described above cannot be justified immediately - that is, the claim $f_p(\gamma)$ is a closed loop is far from immediate, since given an arbitrary curve $\gamma \subseteq \overline{D_\alpha}$ by Prop.3.2 and Cor.3.0.1 there is no reason to assume $f_p(\gamma)$ is even connected. However, as we will now prove, provided we work carefully enough and restrict ourselves to another cross-section $H_p \subseteq D_\alpha$, this heuristic becomes a rigorous proof. Namely, we now prove:

Theorem 3.1. *Let $(a, b, c) = p \in P$ be a trefoil parameter, and let F_p denote the vector field generating the corresponding Rössler system. Now, denote by $\sigma : \{1, 2\}^{\mathbb{N}} \rightarrow \{1, 2\}^{\mathbb{N}}$ the one sided shift - then, there exists a cross-section $H_p \subseteq D_\alpha$ an f_p -invariant $Q \subseteq \overline{H_p}$ s.t. the following holds:*

- $\overline{H_p}$ is a closed topological disc.
- f_p is continuous on Q .
- There exists a continuous $\pi : Q \rightarrow \{1, 2\}^{\mathbb{N}}$ s.t. $\pi \circ f_p = \sigma \circ \pi$.
- Given any $s \in \{1, 2\}^{\mathbb{N}}$ which is **not** the constant $\{1, 1, 1, \dots\}$ nor pre-periodic to it, $s \in \pi(Q)$.
- Let $s \in \{1, 2\}^{\mathbb{N}}$ be periodic of minimal period k . Then, $\pi^{-1}(s)$ contains a periodic point x_s for f_p of minimal period k .

In particular, f_p is chaotic on Q w.r.t. Def.1.1.

Proof. To begin, recall that by Prop.3.2 the discontinuities of f_p in the (open) topological disc D_α are given by $f_p^{-1}(l) \cap D_\alpha$. Now, before sketching the proof of Th.3.1, let us first recall that Prop.3.2 and Cor.3.0.1 together imply that even though f_p is discontinuous at some curves in the cross-section D_α , these discontinuities are mild, in a sense - namely, they occur when the trajectory of some interior point $x \in D_\alpha$ flows to the arc $l \subseteq \partial D_\alpha$. As such, both Prop.3.2 and Cor.3.0.1 motivate us to construct the cross-section H_p and the set Q by analyzing the invariant set of f_p in $\overline{D_\alpha} \setminus l$ - in fact, these two constructions would form the core of the proof of Th.3.1.

Therefore, to achieve these ends we divide the proof of Th.3.1 into three consecutive stages:

- In Stage *I* we construct the cross-section H_p . As remarked above, we do so by studying the discontinuities of f_p in D_α , or more precisely, the topology of the set $f_p^{-1}(l)$. As we will discover, there exists a component H_p of $D_\alpha \setminus f_p^{-1}(l)$ s.t. both fixed points P_{In}, P_{Out} and the curve δ from Prop.3.2 lie in ∂H_p .
- In Stage *II* we analyze the topology of $f_p(H_p)$ and $f_p^{-1}(l)$ inside $\overline{D_\alpha}$. As we will prove, the set $f_p^{-1}(l)$ is in fact a connected curve in $\overline{D_\alpha}$, from which it would follow that for every $n \geq 0$, $f_p^{-n}(\delta_0) \in \overline{H_p}$ (with δ_0 as in Prop.3.2).
- Finally, in Stage *III* we tie these results together and construct the set Q , thus concluding the proof of Th.3.1.

As must be stated, the results in Stages *I* and *II* are strongly dependent on the results and analysis performed in Section 2 - in particular, they are dependent on the analysis of the two cross-sections $\{\dot{x} = 0\}$ and $\{\dot{y} = 0\}$ performed during the proof of Th.2.1 (see Lemmas 2.3, 2.4, 2.5 and Cor.2.1.1).

3.1. **Stage I - constructing the cross-section H_p .** Per the description above, we begin by constructing and defining the cross-section $H_p \subseteq D_\alpha$. To this end, recall the curve σ introduced in Stage I of the proof of Th.2.1 - that is, recall the cross-section $\{\dot{x} = 0\}$ analyzed in Lemmas 2.3 and 2.4, and that the curve $\sigma \subseteq \{\dot{x} = 0\}$ corresponds to the set where the vector field F_p is tangent to $\{\dot{x} = 0\}$. Further recall $\sigma \setminus \{P_{In}, P_{Out}\}$ is composed of four components, $\sigma_1, \sigma_2, \sigma_3$ and σ_4 (see the discussion after the proof of Lemma 2.3 and the illustrations in both Fig.3 and Fig.26). In particular, recall we parameterize σ_3 by $(x, -\frac{x(b+1)}{a+c-x}, \frac{x(b+1)}{a+c-x})$, $x \in (0, c - ab)$. Additionally, recall that given $s \in \mathbf{R}^3$ we denote its trajectory by $\gamma_s(t)$, $\gamma_s(0) = s$ - therefore, using a similar argument to the proof of Lemma 2.4, we conclude:

Lemma 3.1. *Given $s \in \sigma_3$, there exists an $\epsilon > 0$ s.t. $\forall t \neq 0, |t| < \epsilon, \gamma_s(t) \in \{\dot{x} < 0\} \cap \{\ddot{y} > 0\}$ (see the illustration in Fig.27).*

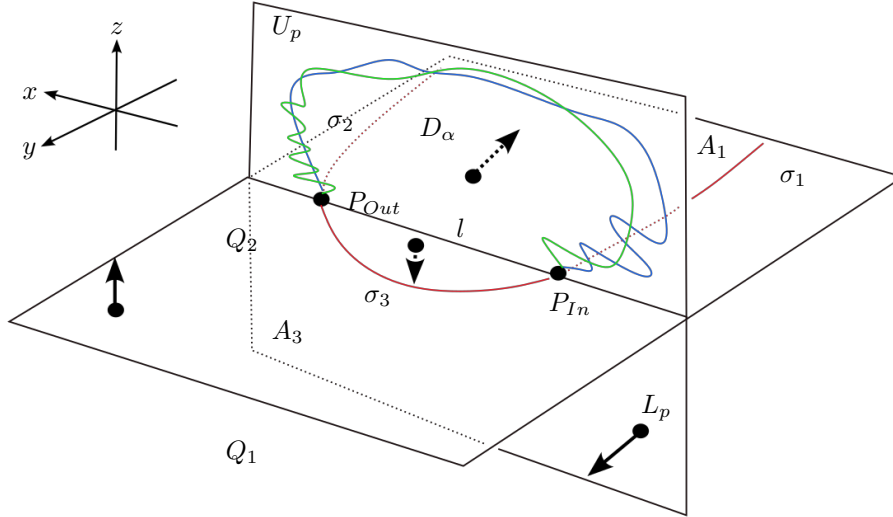


FIGURE 26. The configuration of $\{\dot{y} = 0\}$, $\{\dot{x} = 0\}$ along with the directions of F_p on their respective components.

Now, recall the cross-section U_p (see the discussion before Lemma 2.1), and recall ∂U_p is the curve l_p (see the illustrations in Fig.3 and Fig.5) parameterized by $l_p(x) = (x, -\frac{x}{a}, \frac{x}{a}), x \in \mathbf{R}$ - in particular, recall the arc l corresponds to $\{l_p(x)|x \in (0, c - ab)\}$ (by $P_{In} = l_p(0), P_{Out} = l_p(c - ab)$ we immediately have $P_{In}, P_{Out} \in \bar{l}$). As proven in Lemma 2.5, given $s \in l$, there exists some $\epsilon > 0$ s.t. for $|t| < \epsilon, t \neq 0, \gamma_s(t) \in \{\dot{y} > 0\}$. Now, recall $l_p = \{\dot{x} = 0\} \cap \{\dot{y} = 0\}$ and that $\{\dot{x} > 0\}$ lies **below** the plane $\{\dot{x} = 0\}$ (see Lemma 2.5 and the illustration in Fig.5). Additionally, recall that for $s \in l$ we have $F_p(s)$ points in the negative z -direction (see the proof of Lemma 2.5) - therefore, it follows there exists some maximal $0 < \epsilon_1 \leq \epsilon$ s.t. for $t \in (0, \epsilon_1)$ we have $\gamma_s(t) \in \{\dot{x} > 0\}$ (see the illustration in Fig.26 or Fig.13). Recalling $\{\dot{x} > 0\}$ is the region **below** the plane $\{\dot{x} = 0\}$ (see the illustration in Fig.5 and Fig.26), by this discussion it follows that for $t \in (0, \epsilon_1), \gamma_s(t)$ lies **below** $\{\dot{x} = 0\}$.

To continue, let σ be as above, and recall $\{\dot{x} = 0\} \setminus \sigma$ is composed of three components: A_1, A_2, A_3 s.t. $\sigma_3 \subseteq \partial A_1 \cap \partial A_3$. As shown in the course of proof of Lemma 2.3 and the following discussion in Stage *I* of the proof of Th.2.1, on A_1 the vector field F_p points inside $\{\dot{x} > 0\}$ - that is, F_p points below $\{\dot{x} = 0\}$. Conversely, on A_3 the vector field F_p points inside $\{\dot{x} < 0\}$, i.e. above $\{\dot{x} = 0\}$ (see the illustrations in both Fig.13 and Fig.26). With these ideas in mind, we now prove the following technical Lemma, which, nonetheless, forms an important element in the proof of Th.3.1:

Lemma 3.2. *Let $p \in P$ be a trefoil parameter and let D_α be as in Prop.2.3 - then, there exists a first-hit map $h : \overline{D_\alpha} \rightarrow A_3 \cap \{\dot{y} \geq 0\}$, s.t. the following holds:*

- h is continuous and injective. Moreover, given $s \in \overline{D_\alpha}$, $h(s)$ lies on the interior of the flow-line connecting $s, f_p(s)$.
- $h(l) = l'$ is a Jordan arc in $A_3 \cap \{y > 0\}$ connecting the fixed-points P_{In}, P_{Out} .
- $\overline{D_\alpha}$ is homeomorphic to the topological disc $\overline{T_\alpha} = h(\overline{D_\alpha})$.

Proof. We prove Lemma 3.2 by analyzing the forward-trajectories of initial conditions $s \in \overline{D_\alpha}$ - namely, given $s \in \overline{D_\alpha}$, define $t_1(s) > 0$ as the first positive time s.t. $\gamma_s(t_1(s)) \in \overline{A_3}$ (where defined). As we will now see, Lemma 3.2 will follow provided we prove the function $h : \overline{D_\alpha} \rightarrow \overline{A_3} \cap \{\dot{y} \geq 0\}$ defined by $h(s) = \gamma_s(t_1(s))$ is continuous -

and we will do so by proving that given $s \in \overline{D_\alpha}$, $\gamma_s(t_1(s))$ is a transverse intersection point between γ_s and A_3 , i.e., we will prove $\gamma_s(t_1(s)) \notin \partial A_3$.

Let us begin by proving the assertion above for $s \in l$ - by the proof of Lemma 2.5 we already know that given $s \in l$, $F_p(s)$ points in the negative z -direction. Therefore, by the transverse intersection of $\{\dot{x} = 0\}$ and $\{\dot{y} = 0\}$ and because $\{\dot{x} > 0\}$ is the region **below** $\{\dot{x} = 0\}$ (see the proof of Lemma 2.5 and the illustration in Fig.26) we conclude that given $s \in l$, its forward-trajectory γ_s enters $\{\dot{y} > 0\} \cap \{\dot{x} > 0\}$ immediately upon leaving s - see the illustration in Fig.27). As such, since by definition $\overline{D_\alpha} \subseteq \overline{U_p}$, from $U_p = \{\dot{x} < 0\} \cap \{\dot{y} = 0\}$ it follows that since γ_s , the trajectory of s , must return to $\overline{D_\alpha}$ at $f_p(s)$, γ_s must first exit the open quadrant $Q_1 = \{\dot{x} > 0\} \cap \{\dot{y} > 0\}$ (see the illustration in Fig.26). As shown before the proof of Cor.2.1.1, on $L_p = \{\dot{y} = 0\} \cap \{\dot{x} > 0\}$ the vector field F_p points inside $\{\dot{y} > 0\}$ (see the illustration in Fig.27), hence γ_s can escape Q_1 **only** through hitting $\{\dot{x} = 0\}$ - after which it enters $Q_2 = \{\dot{x} < 0\} \cap \{\dot{y} > 0\}$ (in particular, the sign of \dot{y} along the flow-line connecting $s, f_p(s)$ is non-negative, and vanishes precisely at $s, f_p(s)$ - see the illustration in Fig.26). As discussed after the proof of Lemma 2.3, this can occur **only** at the region $\overline{A_3} \subseteq \{\dot{x} = 0\}$ - which implies that given $s \in l$, $t_1(s)$ is well-defined (see the illustration in Fig.27).

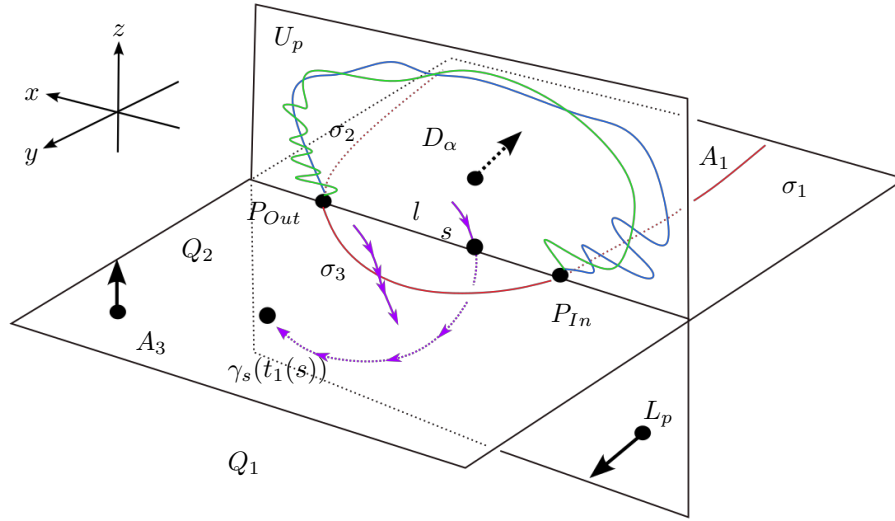
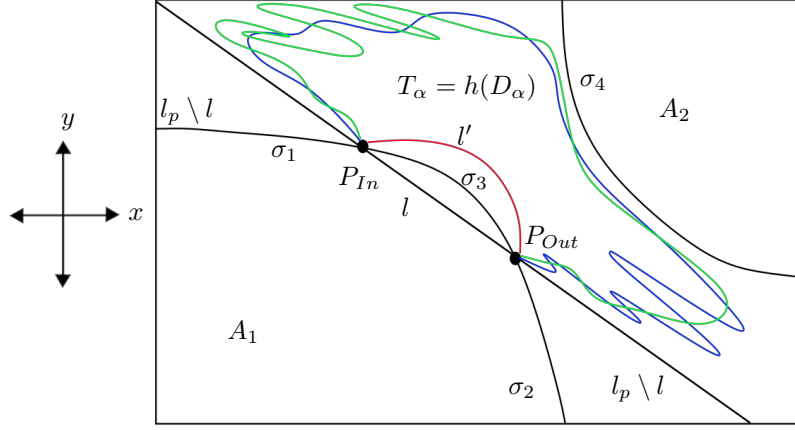


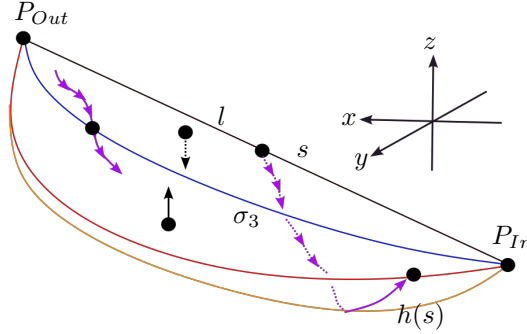
FIGURE 27. The flow line connecting $s, \gamma_s(t_1(s))$ and the local dynamics of F_p on σ_3 .

By this discussion we also conclude $\gamma_s(t_1(s))$ lies strictly in $\overline{A_3} \cap \{\dot{y} \geq 0\}$. Moreover, because γ_s flows from s to $\gamma_s(t_1(s))$ through the quadrant Q_1 , using Lemma 2.5 and Lemma 2.4 a similar argument to the one used in the proof of Prop.2.3 implies $\gamma_s(t_1(s))$ is a **transverse** intersection point between $A_3 \cap \{\dot{y} > 0\}$ and the flow-line γ_s - i.e. $\gamma_s(t_1(s))$ is strictly interior to the region $A_3 \cap \{\dot{y} > 0\}$ (see the illustration in Fig.28). In particular, it follows $l' = \cup_{s \in l} \gamma_s(t_1(s))$ is a curve in $A_3 \cap \{\dot{y} > 0\}$ whose closure connects the fixed-points P_{In}, P_{Out} (see the illustration in Fig.28). Moreover, the collection of flow-lines connecting l, l' form a canoe-shaped surface C which lies wholly inside $\{\dot{x} \geq 0\} \cap \{\dot{y} \geq 0\}$ (see the illustration in Fig.29).

We now use these observations to conclude the proof. To do so, consider an initial condition $s \in \overline{D_\alpha} \setminus l$ which is not a fixed-point - as shown before the proof of Lemma 2.1 and Cor.2.1.1, on U_p the vector field F_p points inside the quadrant Q_2 (see the illustration in Fig.5). Therefore, by $(\overline{D_\alpha} \setminus l) \subseteq U_p$ the same is true for $\overline{D_\alpha} \setminus l$ - which implies $\gamma_s(t), t > 0$ enters $\{\dot{y} < 0\}$ immediately upon leaving $s = \gamma_s(0)$. Since the first-return map $f_p : \overline{D_\alpha} \rightarrow \overline{D_\alpha}$ is well-defined (see Remark 2.2.1) and because flow lines arrive at $\overline{D_\alpha}$ from $\{\dot{y} > 0\}$ (see the discussion in Stage II of the proof of Th.2.1 and Lemma 3.1), the flow-line γ_s connecting $s, f_p(s)$ must escape $\{\dot{y} < 0\}$ **before** reaching $f_p(s)$. Since L_p is the **only** set on which initial conditions escape from $\{\dot{y} < 0\}$ to $\{\dot{y} > 0\}$ (see the illustration in Fig.27), by the discussion preceding Cor.2.1.1 it follows γ_s **must** intersect transversely with the half-plane $L_p = \{\dot{y} = 0\} \cap \{\dot{x} > 0\}$ before hitting $f_p(s)$. Or, put simply, after leaving s the flow-line connecting $s, f_p(s)$ hits L_p transversely before reaching $f_p(s)$. Since $\overline{D_\alpha} \subseteq \{\dot{x} \leq 0\} \cap \{\dot{y} = 0\}$ it follows $f_p(s) \in \{\dot{x} \leq 0\} \cap \{\dot{y} = 0\}$ - therefore, because $L_p \subseteq \{\dot{x} > 0\} \cap \{\dot{y} = 0\}$, and because on L_p the vector field F_p points inside $\{\dot{y} > 0\}$ it follows that γ_s enters Q_1 immediately after hitting L_p .

FIGURE 28. The curves l and l' .

In particular, by the orientation-preserving properties of the flow it follows that after hitting L_p , γ_s now slides **below** the surface C inside $\{\dot{x} > 0\} \cap \{\dot{y} > 0\}$. As such, recalling we originally chose $s \in \overline{D_\alpha} \setminus l$, similar arguments to those used earlier imply both $t_1(s)$ is well defined, and that $\gamma_s(t_1(s))$ is a transverse intersection point between $\gamma_s, A_3 \cap \{\dot{y} > 0\}$. Therefore, all in all, we have proven that given $s \in \overline{D_\alpha}$ which is **not** a fixed point, since $\overline{D_\alpha} = (\overline{D_\alpha} \setminus l) \cup l$, $\gamma_s(t_1(s))$ is always a transverse intersection point between the trajectory γ_s and $A_3 \cap \{\dot{y} > 0\}$. Moreover, by the discussion above we conclude γ_s hits $\gamma_s(t_1(s))$ **before** hitting $f_p(s)$ - which immediately yields $h(s)$ is strictly interior to the flow-line connecting $s, f_p(s)$. As a consequence, the function $h : \overline{D_\alpha} \rightarrow \overline{A_3} \cap \{\dot{y} \geq 0\}$, $h(s) = \gamma_s(t_1(s))$ is continuous. Being a first-hit map, because the sets $\overline{D_\alpha}, \overline{A_3} \cap \{\dot{y} \geq 0\}$ intersect **only** at the fixed points for F_p (i.e., P_{In}, P_{Out}), by the Existence and Uniqueness Theorem h is automatically injective and Lemma 3.2 now follows. \square

FIGURE 29. The body C , and the directions of F_p on it.

Despite its technical nature, Lemma 3.2 has the following geometric meaning - by Lemma 3.2, given any $s \in \overline{D_\alpha}$, its forward trajectory must first hit the disc $\overline{T_\alpha}$ **before** hitting $f_p(s) \in D_\alpha$. Additionally, by Cor.2.2.1, we have $f_p(\overline{D_\alpha}) = \overline{D_\alpha}$ - as such, by $l \subseteq \partial D_\alpha$ we immediately conclude:

Corollary 3.1.1. *Given an initial condition $s \in l$, $f_p^{-1}(s)$ is well defined - and moreover, the **backwards** trajectory of s must hit $\overline{T_\alpha}$ strictly before hitting $f_p^{-1}(s)$.*

Now, given $s \in l$, let $t_2(s) < 0$ denote the maximal time s.t. the backwards trajectory of s , γ_s , satisfies $\gamma_s(t_2(s)) \in \overline{T_\alpha}$. Therefore, by Cor.3.1.1 and Lemma 3.2 we conclude that in order to analyze the topology of $f_p^{-1}(l)$ it would suffice to analyze the topology of the set $\mu = \cup_{s \in l} \gamma_s(t_2(s))$ - since by Lemma 3.2, because $h : \overline{D_\alpha} \rightarrow \overline{T_\alpha}$ is a homeomorphism, $f_p^{-1}(l)$ is simply a homeomorphic copy of μ in $\overline{D_\alpha}$ (i.e. $f_p^{-1}(l) = h^{-1}(\mu)$). We now do just that - namely, using Lemma 3.2, we derive the following fact about the topology of both $\mu, f_p^{-1}(l)$:

Proposition 3.3. *Let $p \in P$ be a trefoil parameter, and let δ be as in Prop.3.2. Then, P_{In}, δ are in the boundary of the **same** component H_p of $D_\alpha \setminus f_p^{-1}(l)$ - and moreover, H_p is a topological disc.*

Proof. We prove Cor.3.3 by contradiction. That is, assume Cor.3.3 is mistaken, i.e., assume the fixed-point P_{In} and the curve δ lie in **different** components of $D_\alpha \setminus f_p^{-1}(l)$, as illustrated in Fig.30. In order to generate a contradiction, we must first study the dynamics of the flow. To this end, recall the sets $T_\alpha = h(D_\alpha)$ from Lemma 3.2 and the set V_α introduced in the proof of Prop.2.3. As proven in Prop.2.3, V_α is a topological disc in the surface

$A_3 \subseteq \{\dot{x} = 0\}$ (see the proof of Prop.2.3), bounded by arcs on $(W_{In}^u \cup W_{Out}^s) \cap A_3$ and the arc σ_3 , parameterized by $\sigma(x) = (x, -\frac{x(b+1)}{a+c-x}, \frac{x(b+1)}{a+c-x})$, $x \in (0, a+c)$ (see the discussion after the proof of Lemma 2.3). In particular, it follows $T_\alpha \subseteq V_\alpha$ - and since during the course of proof of Lemma 3.2 we showed the curve $l' = h(l)$ is disjoint from σ_3 , we conclude $\partial T_\alpha \setminus l' \subseteq \partial V_\alpha$ (see the illustration in Fig.31).

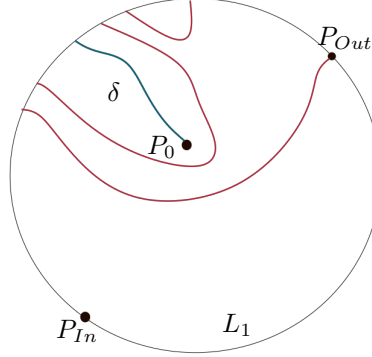


FIGURE 30. The red curves correspond to $f_p^{-1}(l) \setminus \delta$ - and in this scenario they separate P_{In} from δ . We will prove this is impossible. The arc L_1 corresponds to $\partial D_\alpha \setminus l$, i.e., to arcs in $(W_{In}^u \cup W_{Out}^s) \cap U_p$. As such, by Prop.2.3, $f_p^{-1}(l) \cap L_1 = \emptyset$.

Now, set $\Delta = h(\delta)$. Since $p \in P$ is a trefoil parameter and because h is a homeomorphism, it follows Δ is a curve in T_α which connects $P_1 = h(P_0)$, a point on Θ , the bounded heteroclinic connection (see Def.3.2) and $\delta_1 = h(\delta_0)$, a point in l' (see the illustration in Fig.31). In particular, since P_0 is interior to D_α , P_1 is interior to T_α - hence by previous paragraph, because $P_0 \notin (W_{In}^u \cup W_{Out}^s)$ neither is P_1 . Now, denote by $(P_{In}, f_p(\delta_0)]$ the half-closed subarc on l connecting $P_{In}, f_p(\delta_0)$ - by Cor.3.1.1, because $f_p(\delta) = (P_{In}, f_p(\delta_0)] = L$ it follows that every initial condition in Δ connects with some point in $f_p(\delta)$.

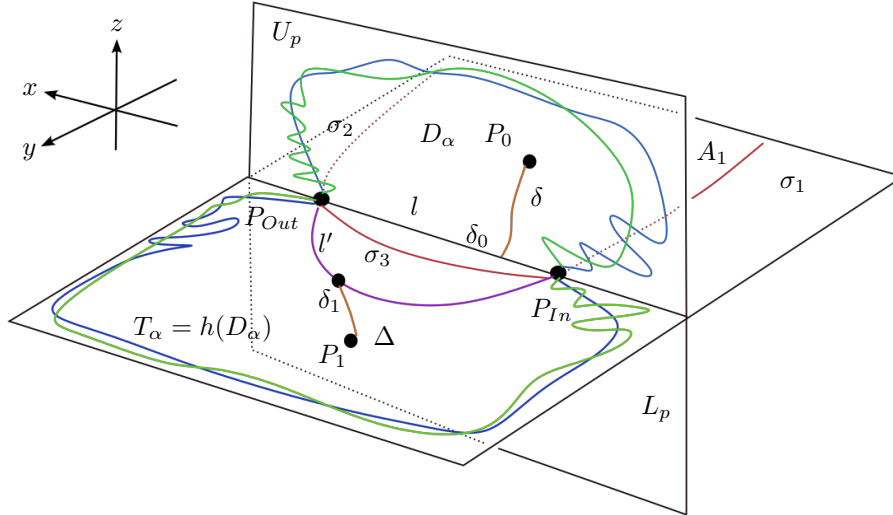


FIGURE 31. The sets $\Delta = h(\delta)$ and the points $\delta_1 = h(\delta_0)$, $P_1 = h(P_0)$.

Now, given $s \in l$ let $t_2(s)$ be as defined before Cor.3.3 - by previous paragraph, we have $\Delta = \cup_{s \in L} \gamma_s(t_2(s))$. Now, recall we assume δ, P_{In} are in different components of $\overline{D_\alpha} \setminus f_p^{-1}(l)$. By Cor.3.1.1 we conclude that setting $\Xi = \cup_{s \in l} \gamma_s(t_2(s))$, Δ and the fixed-points P_{In}, P_{Out} lie in different components of $\overline{T_\alpha} \setminus \Xi$ (by definition, $\Delta \subseteq \Xi$, and by Cor.3.1.1 Ξ is well-defined) - see the illustration in Fig.32 (with the notation of Lemma 3.2, we have $\Xi = h(f_p^{-1}(l))$). Now, recall the curve ρ from Cor.3.0.1 and set $\psi = h(\rho)$ - by Cor.3.0.1 $\rho \neq \delta$ which implies ρ must have two distinct endpoints on l : hence, the same is true for $\psi, l' = h(l)$ (again, we have $\psi \subseteq \Xi$). As must be remarked, similar arguments to those used to prove Lemma 3.2 now imply the flow-lines which connect l to Ξ lie strictly in the quadrant $\{\dot{x} \geq 0\} \cap \{\dot{y} \geq 0\}$ (that is, they all lie **above** the cross-section $\{\dot{x} = 0\}$).

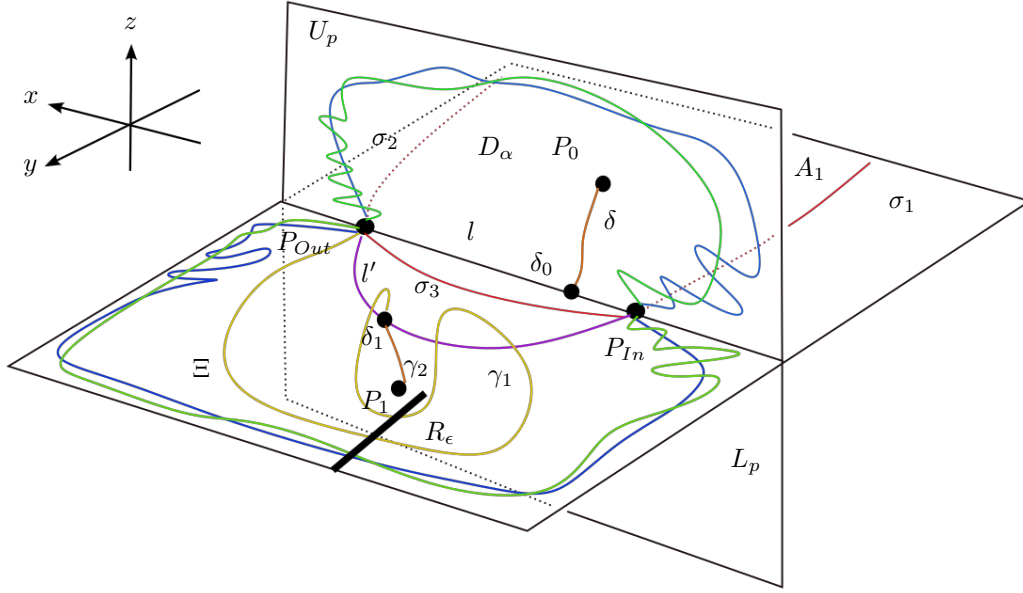


FIGURE 32. The first case - γ_3 is a connected arc in A_3 , with R_ϵ denoting $H_\epsilon \cap A_3$. We will prove this is impossible.

Now, let l_1 be the open arc on l' connecting P_{In}, δ_1 . By Prop.3.2, $\delta_0 \neq P_{In}, P_{Out}$ - hence, by $\delta_1 = h(\delta_0)$, $\psi \neq \delta$ there exists some arc $I \subseteq l$ s.t. $\eta = \cup_{s \in I} \gamma_s(t_2(s))$ includes two curves in \bar{V}_α , γ_1, γ_2 s.t. both connect l_1 with interior points in T_α (see the illustration in Fig.33). In particular, without any loss of generality $\bar{T}_\alpha \setminus \gamma_1$ defines a Jordan domain J , s.t. $\partial J \subseteq \gamma_1 \cup \bar{l}$ - see the illustration in Fig.32. In particular, γ_1 connects **both** components of $l' \setminus \{\delta_1\}$, as illustrated in Fig.32 (let us remark that it is possible $P_{In} \in \bar{l}$ - in which case, we have $\bar{\gamma}_2 = \Delta$). Now, let I_1, I_2 denote the intervals on l s.t. $I_j = \cup_{s \in I_j} \gamma_s(t_2(s))$, $j = 1, 2$. Similarly, let $I_3 \subseteq l$ denote the interval in $l \setminus (I_1 \cup I_2)$ s.t. $I_j \cap I_3 \neq \emptyset$, $j = 1, 2$, and write $\gamma_3 = \cup_{s \in I_3} \gamma_s(t_2(s))$ (see the illustration in Fig.32). Additionally, recall we have $h(P_0) = P_1 = (x_1, y_1, z_1)$ and given $\epsilon \neq 0$ set $H_\epsilon = \{(x, y, z) | x = x_1 - \epsilon, y \geq y_1\}$, and define $V = I_1 \cup I_2 \cup I_3$. There are now two possibilities to consider - namely, either γ_3 is a connected curve in \bar{A}_3 or not. We will show both imply a contradiction, from which Prop.3.3 will follow.

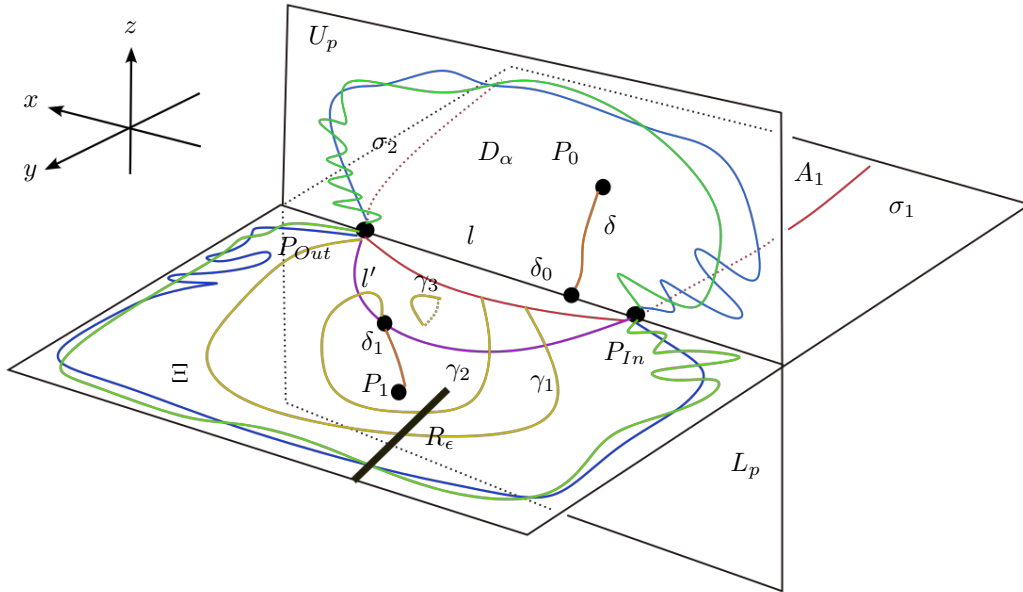


FIGURE 33. The second case - γ_3 is not a connected arc in A_3 (again, R_ϵ denotes $H_\epsilon \cap A_3$). This possibility also cannot occur.

First, assume $\cup_{s \in I_3} \gamma_s(t_2(s))$ is a connected curve in \bar{A}_3 as illustrated in Fig.32, - which implies $\cup_{s \in V} \gamma_s(t_2(s))$ is a curve in \bar{A}_3 . Setting Φ as the surface of flow-lines connecting V , $\cup_{s \in V} \gamma_s(t_2(s))$, it follows A_3 , Φ , and H_ϵ form the

boundary of the three-dimensional body B (provided $|\epsilon|$ is sufficiently small). The vector field F_p is tangent to Φ , and points inside $\{\dot{x} < 0\}$ on A_3 . Because $\Phi \subseteq \Xi$, the flow-lines connecting V, Φ do so through $\{\dot{x} < 0\} \cap \{\dot{y} > 0\}$ we conclude $B \subseteq \{\dot{y} > 0\}$ - and since the normal vector to H_ϵ is $(1, 0, 0)$ we conclude that throughout ∂B , F_p is either tangent or points inside B (see the illustration in Fig.??). Since by definition B is bounded, it implies B contains a bounded-invariant set for F_p - and since $B \subseteq \{\dot{y} > 0\}$, this is a contradiction to Lemma 2.1, hence $\cup_{s \in I_3} \gamma_s(t_2(s))$ cannot be a curve in $\overline{A_3}$.

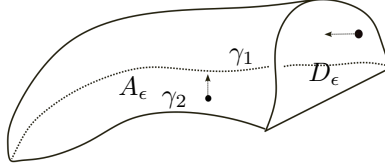


FIGURE 34. The 3-dimensional body B . The vector field F_p points inside it on $A_\epsilon = A_3 \cap \partial B$, $D_\epsilon = H_\epsilon \cap \partial B$ and tangent to ∂B everywhere else.

In the second case, $\cup_{s \in I_3} \gamma_s(t_2(s))$ is not a connected curve in $\overline{A_3}$. Therefore, in order to deal with this case similarly to the previous argument, we need to introduce some notations and definitions. To do so, for $s \in \sigma_3$ define $t_3(s) < 0$ as the maximal time s.t. $\gamma_s(t_3(s)) \in \overline{V_\alpha}$ (by the definition of V_α in Prop.2.3, t_3 is always finite), and set $\Sigma = \cup_{s \in \sigma_3} \gamma_s(t_3(s))$ - again, similar arguments to those used to prove Lemma 3.2 imply the flow-lines which connect σ_3 to Σ lie strictly in the quadrant $\{\dot{x} \geq 0\} \cap \{\dot{y} > 0\}$ (that is, they all lie **above** the cross-section $\{\dot{x} = 0\}$). Now, similarly to the previous paragraph, we conclude there exists a three-dimensional body $B \subseteq \{\dot{y} > 0\}$ trapped between Φ, Σ, A_3 and H_ϵ (again, provided ϵ is sufficiently small - see the illustration in Fig.33). Again, F_p is either tangent or points inside B throughout ∂B hence similarly to the argument in the previous paragraph we again have a contradiction.

All in all, we conclude the assumption δ is separated from P_{In}, P_{Out} by $f_p^{-1}(l)$ yields a contradiction, and it follows P_{In}, P_{Out}, δ are all subsets of ∂H_p . Finally, since no component of $\eta = \cup_{s \in I} \gamma_s(t_2(s))$ is strictly interior to $\overline{T_\alpha}$, every component of $\overline{T_\alpha} \setminus \eta$ is simply connected - therefore, since by Lemma 3.2 $h(H_p)$ is a component of $\overline{T_\alpha} \setminus \eta$ we conclude H_p is a topological disc and Prop.3.3 follows (see the illustration in Fig.39). \square

Remark 3.1. An immediate consequence of Prop.3.3 (and of $f_p(\overline{D_\alpha}) = \overline{D_\alpha}$) is that the function $f_p : \overline{H_p} \setminus \delta \rightarrow \overline{D_\alpha}$ is continuous.

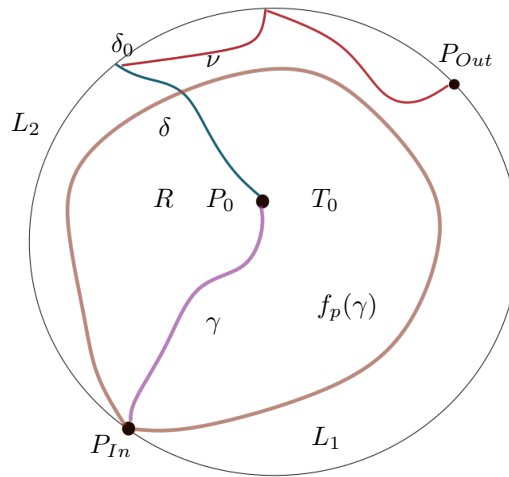


FIGURE 35. The regions R, T_0 and the topological disc H_p , bounded by δ , arcs $\nu \subseteq f_p^{-1}(l)$ and $L_2 = [P_{In}, \delta_0)$. Additionally, γ and $f_p(\gamma)$ are also sketched. Again, the arc L_1 denotes $(W_{In}^u \cup W_{Out}^s) \cap \partial D_\alpha$.

Using Prop.3.3, we conclude Stage I of the proof of Th.3.1 with a justification of the heuristic presented in page 28. To do so, note that by Prop.3.3 we can choose a curve $\gamma \subseteq H_p$ s.t. $\overline{\gamma} \cap \partial H_p = \{P_{In}, P_0\}$ - i.e., γ connects the fixed point P_{In} and the point P_0 , and moreover, by definition $\gamma \cap f_p^{-1}(l) = \emptyset$ - which, by Prop.3.2 proves

f_p is **continuous** on γ . As previously remarked, since P_0 lies on the heteroclinic connection, f_p^{-1} is undefined at P_0 - and in particular, given any $s \in \overline{D_\alpha}$, $f_p(s) \neq P_0$. Additionally, since the trajectory of P_0 tends to the fixed-point P_{In} (in infinite time), we conclude $f_p(\gamma)$ is a closed loop in D_α which begins and terminates at P_{In} - and since $p \in P$ is a trefoil parameter, the discussion immediately before the proof of Th.3.1 implies the curve $f_p(\gamma)$ separates P_0 from $\partial D_\alpha \setminus \{P_{In}\}$, i.e., we can impose $f_p(\gamma)$ on D_α as in Fig.24, Fig.25 and Fig.61. Namely, we have just proven:

Corollary 3.1.2. *Let $p \in P$ be a trefoil parameter and let $H_p \subseteq D_\alpha$ be as in Prop.3.3. Then, there exists a curve $\gamma \subseteq H_p$ satisfying:*

- $\overline{\gamma} \cap \partial H_p = \{P_{In}, P_0\}$.
- $\overline{f_p(\gamma)}$ is a closed loop in D_α , s.t. $\overline{f_p(\gamma)} \cap \partial D_\alpha = \{P_{In}\}$.
- $f_p(\gamma)$ separates P_0 from $\partial D_\alpha \setminus \{P_{In}\}$ (see the illustration in Fig.35).

3.2. Stage II - analyzing the map $f_p : \overline{H_p} \rightarrow \overline{D_\alpha}$. Having proven Cor.3.1.2 we can almost begin proving the existence of chaotic dynamics for the first-return map f_p on some invariant set $Q \subseteq \overline{H_p}$. However, before doing so we must first analyze the behaviour of the function $f_p : \overline{H_p} \rightarrow \overline{D_\alpha}$ - which we will do now. To begin doing so, recall we denote by δ_0 the endpoint of the curve δ in the arc l (see the proof of Prop.3.2). From now on, let us denote by $[P_{In}, \delta_0]$ the component of $\delta \setminus \{\delta_0\}$ (see the illustration in Fig.35). Similarly, we often denote by (P_{In}, δ_0) , $[P_{In}, \delta_0]$ (and so on) the interior and closure of this arc. We first prove:

Lemma 3.3. *Let $p \in P$ be a trefoil parameter. Then, with previous notations, the following holds:*

- f_p is continuous on $[P_{In}, \delta_0]$ - that is, $f_p([P_{In}, \delta_0]) \cap \partial D_\alpha = \{P_{In}\}$.
- $f_p([P_{In}, \delta_0])$ is a loop s.t. for $s \in [P_{In}, \delta_0)$, $s \rightarrow \delta_0$ we have $f_p(s) \rightarrow f_p^2(\delta_0)$ (see the illustration in Fig.61).
- $f_p([P_{In}, \delta_0])$ is a loop, winding once around P_0 - as a consequence, $P_0 \notin \overline{f_p(H_p)}$.

Proof. Let γ denote the curve from Cor.3.1.2. By definition, $\overline{\gamma} \cap [P_{In}, \delta_0] = \{P_{In}\}$, which, due to the injectivity of f_p and because P_{In} is a fixed point yields $f_p(\gamma) \cap f_p([P_{In}, \delta_0]) = \{P_{In}\}$. As shown in the proof of Prop.3.2 f_p is continuous on some neighborhood of the saddle-focus P_{In} in $\overline{D_\alpha}$ - i.e., points on (P_{In}, δ_0) sufficiently close to P_{In} are mapped inside D_α . Now, let us denote by T_0 the component of $D_\alpha \setminus f_p(\gamma)$ s.t. $P_0 \in T_0$ (see the illustration in Fig.35) - by this discussion and by the orientation-preserving properties of the flow, it follows that given $s \in [P_{In}, \delta_0)$, $s \neq P_{In}$ sufficiently close to P_{In} , $f_p(s) \in T_0$. However, since by Cor.3.1.2 we have $f_p(\gamma) \cap f_p([P_{In}, \delta_0]) = \{P_{In}\}$ we conclude $f_p([P_{In}, \delta_0]) \subseteq T_0$ - and since $\overline{T_0} \cap \partial D_\alpha = \{P_{In}\}$, because $P_0 \notin [P_{In}, \delta_0]$ we conclude $\partial T_0 \cap f_p([P_{In}, \delta_0]) = \emptyset$ which implies $f_p([P_{In}, \delta_0])$ is strictly interior to D_α , as illustrated in Fig.61. Or, put simply, f_p is continuous on $[P_{In}, \delta_0]$. Therefore, all that remains to conclude the proof of Lemma 3.3 is to prove that when $x \rightarrow \delta_0$, $x \in [P_{In}, \delta_0)$, $f_p(x) \rightarrow f_p^2(\delta_0)$, and that $P_0 \notin \overline{f_p(H_p)}$.

We first prove that given $x \in [P_{In}, \delta_0)$, when $x \rightarrow \delta_0$, $f_p(x) \rightarrow f_p^2(\delta_0)$. To do so, let us recall that since $\delta_0 \in \delta$, by the definition of δ in Prop.3.2 we have $f_p(\delta_0) \in l$ - and additionally, because $\delta_0 \in l$, by Lemma 2.5 and the definition of D_α as a subset of $\{\dot{y} = 0\}$ it follows the flow-line connecting $\delta_0, f_p(\delta_0)$ lies strictly inside $\{\dot{y} \geq 0\}$, and that \dot{y} vanishes alongside it **precisely** at $\delta_0, f_p(\delta_0)$. Therefore, the y -coordinate for $f_p(\delta_0)$ is strictly greater than that of δ_0 hence $\delta_0 \neq f_p(\delta_0)$ - as such, by $\{\delta_0\} = \delta \cap l$ (see Prop.3.2) it follows $f_p(\delta_0) \notin \delta$.

Now, denote by $[P_{In}, f_p(\delta_0)]$ the closed arc on l connecting $P_{In}, f_p(\delta_0)$ (see the illustration in Fig.61). By Prop.3.2, $(P_{In}, f_p(\delta_0)) = f_p(\delta \setminus \{P_0\})$ - therefore, since by Lemma 2.5 the forwards-trajectory of $f_p(\delta_0)$ enters $\{\dot{y} > 0\}$ immediately upon leaving $f_p(\delta_0)$, similar arguments again prove the y -coordinate of $f_p^2(\delta_0)$ must be strictly greater than that of $f_p(\delta_0)$. Since $f_p(\delta_0) \notin \delta$, we conclude $f_p^2(\delta_0) \notin f_p(\delta \setminus \{P_0\}) = (P_{In}, f_p(\delta_0))$. Recalling we parameterize l by $(x, -\frac{x}{a}, \frac{x}{a})$, $x \in (0, c - ab)$, because the y -coordinate increases along l when $x \rightarrow P_{In}$, $x \in l$, it follows that since $f_p^2(\delta_0)$ **cannot** hit $(P_{In}, f_p(\delta_0))$ it must hit D_α transversely - as such, with previous notations we conclude $f_p^2(\delta_0) \in T_0$. And as consequence, because $f_p^2(\delta_0)$ is the first transverse intersection point between the forward-trajectory of δ_0 and D_α , by the continuity of the flow $f_p^2(\delta_0)$ must be an accumulation point of $f_p([P_{In}, \delta_0])$ - therefore, we conclude that given $x \in [P_{In}, \delta_0)$, $x \rightarrow \delta_0$ we have $f_p(x) \rightarrow f_p^2(\delta_0)$. In particular, $\overline{f_p([P_{In}, \delta_0])}$ includes a closed loop, corresponding to $\overline{f_p([f_p(\delta_0), \delta_0])}$ (see the illustration in Fig.61).

All in all, to conclude the proof of Lemma 3.3 it remains to show $P_0 \notin \overline{f_p(H_p)}$. To do so, consider the region R in $\overline{D_\alpha}$ bounded by δ, γ and $[P_{In}, \delta_0]$. By the previous paragraph and by Cor.3.1.2, the first-return map f_p is continuous on R , hence, by $f_p(\delta) = (P_{In}, f_p(\delta_0))$ and previous paragraphs the boundary of $f_p(R)$ is composed of $f_p([P_{In}, \delta_0] \cap f_p(\gamma))$. As such, by Cor.3.1.2 we conclude the curve $f_p([P_{In}, \delta_0])$ and P_0 lie in the same component of $D_\alpha \setminus f_p(\gamma)$ - and since P_0 has no pre-images under f_p in $\overline{D_\alpha}$ we conclude $P_0 \notin \overline{f_p(R)}$, hence $f_p([P_{In}, \delta_0])$ must

wind around P_0 . Therefore, since $f_p(\overline{H_p} \setminus R)$ and P_0 lie in different components of $\overline{D_\alpha} \setminus f_p(\gamma)$ (see Fig.61) by $\overline{H_p} = R \cup (\overline{H_p} \setminus R)$ we conclude $P_0 \notin \overline{f_p(H_p)}$, and Lemma 3.3 now follows. \square

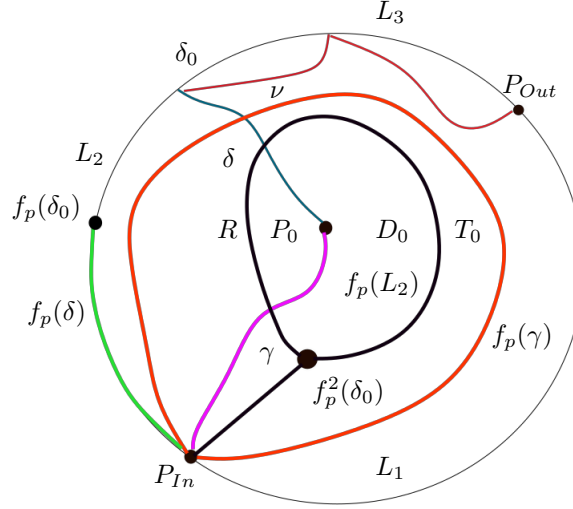


FIGURE 36. The image of $L_2 = [P_{In}, \delta_0]$ under f_p inside the topological disc H_p - in particular, it encloses an open Jordan domain D_0 s.t. $P_0 \in D_0$. Moreover, $f_p(L_2)$ lies inside H_p , the topological disc on D_α bounded by L_1, L_2, δ and ν (with L_1, L_2, ν as in Fig.35). L_3 denotes $[\delta_0, P_{Out}]$, the arc connecting δ_0, P_{Out} on l .

To continue, let us recall that P_0 is the **unique** intersection point of the bounded heteroclinic trajectory with $\overline{D_\alpha}$ (see Def.3.2 and Prop.3.1) - as such, given $x \in \overline{D_\alpha}$ we have $f_p(x) \neq P_0$. To continue, let D_0 denote the component of $\overline{D_\alpha} \setminus f_p([P_{In}, \delta_0])$ s.t. $P_0 \in D_0$ (see the illustration in Fig.61). By Lemma 3.3, D_0 is a Jordan domain and P_0 is strictly interior to it. Using this observation, we now prove:

Corollary 3.1.3. *Let $p \in P$ be a trefoil parameter, and let l be as above. Then, the set $f_p^{-1}(l)$ is connected - in particular, it is a connected curve in $\overline{D_\alpha}$ (see the illustration in Fig.39).*

Proof. Before proving Cor.3.1.3, we first study the behavior of F_p on the set $l \subseteq \partial D_\alpha$. To do so, recall that given $s \in \mathbf{R}^3$, we parameterize its trajectory by $\gamma_s, \gamma_s(0) = s$. Additionally, recall we denote by (P_{In}, δ_0) the component of $l \setminus \{\delta_0\}$ connecting P_{In}, δ_0 . Now, for every $s \in l$, define $t_4(s) > 0$ to be the minimal positive time s.t. $\gamma_s(t_4(s))$ is a **transverse** intersection point between $\gamma_s, \overline{D_\alpha}$ (by Lemma 2.1 and Cor.2.2.1, $t_4(s)$ is well-defined for every $s \in l$). Using a similar reasoning to the one used in the proof of Lemma 3.2, given an initial condition $s \in l$ by Lemma 2.5 we conclude its forward-trajectory leaves s and flows through the half-space $\{\dot{y} \geq 0\}$ until hitting D_α at some interior point $\gamma_s(t_4(s))$. As must be stated, $\gamma_s(t_4(s))$ need not coincide with $f_p(s)$, as the flow-line γ_s can hit $\overline{D_\alpha}$ tangently more than once **before** hitting $\overline{D_\alpha}$ transversely at $\gamma_s(t_4(s))$. For example, as shown in the proof of Lemma 3.3, on the one hand $f_p(\delta_0) \in l$, while on the other $f_p^2(\delta_0)$ is strictly interior to $\overline{D_\alpha}$ (see the illustration in Fig.61). Therefore, we conclude, $\gamma_{\delta_0}(t_4(\delta_0)) = f_p^2(\delta_0) \neq f_p(\delta_0)$.

Let us now consider the set $\Psi = \cup_{s \in l} \gamma_s(t_4(s))$. The set Ψ is composed of curves in $\overline{D_\alpha}$ whose **closures** connect interior points of D_α to l (by definition, $\Psi \cap l = \emptyset$). As must be stated, any given component ψ of Ψ , ψ is a curve which is possibly self-intersecting - however, all such self-intersections of ψ are points at which the curve ψ is tangent to itself (see the illustration in Fig.37). Additionally, for every component ψ in Ψ there exists some connected sub-arc $I \subseteq l$ s.t. $\forall s \in I, \gamma_s$ connects $s, \gamma_s(t_4(s))$ through $\{\dot{y} \geq 0\}$. Conversely, given $\nu \in \psi$, there exists **at least** one $s \in I$ s.t. γ_s connects s, ν through $\{\dot{y} \geq 0\}$. In particular, by the Existence and Uniqueness Theorem it follows that points at which ψ is tangent to itself corresponds to points $s \in I$ at which $\gamma_s(t_4(s)) \neq f_p(s)$, i.e., $\gamma_s(t_4(s)) = f_p^k(s)$ for some $k > 1$, and moreover, for every $0 < j < k$, $f_p^j(s) \in l$ (that is, γ_s is tangent to $\overline{D_\alpha}$ at $f_p^j(s)$). Hence, it is immediate that t_4 is continuous on the interval I corresponding to ψ .

Now, recall $p \in P$ is a trefoil parameter, and that P_0 lies on the bounded heteroclinic connection Θ (see Def.3.2) - therefore, a similar argument to the one used to prove Prop.3.2 implies there exists a component ψ of Ψ , which is a curve beginning at P_0 , s.t. for every $s \in l$ sufficiently close to P_{Out} , $\gamma_s(t_4(s)) \in \psi$ (see the illustration in Fig.37). In particular, $\overline{\psi}$ is a curve which connects P_0 and some unique point P_1 on l . We now claim $P_1 = P_{In}$ - to see why this is so, recall that as mentioned earlier, with previous notations $D_\alpha \setminus f_p(P_{In}, \delta_0)$ includes a Jordan domain D_0

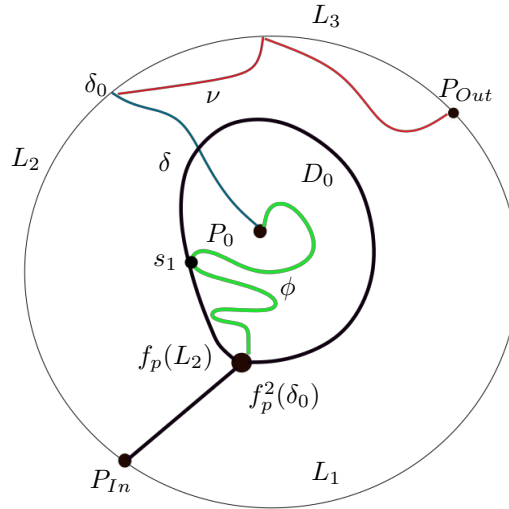


FIGURE 37. In this image, the set Ψ is the union $\phi \cup f_p(L_2)$, with $L_2 = [P_{In}, \delta_0)$. As can be seen, ϕ is tangent to $f_p(L_2)$ at both $s_1, f_p^2(\delta_0)$. L_3 denotes $[\delta_0, P_{Out}]$, the arc connecting δ_0, P_{Out} on l , while $\nu = f_p^{-1}(l) \setminus \delta$.

s.t. P_0 is interior to D_0 (see the illustration in Fig.61). By Lemma 3.3 we therefore conclude ∂D_0 separates P_0 and l .

By Lemma 3.3 it now follows that given $s \in (P_{In}, \delta_0)$, $f_p(s)$ is strictly interior to D_α , which implies $f_p(s)$ is a transverse point of intersection between γ_s and the cross-section $\overline{D_\alpha}$. As such, given $s \in (P_{In}, \delta_0)$ it follows $f_p(s) = \gamma_s(t_4(s))$ - and as remarked earlier, $f_p^2(\delta_0) = \gamma_{\delta_0}(t_4(\delta_0))$. Therefore, since ψ connects P_0 and l , because ∂D_0 separates P_0 and l and since $\partial D_0 \subseteq f_p(P_{In}, \delta_0) = \cup_{s \in (P_{In}, \delta_0)} \gamma_s(t_4(s))$, it follows $f_p(P_{In}, \delta_0) \subseteq \psi$. By the uniqueness of P_1 , it therefore follows $P_1 = P_{In}$. Now, recall that by the discussion above it follows there exists a maximal arc $I \subseteq l$ s.t. every $s \in I$ has a forward-trajectory γ_s connecting $s, \gamma_s(t_4(s))$. Since both $P_0, P_{In} \in \overline{\psi}$, it follows $I = l$, and that t_4 is continuous on l - in particular, $\Psi = \psi$.

Now, recall that per Lemma 3.3, the topological disc H_p is the component of $\overline{D_\alpha} \setminus f_p^{-1}(l)$ s.t. P_{In}, P_{Out} and δ are all subsets of ∂H_p (see Prop.3.3 and the illustration in Fig.35). Additionally, with the notations of Prop.3.3 recall we denote by R the subdomain of H_p bounded by $\delta, [P_{In}, \delta_0)$ and the curve γ (see the illustration in Fig.35). Finally, recalling we denote by T_0 the component of $\overline{D_\alpha} \setminus f_p(\gamma)$ s.t. $P_0 \in T_0$ (see the proof of Lemma 3.3 and the illustrations in Fig.35 and Fig.61), by $f_p(P_{In}, \delta_0) \subseteq T_0$ (see the proof of Lemma 3.3 and Fig.35) it follows $\psi \subseteq T_0$ (see the illustration in Fig.38).

Having made these remarks, we are now ready to conclude the proof of Cor.3.1.3. Namely, we now use the facts above to prove $f_p^{-1}(l)$ is connected in $\overline{D_\alpha}$ - to do so, assume this is not the case, i.e., that $f_p^{-1}(l)$ includes at least two components (one of which has to include the curve δ_0). Since l is a curve, every component of $f_p^{-1}(l)$ in $\overline{D_\alpha}$ is also a curve (which is possibly a singleton) - by Prop.3.2 and the continuity of the flow, if γ is a component of $f_p^{-1}(l)$ which **does not** include the curve δ , the curve γ does not have an endpoint strictly interior to D_α . Additionally, since we assume $f_p^{-1}(l)$ is disconnected in $\overline{D_\alpha}$, $f_p^{-1}(l)$ **cannot** separate the arc $l_1 = l \setminus [P_{I_n}, \delta_0]$ from the interior of H_p - i.e. there exists a point $s \in l_1 \cap \partial H_p$ (see the illustration in Fig.38).

Now, recall we denote by R the region in H_p bounded by $[P_{In}, \delta_0]$, δ , and the curve γ from Cor.3.1.2. Since $s \in l_1 \cap \partial H_p$, by $\overline{R} \cap l = [P_{In}, \delta_0]$ we conclude $\overline{R} \cap l_1 = \emptyset$, hence $s \notin \overline{R}$ - hence, by the arguments found at the end of the proof Lemma 3.3 it follows $\overline{f_p(R)}$, $f_p(s)$ lie in different components of $D_\alpha \setminus f_p(\gamma)$ (see the illustration in Fig.38). However, by the discussion above we must have $s \in \psi$, and as proven earlier, $\psi \subseteq \overline{T_0}$ - i.e., ψ lies at the closure of precisely one component of $D_\alpha \setminus f_p(\gamma)$. This is a contradiction, hence $f_p^{-1}(l)$ is connected. Therefore, since l is a curve so is $f_p^{-1}(l)$ and Cor.3.1.3 now follows - see the illustration in Fig.39. \square

We now use both Cor.3.1.3 and ideas from the proof of Prop.3.3 to prove the following technical (yet useful) fact. To do so, recall we denote by $[\delta_0, P_{Out}]$ the closed arc on l connecting P_{Out}, δ_0 - conversely, further recall we denote by $[P_{In}, \delta_0]$ the semi-open arc on l connecting P_{In}, δ_0 (see the illustration in Fig.61). We now prove the following list of properties of $f_p^{-n}(l)$, $n \geq 2$, which generalize Cor.3.1.3 and Prop.3.3. As we will see in Stage III, Prop.3.4 (and its corollaries) would form a major tool in proving the existence of symbolic dynamics for the first-return map in H_n .

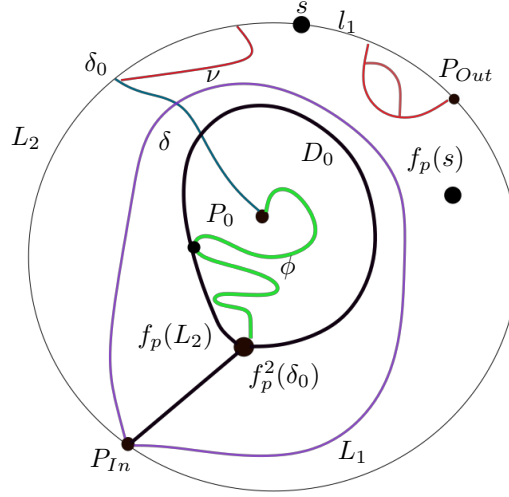


FIGURE 38. The red arcs correspond to $\nu = f_p^{-1}(l) \setminus \delta$ - as can be seen, ν is disconnected, thus there exists an arc $l_1 \subseteq l \cap \partial H_p$. Moreover, $\Psi = \phi \cup f_p(L_2) \subseteq T_0$, with T_0 denoting the area trapped inside the purple loop. In particular, there exists a point $s \in l_1$ s.t. $f_p(s) \notin \overline{T_0}$ - which generates a contradiction.

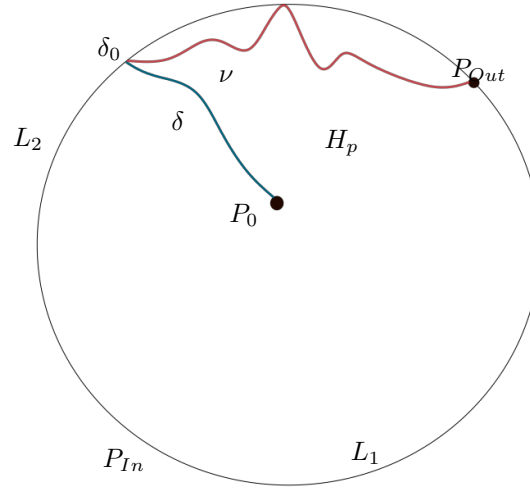


FIGURE 39. The cross-section H_p , homeomorphic to a slit disc, bounded by $L_2 = [P_{In}, \delta_0]$, $f_p^{-1}(l) = \delta \cup \nu$ and $L_1 \subseteq (W_{In}^u \cup W_{Out}^s) \cap \{\dot{y} = 0\}$. By Prop.3.3, $f_p^{-1}(l)$ is a curve connecting P_{Out}, δ_0 .

Proposition 3.4. *Let $p \in P$ be a trefoil parameter and let H_p be as in Prop.3.3. Furthermore, denote by $\Delta_0 = f_p^{-1}(l)$ - then, the following holds:*

- For $n \geq 2$, $f_p^{-n}(l) \cap \overline{H_p}$ includes a component $\Delta_{n-1} \subseteq \overline{H_p}$ s.t. Δ_{n-1} is a curve connecting $P_{Out}, f_p^{-n+1}(\delta_0)$ and some $\delta_{n-1} \in [P_{In}, \delta_0]$.
- For every $n > 0$, Δ_n includes a curve $\Gamma_n \subseteq \Delta_n$ s.t. $f_p^{n+1}(\Gamma_n) = [\delta_0, P_{Out}]$.
- For $n \geq 1$, $\Delta_n \cap \delta = \emptyset$.
- With the same notations, for every $n, k \geq 0$, $\Gamma_n \subseteq f_p^k(\overline{H_p})$ - and in particular, $f_p^{-n}(\delta_0) \in f_p^k(\overline{H_p})$.
- For every $n \geq 1$, $f_p^{-n+1}(\delta_0) \in \Delta_n \cap \Delta_{n-1}$.
- Write $\mu_n = \Delta_n \cap f_p^{-n}(\delta)$ - then, given $n \neq k$, we have $\mu_n \cap \mu_k = \emptyset$.

Proof. Before proving Cor.3.4, let us first make some general remarks. To begin, note that since the saddle-focus P_{Out} is a fixed-point, for every $n > 0$ we have $f_p^{-n}(P_{Out}) = P_{Out}$. Additionally, recalling P_{Out} is a saddle-focus with two-dimensional stable manifold W_{Out}^s transverse to the cross-section $U_p = \{\dot{y} = 0\} \cap \{\dot{x} = 0\}$ at P_{Out} , by the definition of $D_\alpha \subseteq U_p$ in Section 2.2 we conclude that a similar argument to the proof of Cor.3.0.1 implies that for every $n > 0$, $f_p^{-n-1}([\delta_0, P_{Out}]) \cap \overline{D_\alpha}$ includes a component Δ_n s.t. $P_{Out} \in \Delta_n$ (see the illustration in Fig.40). Moreover, by the definition of H_p in Cor.3.3 it follows that for every n , at least locally around P_{Out} the curve Δ_n

lies in $\overline{H_p}$. With these remarks, we can now begin proving Cor.3.4 - and we do so by induction on n . Namely, we first prove that given $n \geq 1$ the curve Δ_n satisfies $\Delta_n \subseteq f_p^{-n-1}(l) \cap \overline{H_p}$, $P_{Out} \in \Delta_n$ s.t.:

- For $n \geq 1$, $\Delta_n \cap \delta = \emptyset$.
- Δ_n is a curve in $\overline{H_p}$ connecting $P_{Out}, f_p^{-n+1}(\delta_0)$.
- For every $n > 0$, Δ_n includes a curve $\Gamma_n \subseteq \Delta_n$ s.t. $f_p^{n+1}(\Gamma_n) = [\delta_0, P_{Out}]$.
- Δ_n connects P_{Out} with some $\delta_n \in [P_{In}, \delta_0)$.

As we will see, these four facts will imply the entire list of properties in Prop.3.4. For the base of the induction, consider for $n = 1$ - namely, we will now prove that the curve $\Delta_1 \subseteq f_p^{-2}(l) \cap \overline{H_p}$ connects $P_{Out}, f_p^{-1}(\delta_0)$ and some $\delta_1 \in [P_{In}, \delta_0)$, that it contains a curve Γ_1 s.t. $f_p^2(\Gamma_1) = [\delta_0, P_{Out}]$, and satisfies $\Delta_1 \cap \delta = \emptyset$. To do so, let us first remark that by its definition in Prop.3.2, we have $\delta_0 \in l \cap f_p^{-1}(l)$ from which it follows $f_p^{-1}(\delta_0) \in f_p^{-1}(l) \cap f_p^{-2}(l)$. With previous notations, since by Prop.3.2 we have $f_p(\delta) \subseteq [P_{In}, \delta_0)$, by Cor.3.3 it follows $f_p^2(\delta)$ is interior to D_α - i.e., $f_p^2(\delta) \cap l = \emptyset$. Hence, $\delta \cap f_p^{-2}(l) = \emptyset$ - which, by $\Delta_1 \subseteq f_p^{-2}(l)$, implies both $f_p^{-1}(\delta_0) \notin \delta$ and $\delta \cap \Delta_1 = \emptyset$.

For the first-two properties of Δ_1 we need to work a little harder. To do so, first, recall the homeomorphism $h : \overline{D_\alpha} \rightarrow \overline{T_\alpha} \subseteq A_3$ from Lemma 3.2, and define $\nu_1 = h(\Delta_1)$ - by the definitions for both h and ρ_1 it follows there exists a connected sub-arc on $f_p^{-1}(l)$, I_1 , s.t. $P_{Out} \in I_1$ and the **backwards** trajectory of every $s \in I_1$ connects with some $x \in \Delta_1$ (see the illustration in Fig.40) - and moreover, the flow-line connecting s, x lies strictly inside the quadrant $Q_2 = \{\dot{x} < 0\} \cap \{\dot{y} > 0\}$, that is, above the cross-section $\{\dot{x} = 0\}$ (see the illustration in Fig.27). Writing $L = h(f_p^{-1}(l))$, a similar argument proves that given any initial condition $s \in l$, its backwards trajectory is connected to some $x \in L$ by its backwards trajectory - and again, the flow-line connecting s, x lies inside Q_2 (see the illustration in Fig.40). As such, the collection of flow-lines connecting l, L form a surface S , which stretches from l to L through Q_2 - and conversely, the flow-lines connecting I_1 to ν_1 also form a surface, β_1 . By Prop.3.4 $f_p^{-1}(l)$ is a connected arc in $\overline{D_\alpha}$, which is (at most) tangent to l at $f_p^{-1}(l) \cap l$ - therefore, it follows the surface β_1 **cannot** intersect S transversely.

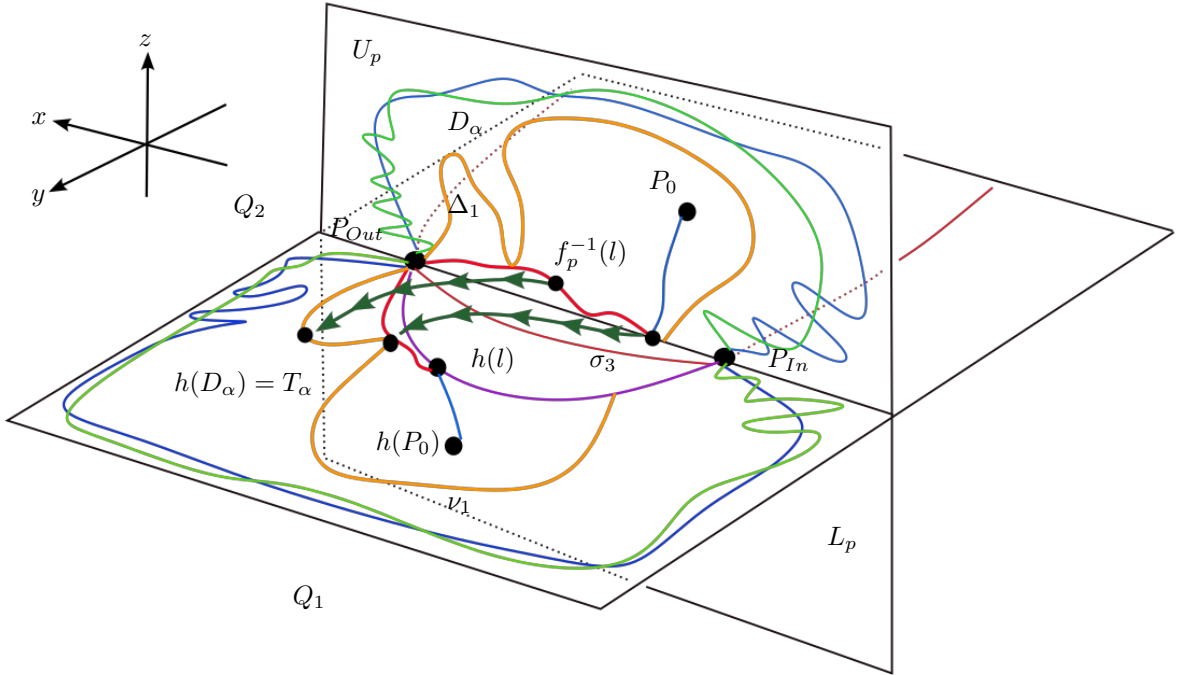


FIGURE 40. The backward trajectories connecting points in l with points in $h(f_p^{-1}(l))$ and points from $f_p^{-1}(l)$ with $h(\Delta_1) = \nu_1$. Both flow lines lie strictly in the quadrant $Q_2 = \{\dot{x} < 0\} \cap \{\dot{y} > 0\}$.

As a consequence, because $\Delta_1 = h^{-1}(\nu_1)$, we conclude Δ_1 never intersects $f_p^{-1}(l)$ transversely as well. Since ∂H_p is composed of $f_p^{-1}(l)$, the arc $L_1 \subseteq (W_{In}^u \cup W_{Out}^s) \cap H_p$ and the arc $[P_{In}, \delta_0)$ (see Cor.4.0.1), we conclude $\Delta_1 \subseteq \overline{H_p}$ (see the illustration in Fig.40). We now claim Δ_1 is a curve connecting $P_{Out}, f_p^{-1}(\delta_0)$ in $\overline{H_p}$ (thus almost completing the base of the induction) - and we will prove so by contradiction. To this end, assume this is not the case, i.e., assume that the curve Δ_1 **does not** connect $P_{Out}, f_p^{-1}(\delta_0)$ in $\overline{H_p}$ - as such, ν_1 **does not** connect $P_{Out}, h(f_p^{-1}(\delta_0))$ in $h(\overline{H_p})$. Now, recall the curve δ from Prop.3.2 - with previous notations, $h(\delta) \subseteq S$, therefore, by

$\Delta_1 \cap \delta = \emptyset$ we have $h(\delta) \cap \nu_1 = \emptyset$. Since $f_p^{-1}(l)$ separates the arc $[\delta_0, P_{Out}]$ from Δ_1 (and since $\Delta_1, f_p^{-1}(l)$ are **at most** tangent) it follows the curve ν_1 connects P_{Out} with $l' = h(l)$ through $h(\overline{H_p})$, and it does so without **ever** touching $h(f_p^{-1}(\delta_0))$ (see the illustration in Fig.41).

To continue, since $f_p^{-1}(\delta_0) \in f_p^{-1}(l) \cap f_p^{-2}(l)$, because we assume $f_p^{-1}(\delta_0) \notin \Delta_1$ a similar argument to the one above proves there exists an arc $\rho_2 \subseteq f_p^{-2}(l)$ connecting $f_p^{-1}(\delta_0), l$ s.t. $\rho_2 \subseteq f_p^{-2}(l)$ - by $\delta \cap f_p^{-2}(l) = \emptyset$ we have $\rho_2 \cap \delta = \emptyset$. Now, setting $\nu_2 = h(\rho_2)$, a similar argument to the one used in the proof of Prop.3.3 (with ν_1, ν_2 taking the respective places of γ_1, γ_2) implies a contradiction. Therefore, it follows Δ_1 is a curve in $\overline{H_p} \cap f_p^{-2}(l)$ connecting $P_{Out}, f_p^{-1}(\delta_0)$. Additionally, by $\Delta_1 \subseteq f_p^{-2}(l)$ and previous discussion it also follows $\Delta_1 \cap \delta = \emptyset$ - hence, with previous notations, $\mu_1 \cap \mu_0 = \emptyset$. Moreover, since Δ_1 connects $f_p^{-1}(\delta_0), P_{Out}$ it follows $[\delta_0, P_{Out}] \subseteq f_p^2(\Delta_1)$. Therefore, all in all we see that to conclude the proof of the base of the induction it remains to prove Δ_1 connects $\delta_1 \in [P_{In}, \delta_0)$.

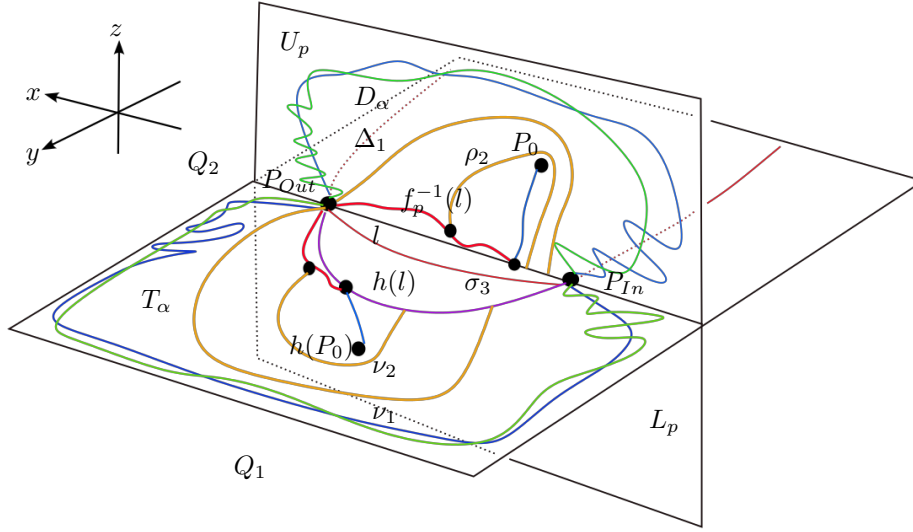


FIGURE 41. The curves Δ_1, ρ_2 and ν_1, ν_2 . The existence of ν_2 generates a contradiction.

To do so, assume this is not the case - i.e., assume Δ_1 **does not** connect $f_p^{-1}(\delta_0)$ with $[P_{In}, \delta_0)$. Recall we denote by $\nu_1 = h(\Delta_1)$ - similarly to the previous arguments, it follows there exists an arc $J_1 \subseteq f_p^{-1}(l)$ s.t. the flow-lines connecting J_1 to ν_1 through the quadrant Q_2 glide above the surface S . Again, recall that since $\Delta_1, f_p^{-1}(l)$ cannot intersect transversely, the curve ν_1 cannot intersect transversely with $h(f_p^{-1}(l))$ as well, and that by $\Delta_1 \cap \delta = \emptyset$, we have $\nu_1 \cap h(\delta) = \emptyset$. Therefore, since $f_p^{-1}(l)$ separates $[\delta_0, P_{Out}]$ from Δ_1 (see Fig.40) it follows the curve Δ_1 **cannot** terminate at any point $[\delta_0, P_{Out}]$ - as that would necessitate a transverse intersection between $\nu_1, h(f_p^{-1}(l))$ (see the illustration in Fig.40). Now, recall $p \in P$ is a trefoil parameter (see Def.3.2). Therefore, since the point P_0 is the **unique** intersection point of the bounded heteroclinic trajectory Θ with $\overline{D_\alpha}$ (see Cor.3.1), the **backwards**-trajectories of initial conditions on δ flow along Θ back towards P_{Out} .

Let us further recall ∂D_α is the union of L_1, l and $\{P_{In}, P_{Out}\}$, s.t. L_1 is a collection of arcs on $(W_{Out}^s \cup W_{In}^u) \cap \overline{D_\alpha}$ satisfying $f_p(L_1) = L_1$. Additionally, since P_{In}, P_{Out} are saddle-foci of opposing indices whose 2-dimensional manifolds are transverse to $\{y = 0\}$ (see Lemma 2.3 and Cor.2.1.1) - therefore, it follows that given $x \in \overline{D_\alpha}$ s.t. $x \notin \{P_{In}, P_{Out}, P_0\}$, we also have $f_p^{-1}(x) \notin \{P_{In}, P_{Out}, P_0\}$. As such, if Δ_1 does not hit $[P_{In}, \delta_0)$, by previous paragraph it follows Δ_1 never intersects $\partial D_\alpha \setminus (l \cup L_1)$. Therefore, if Δ_1 never hits l there **must** exist a Jordan curve $\alpha_1 \subseteq \Delta_1$ which encloses a domain R_1 s.t. $P_{Out} \in \alpha_1$ (see the illustration in Fig.42). Therefore, there exists some $y_0 \in \mathbf{R}$ s.t. $R_1 \setminus H_{y_0}, H_{y_0} = \{(x, y_0, z) | x, z \in \mathbf{R}\}$ consists of at least two components (see Fig.42). Again, similarly to the proof of Prop.3.3, since the normal vector to H_{y_0} is $(0, 1, 0)$, there exists a three-dimensional body B trapped between A_3, H_{y_0} and the flow-lines connecting $\nu_1, f_p^{-1}(l)$ - it follows F_p is either tangent to ∂B or points inside B . Similarly to the proof of Prop.3.3, this implies a contradiction - therefore Δ_1 must connect $f_p^{-1}(\delta_0)$ with some $\delta_1 \in [P_{In}, \delta_0)$ and the base of the induction now follows (see the illustrations in Fig.40 and Fig.43). For simplicity, we set δ_1 as the **first** point of intersection of Δ_1 with $[P_{In}, \delta_0)$ after it leaves $f_p^{-1}(\delta_0)$.

For the step of the induction, assume that for all $0 < k \leq n, n \geq 1$ Δ_k is a curve in $f_p^{-k-1}(l) \cap \overline{H_p}$ s.t. the following is satisfied:

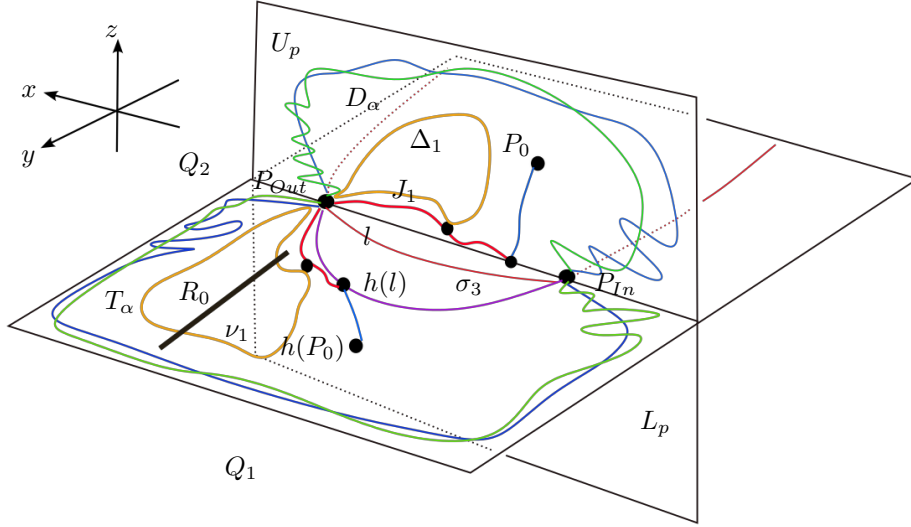


FIGURE 42. The Jordan curve ν_1 and $R_0 = H_{y_0} \cap T_\alpha$. This situation generates a contradiction.

- Δ_k connects $f_p^{-k}(\delta_0), P_{Out}$ and some $\delta_k \in [P_{In}, \delta_0]$. Analogously δ_k would be defined as the first point of intersection as described above.
- $\Delta_k \cap \delta = \emptyset$.
- Δ_k includes a sub-arc Γ_k s.t. $f_p^{k+1}(\Gamma_k) = [\delta_0, P_{Out}]$.

We will now prove the same is true for Δ_{n+1} as well. To do so, note that similarly to the proof in the base of the induction, the backward-trajectories connecting $\Delta_{n-1} \subseteq \overline{D_\alpha}$ to $h(\Delta_n) \subseteq \overline{T_\alpha}$ generate a surface S_n (recall that when $n = 1$, we take $\Delta_0 = f_p^{-1}(l)$). As such, there exists an arc $I_1 \subseteq \Delta_n$ whose backwards trajectories all glide over S_n and hit $\nu_{n+1} = h(\Delta_{n+1})$. Again, similarly to the previous arguments, the collection of flow lines connecting ν_{n+1}, Δ_n , denoted by β_n , **cannot** intersect S_n transversely - hence again it follows $\nu_{n+1} \subseteq h(\overline{H_p})$, i.e., $\Delta_{n+1} \subseteq \overline{H_p}$. Again, a similar argument to the one used in the base of the induction proves Δ_{n+1} must connect $P_{Out}, f_p^{-n}(\delta_0)$. Additionally, since Δ_{n-1} connects P_{Out} and δ_n , because S_n, β_n cannot intersect transversely it follows S_n is a surface which separates β_n from $h(\delta)$ in $\overline{T_\alpha}$ - therefore, $h(\delta) \cap \nu_{n+1} = \emptyset$ which implies $\delta \cap \Delta_{n+1} = \emptyset$. Similarly to the argument in the base of the induction, again we conclude Δ_{n+1} must connect P_{Out} and some $\delta_{n+1} \in [P_{In}, \delta_0]$, the **first** point of intersection between Δ_{n+1} and $[P_{In}, \delta_0]$ (see the illustration in Fig.42). Finally, because Δ_{n+1} connects $P_{Out}, f_p^{-n-1}(\delta_0)$ again, by the definition of Δ_{n+1} , it follows there exists some $\Gamma_{n+1} \subseteq \Delta_{n+1}$ s.t. $f_p^{n+2}(\Gamma_{n+1}) = [\delta_0, P_{Out}]$.

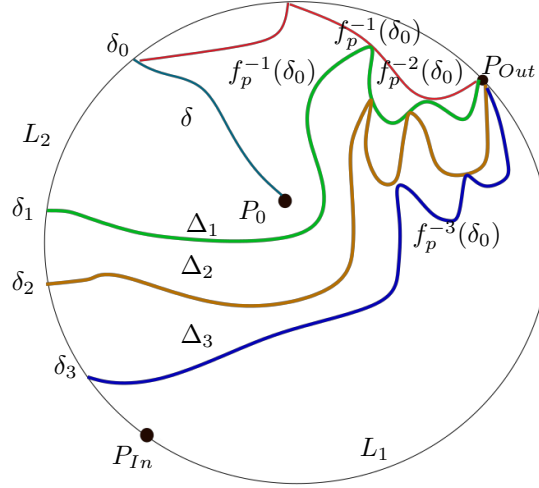
All in all, we have proven that given $n \geq 1$ there exists a component $\Delta_n \subseteq f_p^{-n-1}(l) \cap \overline{H_p}$ s.t. the following holds:

- Δ_n is a curve connecting $P_{Out}, f_p^{-n+1}(\delta_0)$ and some point $\delta_n \in [P_{In}, \delta_0]$.
- For every $n > 0$, Δ_n includes a curve $\Gamma_n \subseteq \Delta_n$ s.t. $f_p^{n+1}(\Gamma_n) = [\delta_0, P_{Out}]$.
- For $n \geq 1$, $\Delta_n \cap \delta = \emptyset$.

We now conclude the proof of Prop.3.4. By Lemma 3.2 and by the existence of the surface S_n connecting Δ_{n-1}, ν_n it immediately follows $f_p(\Delta_n) \subseteq \Delta_{n-1}$ - and since for every n , $f_p^{-n}([\delta_0, P_{Out}]) \subseteq \Delta_{n-1}$, it also follows that for every $n, k > 0$ we have both $f_p^{-n}([\delta_0, P_{Out}]) = \Gamma_n \subseteq f_p^k(\overline{H_p})$ and $f_p^{-n+1}(\delta_0) \in \Delta_n \cap \Delta_{n-1}$. In particular, for every $n, k > 0$ we have $f_p^{-n}(\delta_0) \in f_p^k(\overline{H_p})$. Finally, recalling we denote by $\mu_n = f_p^{-n}(\delta) \cap \Delta_n$, to conclude the proof of Cor.3.4 all that remains to proven is that given $n \neq k$, $\mu_n \cap \mu_k = \emptyset$. To do so, recall we have already proven $f_p^{-1}(\delta) \cap \delta = \emptyset$ - therefore, applying f_p^{-1} we see $\mu_2 \cap \mu_1 = \emptyset$, and in general, for $n \geq 1$, $\mu_{n+1} \cap \mu_n = \emptyset$. However, since by construction μ_n is separated from μ_{n+2} in $\overline{H_p} \setminus \cup_{n \geq 1} \Gamma_n$ by μ_{n+1} it follows $\mu_n \cap \mu_{n+2} = \emptyset$ - and by iterating this argument, Prop.3.4 follows (see the illustration in Fig.43). \square

Now, recall the curve δ from Prop.3.2. As proven earlier, $f_p(\delta) = (P_{In}, f_p(\delta_0))$ (i.e., the semi-open arc connecting $P_{In}, f_p(\delta_0)$ on l), which $f_p^2(\delta)$ is strictly interior to the cross-section D_α . Having proven Prop.3.4, we conclude Stage II with a proof of the following Lemma, which follows immediately from Prop.3.4:

Lemma 3.4. *Let $p \in P$ be a trefoil parameter and let H_p be the cross-section from Prop.3.3 - then, with the notations of Cor.3.4, for every $n \geq 1$, $\delta_n \notin f_p(\delta)$. As a consequence, for every n we have the following:*

FIGURE 43. The cross-section H_p , with Δ_1, Δ_2 and Δ_3 imposed on it.

- For every $n \geq 1$, both $\Delta_n \cap f_p(\delta) = \emptyset$.
- For every $n \geq 1$, $\Delta_n \cap f_p^2(\delta) = \emptyset$.

As an immediate consequence, $f_p^2(\delta)$ is disjoint from δ , hence $f_p^2(\delta) \subseteq H_p$.

Proof. We first prove that as a consequence from $\Delta_n \cap f_p^2(\delta) = \emptyset$, $n \geq 1$, it follows $f_p^2(\delta) \subseteq H_p$. Assume these assertions hold - then, since Prop.3.4 implies $\Gamma_n = f_p^{-n-1}([\delta_0, P_{Out}]) \subseteq f_p^k(\overline{H_p})$, $n \geq 1$, $k \geq 0$, by $f_p^2(\delta) \subseteq \partial f_p(H_p)$ it follows $f_p^2(\delta)$ cannot intersect transversely with Γ_n , $n \geq 1$. Additionally, if $f_p^2(\delta) \cap \delta \neq \emptyset$ it would follow $f_p^2(\delta) \cup \delta$ would separate Γ_n , $n \geq 1$ from $[P_{In}, \delta_0]$ in $\overline{H_p}$ - therefore, since $\Gamma_n \subseteq \Delta_n$, because Prop.3.4 proves Δ_n connects Γ_n to $\delta_n \in [P_{In}, \delta_0]$ it follows immediately that Δ_n has to intersect with either δ or $f_p^2(\delta)$. This is a contradiction to both Prop.3.4 and our assumption that $\Delta_n \cap f_p^2(\delta) = \emptyset$ - therefore, to prove Lemma 3.4 it would suffice to show $\Delta_n \cap f_p^2(\delta) = \emptyset$ - and we will do so by first proving $\Delta_n \cap f_p(\delta) = \emptyset$.

To begin, using the notations used in the proof of Prop.3.4, recall we denote by $\nu_1 = h(\Delta_1)$ (with h as in Lemma 3.2), and recall the surface $A_3 \subseteq \{\dot{x} = 0\}$ (see the illustration in Fig.44) - in particular, recall the curve $\sigma_3 \subseteq \partial A_3$, one of the tangency curves of F_p to $\{\dot{x} = 0\}$ (see Lemma 3.1, and the discussion after Lemma 2.3 and Lemma 2.4). As shown in Stage I of the proof of Th.2.1, σ_3 connects P_{In}, P_{Out} , the fixed points for F_p in \mathbf{R}^3 . Now, recall that as proven earlier, under the inverse flow the backwards trajectory of every initial condition $s \in \overline{D_\alpha}$ must hit $\overline{A_3}$ **before** returning to $\overline{D_\alpha}$. Therefore, recalling we denote the trajectory of $s \in \mathbf{R}^3$ by $\gamma_s(t)$, $\gamma_s(0) = s$, we are motivated to make the following definition - for $s \in \overline{D_\alpha}$ (which is not a fixed-point) let $t_5(s) < 0$ denote the **maximal** time s.t. $\gamma_s(t_5(s)) \in \overline{A_3}$. Since every backwards trajectory of $s \in \overline{D_\alpha}$ which is not a fixed point returns to $\overline{D_\alpha}$ at some negative time, it follows $t_5(s)$ is always negative and finite. Additionally, with the notations of Lemma 3.2 and Prop.3.3, the flow-line connecting $s, \gamma_s(t_5(s))$ does so through the quadrant $Q_2 = \{\dot{x} < 0\} \cap \{\dot{x} > 0\}$ (see, for example, the illustration in Fig.40 or Fig.46).

Now, let δ be the same curve as in Prop.3.2 and set $\rho = \cup_{s \in f_p^{-1}(l)} \gamma_s(t_5(s))$ - with previous notations, $\nu_1 = h(\Delta_1) \subseteq \rho$. We begin by proving the component of ν which contains ν_1 is a curve which connects P_{Out} and some point $x_1 \in \sigma_3$ - as we will see, given any n , this will force the point δ_n to lie **away** from $f_p(\delta)$. To do so, assume this is not the case - i.e., assume ρ is a curve on $\overline{A_3}$ which never terminates σ_3 - i.e., the intersection between ρ, σ_3 is **at most** tangent. Since $p \in P$ is a trefoil parameter (see Def.3.2), by the definition of δ we know it intersects with the heteroclinic connection Θ - that is, $P_0 \in \delta$. Therefore, we have $\lim_{s \rightarrow P_0} \gamma_s(t_5(s)) = P_{Out}$. This implies ρ is a Jordan curve in $\overline{A_3}$, which begins and terminates at P_{Out} - and moreover, every s in the arc $f_p^{-1}(l)$ connects with some **unique** $\gamma_s(t_5(s)) \in \overline{A_3}$ (see the illustration in Fig.44). Therefore, using a similar argument to the base of the induction in the proof of Cor.3.4 (namely, the proof Δ_1 connects P_{Out} and $\delta_1 \in l$), we derive a contradiction. As a consequence, we conclude that since $\nu_1 \subseteq \rho$, after ρ leaves $h(\delta_1)$, ρ terminates at some point $x_1 \in \sigma_3$ (see the illustration at Fig.45).

Now, as shown during the proof of Prop.3.4, for every $n \geq 2$, the surface of flow lines connecting $\Delta_n \subseteq \overline{H_p}$ with $\nu_{n-1} = h(\Delta_{n-1}) \subseteq h(\overline{H_p})$, β_n , is at most tangent to S'_1 . Now, for every $n \geq 1$ set ρ_n as the component of $T_n = \cup_{s \in f_p^{-n+1}(l)} \gamma_s(t_5(s))$ s.t. $\nu_n \subseteq \rho_n$ (by definition, $\rho_1 = \rho$). Now, since the intersections $f_p^{-1}(l) \cap l$ are at

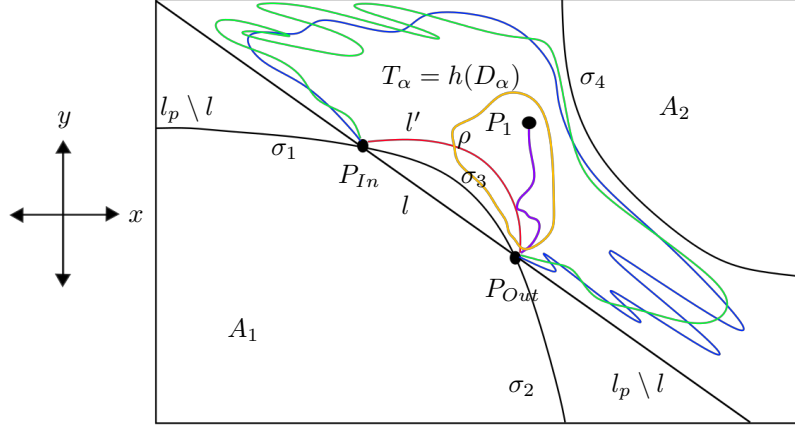


FIGURE 44. ρ is denoted by the yellow curve - in this scenario, ρ is a Jordan curve, which we show to be impossible. The purple arc denotes $h(\delta)$, and $P_1 = h(P_0)$.

most connected by Lemma 3.1.3, it follows the same is true for $f_p^{-2}(l) \cap f_p^{-1}(l)$ - and consequentially, for T_1, T_2 . Therefore, by the existence of $x_1 \in \rho_1$ we conclude there exists some $x_2 \in \sigma_3$ s.t. the component ρ_2 is a curve which begins at P_{Out} and terminates at x_2 . Iterating this argument, we conclude that for every n , ρ_n is a curve which begins at P_{Out} and terminates at $x_n \in \sigma_3$ (see the illustration in Fig.45).

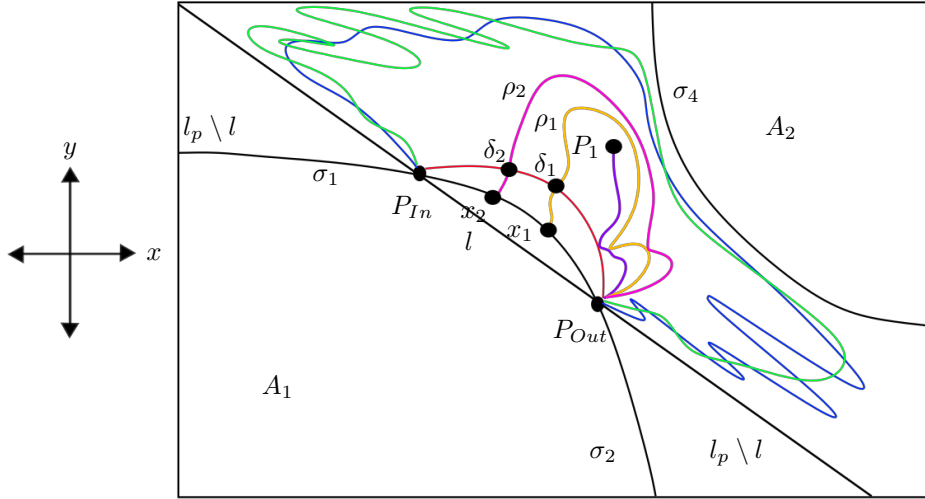


FIGURE 45. The points $x_1, x_2, \delta_1, \delta_2$. The curve ρ_1 is the same as ρ .

We can now prove that given $n \geq 1$, $\Delta_n \cap f_p(\delta) = \emptyset$ - and to do so, we first prove $\delta_n \notin f_p(\delta)$. We do so by contradiction, for $n \geq 2$ - that is, there exists some $n \geq 2$ s.t. we have $\delta_n \in (P_{In}, f_p(\delta_0)] = f_p(\delta)$. In that case, by $\Delta_n \subseteq f_p^{-n-1}(l)$ it follows $f_p^{-n-1}(l)$ intersects δ - therefore, it follows T_{n+1} includes two components - ρ_{n+1} , connecting P_{Out}, x_{n+1} and passing through $\nu_{n+1} = h(\Delta_{n+1})$, and another, ψ_{n+1} , which begins at $f_p^{-1}(\delta_n) \in \delta$ - and since the arc $\mu_n = f_p^{-n}(\delta) \cap \Delta_n$ **does not** include P_0 , ψ_{n+1} also connects with σ_3 at some point y_{n+1} - in particular, x_n is interior to the arc V on σ_3 connecting x_{n+1}, y_{n+1} (with x_n denoting the termination point of ρ_n is σ_3 - see the illustration in Fig.46. Now, write $x_n = (v_1, v_2, v_3)$ and consider the plane $H = \{(v_1, y, z) | y, z \in \mathbf{R}\}$. As such, similarly to the argument used in the proof of Prop.3.3, the body B trapped between H , the flow lines connecting $f_p^{-n}(l)$ to $\cup_{s \in f_p^{-n-1}(l)} \gamma_s(t_5(s))$ **and** the flow lines emanating from V is a three-dimensional set nothing can escape (see the argument at the end of the proof of Prop.3.3 illustrated in Fig.33). Since that body B is trapped inside $\{\dot{y} \geq 0\}$, similarly to the proof of Prop.3.3 its existence generates a contradiction.

Therefore, it follows that for every $n \geq 2$, $\delta_n \notin f_p(\delta)$. Now, since by definition δ_1 is separated from δ_3 on l by δ_2 , it follows immediately $\delta_1 \notin f_p(\delta)$ (see the illustration in Fig.47). Now, recall that for every $n \geq 1$ we defined δ_n in the proof of Prop.3.4 as the first intersection point of Δ_n with $[P_{In}, \delta_0]$ after it leaves $f_p^{-n}(\delta_0)$. Therefore, since $\delta_n, \delta_{n+1} \notin f_p(\delta)$, it follows $\Delta_n \cap l$ is trapped on the arc $[\delta_{n+1}, \delta_n] \subseteq l$ connecting δ_n, δ_{n+1} - or, in other words,

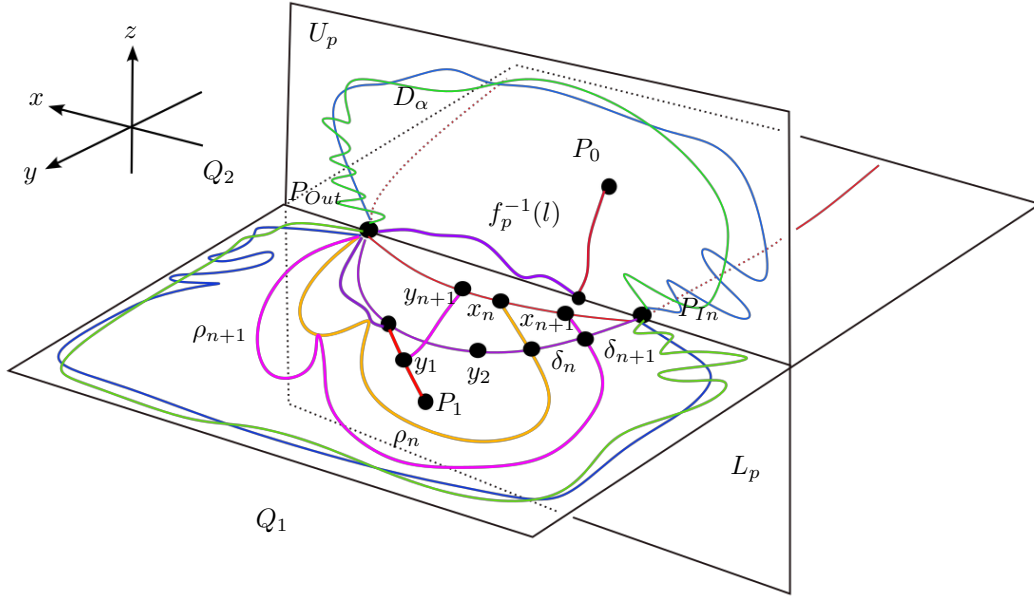


FIGURE 46. The scenario where $\Delta_n \cap f_p(\delta) \neq \emptyset$. In this case, $y_1 = h(f_p^{-1}(\delta_n))$, $y_2 = h(f_p(\delta_0))$ - we show this scenario cannot occur.

$$\Delta_n \cap f_p(\delta) = \emptyset.$$

Now, having proven that for $n \geq 1$, $\Delta_n \cap f_p(\delta) = \emptyset$, to conclude the proof of Lemma 3.4 we must show that for every $n \geq 1$ we have $\Delta_n \cap f_p^2(\delta) = \emptyset$. To do so, recall we defined $\delta_n, n \geq 1$ as the first intersection point of Δ_n with $[P_{In}, \delta_0)$ after leaving $f_p^{-n}(\delta_0)$ (see the proof of Prop.3.4). As a consequence, recalling $f_p(\delta) \subseteq [P_{In}, \delta_0)$, because by definition $f_p(\Delta_{n+1}) \subseteq \Delta_n$, it follows that $f_p(\delta_{n+1})$ is the **first** intersection point of Δ_n with $f_p([P_{In}, \delta_0))$ - and since $\delta_{n+1} \notin f_p(\delta)$, it follows $f_p(\delta_{n+1}) \notin f_p^2(\delta)$ (see the illustration in Fig.47). Therefore, it follows again that given $n \geq 1$, $f_p(\delta_{n+1}) \notin f_p^2(\delta)$. Therefore, since Δ_n is separated from the fixed-point P_{In} by Δ_{n+1} , because $f_p(\delta_{n+2}) \notin f_p^2(\delta)$ it follows $\Delta_n \cap f_p^2(\delta) = \emptyset$ and the assertion follows - and with this conclusion, the Lemma 3.4 follows. \square

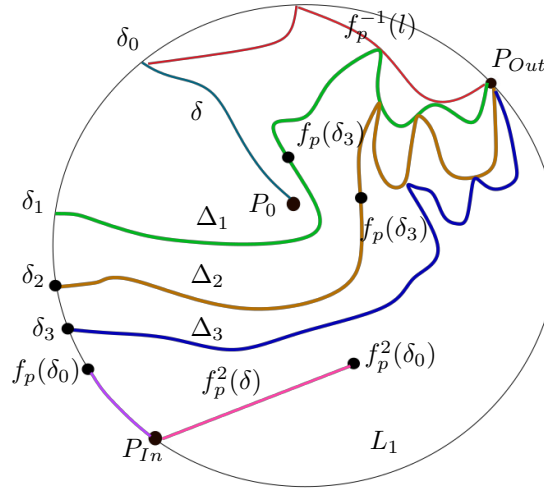


FIGURE 47. The arc $f_p(\delta)$ on l , imposed on the cross-section D_α . Again, $L_1 = (W_{In}^u \cup W_{Out}^s) \cap U_p$.

3.3. Stage III - concluding the proof of Th.3.1. Having analyzed the topology of $f_p^{-1}(l)$, we are now finally ready to prove f_p is chaotic on some invariant subset $Q \subseteq \overline{D_\alpha}$ - thus concluding the proof of Th.3.1. We will do so by analyzing the invariant set of f_p in the cross-section $H_p \subseteq D_\alpha$ introduced in the proof of Cor.3.3. To begin, recall Cor.3.1.2 and Lemma 3.3 - by both these assertions, it follows $f_p(H_p)$ is the banana-shaped region which

intersects H_p as in Fig.48. By Lemma 3.4, we can sketch that image s.t. $f_p^2(\delta) \cap \delta = \emptyset$.

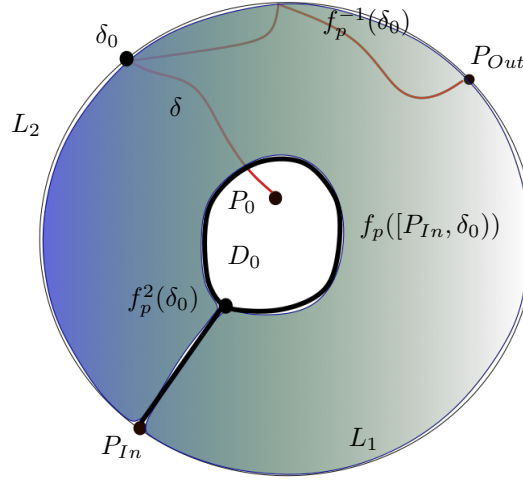


FIGURE 48. $f_p(H_p)$ imposed on the disc $\overline{D_\alpha}$ as the blue-green region, bounded by ∂D_α and the curve $f_p([P_{In}, \delta_0])$. In particular, $f_p(H_p) \cap \delta$ includes a sub-arc of δ connecting both components of ∂H_p . $\overline{D_\alpha} \setminus f_p(H_p)$ is the Jordan region D_0 .

Therefore, using Cor.3.4, we now prove:

Proposition 3.5. *Let $p \in P$ be a trefoil parameter. Then, there exists an invariant $Q \subseteq \overline{H_p}$ and a continuous $\pi : Q \rightarrow \{1, 2\}^{\mathbb{N}}$ s.t. the following holds:*

- $\pi(Q)$ includes every sequence in $\{1, 2\}^{\mathbb{N}}$ which is **not** strictly pre-periodic to the constant $\{1, 1, 1, \dots\}$.
- f_p is continuous on Q and satisfies $\pi \circ f_p = \sigma \circ \pi$.
- Given any $s \in \pi(Q)$, $\pi^{-1}(s) = D_s$ is compact, connected, and homeomorphic to a convex set.
- With the same notations, provided $s \in \{1, 2\}^{\mathbb{N}}$ is not the constant $\{1, 1, 1, \dots\}$ nor pre-periodic to it, $P_{Out}, P_{In} \notin D_s$.

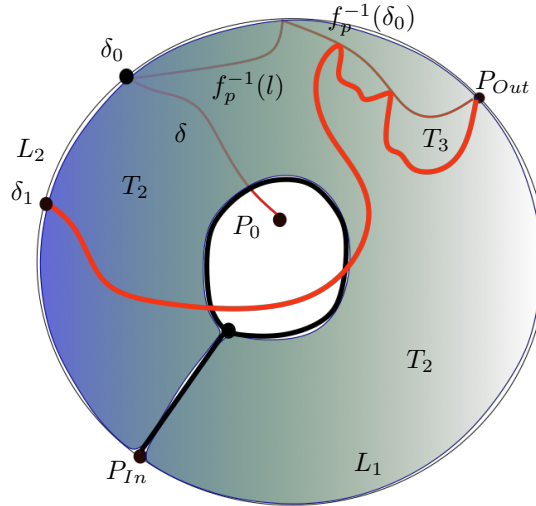


FIGURE 49. The red curve is a component of $f_p^{-2}(l) \cap H_p$, which intersects l at some point δ_1 - or, in the notation of Prop.3.4, the red curve is Δ_1 . The sets T_1, T_2, T_3 are imposed on $\overline{H_p}$ - while $\partial H_p = l \cup L_1 \cup f_p^{-1}(l)$.

Proof. We prove Prop.3.5 constructively. To do so, recall the curve $\delta \subseteq f_p^{-1}(l)$ introduced in Prop.3.2. Moreover, recall the component H_p of $\overline{D_\alpha} \setminus f_p^{-1}(l)$ introduced in the proof of Cor.3.3 has a boundary which is composed of three sets - $f_p^{-1}(l)$, $[P_{In}, \delta_0]$, and the arc $L_1 = (W_{Out}^s \cup W_{In}^u) \subseteq \partial D_\alpha$. By Prop.3.4 and Lemma 3.4, $\Delta_1 \subseteq \overline{H_p}$

is a component of $f_p^{-2}(l)$ which connects $P_{Out}, f_p^{-1}(\delta_0)$ and some $\delta_1 \in [P_{In}, \delta_0] \setminus f_p(\delta)$ - see the illustration in Fig.49.

Therefore, $\overline{H_p} \setminus f_p^{-2}(l)$ is composed of three sets - T_1, T_2, T_3 s.t. the following conditions are satisfied (see the illustration in Fig.49):

- $P_{In}, P_{Out} \in \partial T_1$ and P_0 in ∂T_2 .
- For $i = 1, 2$, $f_p(T_i) \subseteq \overline{H_p} \setminus f_p^{-1}(l)$, while $f_p(T_3) \cap H_p = \emptyset$ - i.e., T_3 is mapped outside of the cross-section $\overline{H_p}$ by f_p , while **both** T_1, T_2 are mapped inside $\overline{H_p}$.
- Since $f_p^{-1}(l)$ does not include self-intersecting curves, both T_1, T_2 include Jordan domains D_1, D_2 s.t. $f_p(D_i) \cap D_j \neq \emptyset, i, j \in \{1, 2\}$.
- $\{P_{In}, P_{Out}\} \subseteq \partial D_1 \setminus \partial D_2$, while $P_0 \in \partial D_2 \setminus \partial D_1$. Moreover, $f_p(D_i) \cap H_p, i = 1, 2$ both connect P_{In}, δ .
- As such, there exists an arc $\theta \subseteq \Delta_1$ s.t. $f_p^2(\theta) \subseteq \delta$ **and** the endpoints of θ on ∂H_p are $f_p^{-1}(\delta_0)$ and some $\delta_1 \in [P_{In}, \delta_0] \setminus f_p(\delta)$. Additionally, by Lemma 3.4, $\theta \cap f_p(\delta) = \emptyset, \theta \cap f_p(\delta) = \emptyset$.

Now, denote by $I = [\delta_0, P_{Out}]$ the subarc of l connecting δ_0, P_{Out} - by Cor.3.4 we have $\cup_{n \geq 1} f_p^{-n}(I) \subseteq f_p(\overline{H_p}) \cap \overline{H_p}$ - and since for every n we have $\Delta_n \subseteq \overline{H_p}$, by their construction in the proof of Cor.3.4 it follows $\cup_{n \geq 1} \Delta_n \subseteq (\overline{D_1} \setminus (f_p(\delta)) \cup f_p^2(\delta))$. Now, choose some $i \in \{1, 2\}$ - because $f_p^{-1}(\delta_0) \in f_p(\overline{H_p})$, it follows $f_p(\overline{H_p}) \cap \Delta_1$ has at least two components (see the illustration in Fig.50). Therefore, it immediately follows $f_p^{-3}(l)$ has pre-images θ_i in $D_i, i = 1, 2$ which divide D_i to the sets $T_{i,1}, T_{i,2}, T_{i,3}$ s.t. $f_p(T_{i,j}) \subseteq T_j$, with $j \in \{1, 2, 3\}$. Because θ lies away from both $f_p(\delta), f_p^2(\delta)$ by Prop.3.2 it follows θ_1, θ_2 both lie away from δ . As a consequence, θ_1 connects $f_p^{-1}(l) \cap [P_{In}, \delta_0] \setminus f_p(\delta)$ in T_1 - and conversely, θ_2 connects the two components of $\partial H_p \setminus \delta$ in T_2 . Again, there exists a Jordan region $D_{i,j}, j = 1, 2$ s.t. $f_p(D_{i,j}) \subseteq D_j$ - see the illustration in Fig.50. In particular, $f_p^2(D_{i,j}) \cap H_p$ both connect δ, P_{In} .

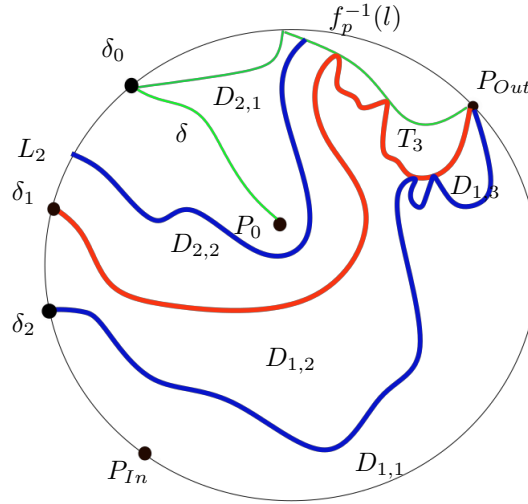


FIGURE 50. The green curve denotes $f_p^{-1}(l)$, the red denotes $f_p^{-2}(l) \cap H_p$ while the blue curves are the components of $f_p^{-3}(l) \cap H_p$, i.e., θ_1 and θ_2 . For simplicity, in this scenario we have $D_1 = T_1$, $T_2 = D_2$, and $D_1 = D_{1,1} \cup D_{1,2} \cup D_{1,3}$, $D_2 = D_{2,1} \cup D_{2,2}$.

Repeating this process, given $k \in \{1, 2\}$, because $f_p^{-2}(\delta_0) \in \overline{f_p^2(H_p)} \cap \overline{D_1}$ it again follows that given $i, j \in \{1, 2\}$ we can find a Jordan subdomain $D_{i,j,k} \subseteq D_{i,j}$ s.t. $f_p^2(D_{i,j,k}) \subseteq D_k$, and $f_p^3(D_{i,j,k}) \cap H_p$ connects P_{In}, δ . We may, of course, proceed in this fashion and conclude the following - let $s \in \{1, 2\}^{\mathbb{N}}$, $s = \{i_0, i_1, i_2, \dots\}$ be a symbol **not** strictly pre-periodic to the constant $\{1, 1, 1, \dots\}$. Define $D_s = \cap_{n \geq 0} \overline{D_{i_0, \dots, i_n}}$ - being an intersection of nested, compact sets, D_s is compact and non-empty. Additionally, since for every $n \geq 0$ D_{i_0, \dots, i_n} is a Jordan domain it follows D_s is homeomorphic to the intersection of a sequence of nested discs - hence, D_s is homeomorphic to the intersection of nested, convex sets, thus it is also homeomorphic to a convex set.

Moreover, by construction, for every $n \geq 0$, $f_p^n(D_s) \subseteq D_{i_n}$ - from which it follows that provided s is **not** the constant $\{1, 1, 1, \dots\}$, there exists some n s.t. $f_p^n(D_s) \subseteq D_2$, hence by the discussion above, $P_{In}, P_{Out} \notin D_s$. Additionally, since we constructed D_s s.t. it lies **away** from $\cup_{n \geq 0} f_p^{-n}(l)$, by Prop.3.2 it follows that for every $k > 0$, f_p^k is continuous on D_s . Now, set Q as the collection of such D_s (for all $s \in \{1, 2\}^{\mathbb{N}}$ which are not strictly pre-periodic to $\{1, 1, 1, \dots\}$). Denoting by $\sigma : \{1, 2\}^{\mathbb{N}} \rightarrow \{1, 2\}^{\mathbb{N}}$ the one-sided shift, by this discussion it follows there exists a function $\pi : Q \rightarrow \{1, 2\}^{\mathbb{N}}$ s.t. the following holds:

- $\pi \circ f_p = \sigma \circ \pi$.
- Since f_p is continuous on Q , π is also continuous on Q .

And moreover, given any $s \in \{1, 2\}^{\mathbb{N}}$ which is **not** strictly pre-periodic to the constant $\{1, 1, 1, \dots\}$ the following is also satisfied:

- $s \in \pi(Q)$.
- $\pi^{-1}(s) = D_s$ is a connected, compact set homeomorphic to a convex set.
- If s is not the constant $\{1, 1, 1, \dots\}$, then $P_{In}, P_{Out} \notin D_s = \pi^{-1}(s)$.

And with that, the proof of Prop.3.5 is complete. \square

Remark 3.2. Let $s \in \{1, 2\}^{\mathbb{N}}$ which is strictly pre-periodic to $\{1, 1, 1, \dots\}$. As must be remarked, there exists a **unique** point $x \in \overline{H_p}$ whose trajectories tends to $P_{In} - P_0$. Because P_0 has no preimages in $\{y = 0\}$ (let alone H_p) any attempt to define D_s for such symbols is probably futile.

Remark 3.3. Consider some $s \in \{1, 2\}^{\mathbb{N}}$, $s = \{i_0, i_1, i_2, \dots\}$, and let J denote the boundary arc of ∂D_2 s.t. $\delta_0 \in J$. It is immediate that θ_2 connects the two components of $J \setminus \{\delta_0\}$, and in fact, for every $j > 2$, $n > 0$, $f_p^{-j}(\Delta_n) \cap D_2$ includes an arc connecting the two components of $J \setminus \{\delta_0\}$. As such, it follows that when $i_0 = 2$, for every n the domain D_{i_0, \dots, i_n} also connects the two components of $J \setminus \{\delta_0\}$ - and as a consequence, so does D_s .

Remark 3.4. As must be remarked, the dynamics of the first-return map observed numerically at trefoil parameters in [27] were associated with bimodal rather than unimodal dynamics - i.e., the first-return map appeared to correspond to some subshift of finite type on three symbols rather than two. This suggests the dynamics of f_p on $\overline{D_\alpha}$ are possibly more complex than those of f_p on $\overline{H_p}$ - or, in other words, the set T_3 from the proof of Prop.3.5 possibly plays a larger part in the dynamics than what initially appears.

As an immediate consequence from Prop.3.5 we obtain:

Corollary 3.1.4. Let $p \in P$ be a trefoil parameter, and let $s \in \{1, 2\}^{\mathbb{N}}$ be periodic of minimal period $k > 0$ - then, $\pi^{-1}(s) = D_s$ includes a periodic point x for f_p of minimal period k .

Proof. With the notations of the proof of Prop.3.5, by the construction of $D_s = \pi^{-1}(s)$ in the proof of Prop.3.5, D_s is homeomorphic to a compact convex set. Therefore, because Prop.3.5 proves $f_p^k : D_s \rightarrow D_s$ is continuous, by the Brouwer Fixed Point Theorem there exists a point $x \in D_s$ s.t. $f_p^k(x) = x$. Therefore, to conclude the proof it remains to show the minimal period of x is also k . To do so, recall we denote by $\sigma : \{1, 2\}^{\mathbb{N}} \rightarrow \{1, 2\}^{\mathbb{N}}$ the one-sided shift. Since the minimal period of s under σ is k , given $i, j \in \{0, \dots, k-1\}$, $i \neq j$, $\sigma^j(s) \neq \sigma^i(s)$ - which, by Prop.3.5 implies $\pi^{-1}(\sigma^i(s)) \cap \pi^{-1}(\sigma^j(s)) = \emptyset$. Therefore, since for $0 \leq i \leq k-1$ we have $f_p^i(D_s) \subseteq D_{\sigma^i(s)}$ we conclude $f_p^i(D_s) \cap D_s \neq \emptyset$ only when $i = k$, and the conclusion follows. \square

Remark 3.5. When s is the constant $\{1, 1, 1, \dots\}$, Cor.3.1.4 remains true - in that case, the argument used to prove Prop.3.5 shows $P_{In} \in D_{\{1, 1, 1, \dots\}}$, and by $f_p(P_{In}) = P_{In}$ the assertion follows.

We can now conclude the proof of Th.3.1. Let Q be the set given by Prop.3.5. As proven in Lemma 3.3, H_p is a topological disc, and so is $\overline{H_p}$ - and by Prop.3.5 there exists an f_p -invariant $Q \subseteq \overline{H_p}$ s.t.:

- f_p is continuous on Q .
- There exists a continuous $\pi : Q \rightarrow \{1, 2\}^{\mathbb{N}}$ s.t. $\pi \circ f_p = \sigma \circ \pi$.
- $\pi(Q)$ includes every $s \in \{1, 2\}^{\mathbb{N}}$ **not** pre-periodic to the constant $\{1, 1, 1, \dots\}$.
- Let $s \in \{1, 2\}^{\mathbb{N}}$ be periodic of minimal period k . Then, by Cor.3.1.4 and Remark 3.5, $\pi^{-1}(s)$ contains a periodic point x_s for f_p of minimal period k .

As a consequence, f_p is chaotic on Q (w.r.t. Def.1.1). In addition, Q includes infinitely many periodic points for f_p - of all minimal periods. Th.3.1 is now proven. \square

At this point, let us remark that the proof of Th.3.1 can probably be generalized to other heteroclinic parameters for the Rössler system, which generate knots more complex than a trefoil (see Def.3.1). **However**, it should also be stressed that the proof of any such generalization would greatly depend on the topology of the heteroclinic knot involved.

Another remark which must be made is that in light of the proof of Th.3.1, we can now reformulate it as follows. To begin, recall the cross-section U_p (see the discussion before Lemma 2.1), the curve Δ_1 from Cor.3.4 and the regions D_1, D_2 from Prop.3.5 (in particular, recall the chain of inclusions $\overline{H_p} \subseteq \overline{D_\alpha} \subseteq \overline{U_p}$). As proven in Cor.3.4, Δ_1 connects P_{Out} and some point $\delta_1 \in l$. Let ρ denote the component of $\Delta_1 \setminus l$ s.t. $\delta_1 \in \rho$ (similar arguments to those used to prove Cor.3.4 prove $\delta_1 \neq P_{In}$). As a consequence, ρ is a curve connecting δ_1 and l , s.t. $\overline{U_p} \setminus \Delta_1$ is composed of **precisely** two components, U_1, U_2 - indexed by $D_i \subseteq U_i, i = 1, 2$ (see the illustration in Fig.51).

Now, set I as the maximal invariant set of f_p in $\overline{U_p} \setminus \rho$ - that is, I is the collection of initial conditions in the cross-section U_p whose trajectories both never hit ρ **and** never escape to ∞ . With these ideas in mind we now restate Th.3.1, and with this result we conclude Section 3:

Corollary 3.1.5. *Let $p \in P$ be a trefoil parameter, and let $f_p : \overline{U_p} \rightarrow \overline{U_p}$ denote the first-return map for the corresponding Rössler system (wherever defined). Now, let I be as above and recall we denote by $\sigma : \{1, 2\}^{\mathbb{N}} \rightarrow \{1, 2\}^{\mathbb{N}}$ the one-sided shift - then, the dynamics of f_p on I include an f_p -invariant $Q \subseteq I$, s.t. the following holds:*

- f_p is continuous on Q .
- There exists a continuous $\pi : Q \rightarrow \{1, 2\}^{\mathbb{N}}$ s.t. $\pi \circ f_p = \sigma \circ \pi$.
- $\pi(I)$ includes every $s \in \{1, 2\}^{\mathbb{N}}$ which is **not** strictly pre-periodic to $\{1, 1, 1, \dots\}$.
- If $s \in \{1, 2\}^{\mathbb{N}}$ is periodic of minimal period $k > 0$, then $\pi^{-1}(s)$ includes **at least** one periodic point for f_p of the same minimal period.

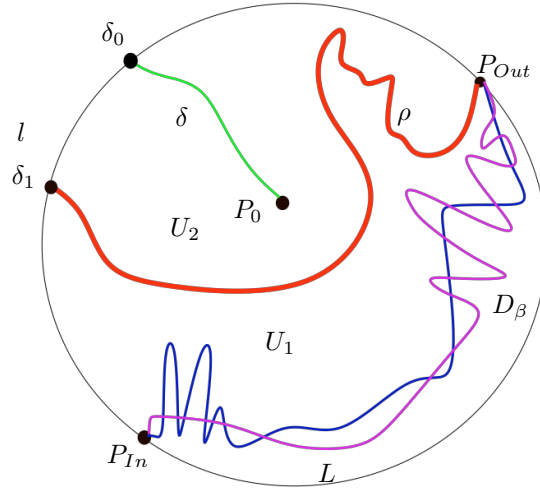


FIGURE 51. The cross-section U_p . The curve ρ bisects U_p to U_1, U_2 , with L denoting the curves $(W_{In}^u \cup W_{Out}^s) \cap U_p$ (see Cor.2.3).

4. THE IMPLICATIONS:

Th.3.1 teaches us that at trefoil parameters, the dynamics of the Rössler system are complex essentially like those of a Smale Horseshoe, suspended around a heteroclinic trefoil knot - or, more precisely, it teaches us that the dynamics are complex **at least** like those of a suspended Smale Horseshoe map. Motivated by the theory of homoclinic bifurcations (and in particular, Shilnikov's Theorem - see [3]), in this section we use Th.3.1 to prove several results about the dynamical complexity of the Rössler system and its bifurcations around trefoil parameters.

To begin, recall P always denote the parameter space introduced in page 3, and let $p \in P$ **always** denote a trefoil parameter. Recall we denote by F_p the vector field corresponding to $p = (a, b, c)$ (see Eq.2). This section is organized as follows - first we study the question of hyperbolicity of the dynamics at trefoil parameter: namely, in Prop.4.1 we prove the flow at trefoil parameters $p \in P$ does not satisfy any dominated splitting condition, a weaker form of hyperbolicity. Following that, we prove that in the space of C^∞ vector fields (on \mathbf{R}^3), trefoil parameters are inseparable from period-doubling and saddle-node bifurcation sets (for a more precise formulation, see Prop.4.2). Finally, we conclude this Section (and this paper) with the following result: given a trefoil parameter $p \in P$, a positive $n > 0$ and $v \in P$, provided v is sufficiently close to p the vector field F_v generates **at least** n distinct periodic trajectories (see Th.4.1).

To begin, let us first recall the cross-section $\overline{D_\alpha} \subseteq \overline{U_p}$ introduced in Section 2.2 (see Lemma 2.15 and Prop.2.3) - by Cor.2.2.1, the first-return map $f_p : \overline{D_\alpha} \rightarrow \overline{D_\alpha}$ is well-defined. As proven in Section 3, the first-return map is continuous on each of the components of $\overline{D_\alpha} \setminus f_p^{-1}(l)$ (with l denoting the arc $\{(x, -\frac{x}{a}, \frac{x}{a}) | x \in (0, c - ab)\}$ - see the discussion at the beginning of Section 3 - and in particular, Prop.3.2). This motivates us to define $R = \bigcap_{n \geq 0} (\overline{D_\alpha} \setminus f_p^{-n}(l))$, the maximal invariant set of f_p in $\overline{D_\alpha} \setminus l$. Since we have the inclusion $\overline{H_p} \subseteq \overline{D_\alpha}$, by the construction of Q in Th.3.1 we conclude $Q \subseteq R$, hence $R \neq \emptyset$. By this definition, using a similar argument to the proof of Prop.3.5 it immediately follows:

Corollary 4.0.1. *Let C be a component of R . Then, for every $n > 0$, f_p^n is continuous on C - and moreover, R is dense in $\overline{D_\alpha}$.*

Proof. By definition, given C as above, f_p^n is continuous on C - for every n . Therefore, it remains to show R is dense in $\overline{D_\alpha}$. To do so, recall that since f_p is a first-return map, iterating the arguments used to prove Prop.3.2 we conclude that given $n \in \mathbf{N}$, $f_p^{-n}(l)$ is a collection of curves (possibly singletons), each with endpoints on $\cup_{0 \leq k \leq n} f_p^{-k}(l)$ - and provided $n > 1$, any component of $f_p^{-n}(l)$ has no endpoints strictly interior to $\overline{D_\alpha}$ (see the illustration in Fig.52). As such, for every $n \geq 0$, $R_n = \overline{D_\alpha} \setminus (\cup_{0 \leq k \leq n} f_p^{-k}(l))$ is dense in $\overline{D_\alpha}$. $\overline{D_\alpha}$ is both complete and separable, hence, by the Baire Category Theorem it follows $R = \cap_{n \geq 1} R_n$ is dense in $\overline{D_\alpha}$ and Cor.4.0.1 follows. \square

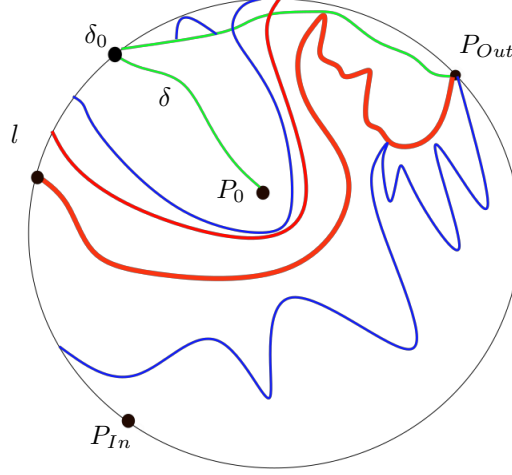


FIGURE 52. The set R_3 - the green curves correspond to $f_p^{-1}(l)$, the red to $f_p^{-2}(l)$, and the blue to $f_p^{-3}(l)$.

Using Cor.4.0.1, we now conclude the following result about the **non-hyperbolic** nature of the Rössler system:

Proposition 4.1. *Let $p \in P$ be a trefoil parameter - then, with previous notations, F_p does not satisfy any dominated splitting condition on the trajectories of initial conditions in R .*

Proof. Let us first recall the notion of **Dominated Splitting** - let M be a Riemannian manifold, and $\phi_t : M \rightarrow M, t \in \mathbf{R}$ be a smooth flow. Also, given a hyperbolic point $x \in M$ (w.r.t. ϕ_t) let us denote the components of the decomposition of the tangent space by $T_x M = E(x) \oplus F(x)$ - with $E(x), F(x)$ denoting the respective stable and unstable parts of the decomposition. A compact, ϕ_t -invariant set Λ is said to satisfy a **dominated splitting** condition if the following conditions are satisfied:

- The tangent bundle satisfies $T\Lambda = E \oplus F$, s.t. $E = \cup_{x \in \Lambda} E(x) \times \{x\}$, $F = \cup_{x \in \Lambda} F(x) \times \{x\}$.
- $\exists c > 0, 0 < \lambda < 1$, s.t. $\forall t > 0, x \in \Lambda$, $(\|D\phi_t|_{E(x)}\|)(\|D\phi_{-t}|_{F(\phi_t(x))}\|) < c\lambda^t$.
- $\forall x \in \Lambda, t > 0$, $E(x), F(x)$ vary continuously to $E(\phi_t(x)), F(\phi_t(x))$.

Now, let p be a trefoil parameter and let Λ be the **closure** in \mathbf{R}^3 of trajectories for initial conditions in R - by definition, Λ is also F_p -invariant. By Lemma 4.0.1, Λ is inseparable from P_{In} - as such, since the two dimensional manifolds W_{In}^u, W_{Out}^s intersect transversely (see page 16), we conclude Λ is also inseparable from P_{Out} . Now, recall P_{In}, P_{Out} are hyperbolic saddle-foci of opposing indices (see the discussion at page 3), connected by a bounded heteroclinic connection Θ (see Def.3.2) - with Θ being a component of **both** one-dimensional invariant manifolds W_{In}^s, W_{Out}^u . As such, by previous discussion and the compactness of Λ , we conclude $\Theta, P_{In}, P_{Out} \subseteq \Lambda$. Now, assume we can decompose $T\Lambda$ to $T\Lambda = E \oplus F$ as in the definition above - with previous notations, this implies $F(P_{Out})$ is one-dimensional, while $F(P_{In})$ is two dimensional. Hence, for $x \in \Theta$, $F(x)$ cannot vary continuously, and we have a contradiction. This contradiction proves F_p cannot satisfy any Dominated Splitting condition on Λ , and Lemma 4.1 follows. \square

Now, let $p \in P$ be a trefoil parameter, and recall we denote the saddle-indices for the saddle-foci P_{In}, P_{Out} by ν_{In}, ν_{Out} - respectively (see the definition at page 3). Additionally, recall that we assume that given $v \in P$, the saddle-indices corresponding to v always satisfy either $\nu_{In} < 1$ or $\nu_{Out} < 1$, i.e. $(\nu_{In} < 1) \vee (\nu_{Out} < 1)$. As must be remarked, the proof of Th.3.1 and Th.2.1 (and later on, Th.4.1) are both independent of the assumption that $\nu_{Out} < 1 \vee \nu_{In} < 1$ - that is, Th.3.1 and Th.?? are both independent of the assumption that at least one of the fixed points for F_p satisfies the Shilnikov condition. Plugging in this assumption, we derive the following result:

Proposition 4.2. *Let $p \in P$ be a trefoil parameter. Then, p is an accumulation point in the space of vector fields for infinitely many period-doubling and saddle-node bifurcation sets in the space of C^∞ vector fields on \mathbf{R}^3 .*

Proof. For completeness, let us recall sections 2,3 of [10]. In that paper, the setting is that of a smooth, two-parameter family of vector fields $\{X_{(a_1, a_2)}\}_{(a_1, a_2) \in O}$, with (a_1, a_2) varying smoothly in some open set $O \subseteq \mathbf{R}^2$. Assume there exists a curve $\gamma \subseteq O$ corresponding to the existence of homoclinic trajectories. Also assume the saddle indices along γ are all strictly lesser than 1 - that is, by Shilnikov's Theorem the dynamics around these homoclinic trajectories all generate infinitely many suspended Smale horseshoes.

As proven in [10], under these assumptions one can construct a function B from the phase space to O . The analysis of B allows one to find a family of spirals, $\{\delta_o\}_{o \in \gamma}$, s.t. δ_o is a curve in O , spiralling towards o . Each δ_o corresponds to the existence of a periodic trajectory, which undergoes a cascade of period-doubling and saddle-node bifurcations as δ_o accumulates on o . Moreover, this family of spirals varies continuously when $o \in \gamma$ varies - and provided the saddle index along γ is bounded, there exists some $c > 0$ s.t. $\forall o \in \gamma, \text{diam}(\delta_o) > c$ (with that diameter taken w.r.t. the Euclidean metric in O). When the function B was analyzed, its critical values corresponded to curves of period-doubling and saddle-node bifurcations - and these critical values accumulated around every point in γ (see Sections 2,3 in [10] for more details). That is, for any $\epsilon < 0$ and any $o \in \gamma$ there exist Γ_1, Γ_2 , a saddle node bifurcation curve and a period doubling bifurcation curve (respectively) s.t. $d(\Gamma_i, o) < \epsilon, i = 1, 2$.

Now, back to the Rössler System - without any loss of generality, assume that w.r.t. the vector field F_p we have $\nu_{In} < 1$ (by assumption, we have $\nu_{In} < 1 \vee \nu_{Out} < 1$). Now, let us approximate F_p by a curve γ_{In} in the space of C^∞ vector fields on \mathbf{R}^3 , s.t. $\forall \omega \in \gamma_{In}$, the vector field corresponding to ω generates a homoclinic curve to P_{In} - moreover, we construct these approximations by perturbing F_p in some small neighborhood of P_{Out} , s.t. the local dynamic of F_p around P_{In} are unaffected by this perturbation. In other words, we construct γ_{In} s.t. the saddle index ν_{In} remains constant $\forall \omega \in \gamma_{In}$. As $\nu_{In} < 1$ by assumption, the discussion above implies the period-doubling and saddle node bifurcations sets are dense around γ_{In} (in the space of C^∞ vector fields on \mathbf{R}^3). Since $F_p \in \overline{\gamma_{In}}$, the conclusion follows. \square

Remark 4.1. Assume *both* $\nu_{In}, \nu_{Out} < 1$. In that case, the proof of Prop.4.2 essentially proves the bifurcations around trefoil parameters in the space of C^∞ vector fields on \mathbf{R}^3 are **doubly as complicated** when compared to homoclinic bifurcations. This should be contrasted with the results of [14], where it was proven a two-dimensional parameter space **cannot** be used to completely describe the bifurcations around heteroclinic parameters.

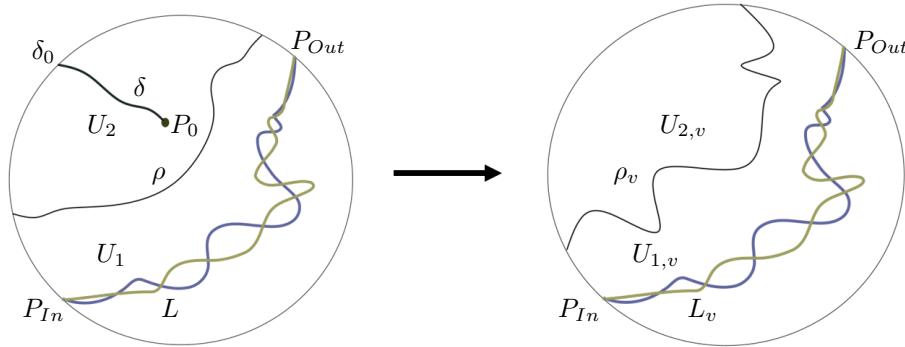


FIGURE 53. the deformation of U_p (on the left) to U_v (on the right). The curve ρ is deformed to ρ_v , while $L = (W_{In}^u \cup W_{Out}^s) \cap U_p$ is deformed to $L_v = (W_{In}^u \cup W_{Out}^s) \cap U_v$.

We are now ready to state and prove Th.4.1, with which we conclude this paper - namely, we will now prove that given a trefoil parameter $p \in P$ and given any $n > 0$, provided $v \in P$ is sufficiently close to p the vector field F_v generates **at least** n periodic trajectories. Or, in other words, Theorem 4.1 has the following meaning - the closer a parameter $v \in P$ is to a trefoil parameter p , the more complex its dynamics become. The idea behind the proof is based on the following intuition - if $p \in P$ is a trefoil parameter, by Th.3.1 the dynamics of f_p on the invariant set Q are complex at least like those of a Smale Horseshoe. As such, we would expect the periodic orbits of the first-return map f_p to be hyperbolic, thus they should persist under perturbations of the first-return map in P . In practice however, due to Prop.4.1 this line of reasoning simply **cannot** hold - or, put simply, there is no reason whatsoever to assume any hyperbolicity on the invariant set Q given by Th.3.1.

Therefore, to bypass this difficulty we will take a different route, and apply the notion of the Fixed-Point Index to prove the persistence of periodic dynamics (see [5]). As we will see, to prove the persistence of periodic dynamics it would be enough to construct a homotopy between the first-return map $f_p : \overline{H_p} \rightarrow \overline{H_p}$ to a Smale-Horseshoe. To begin, let us first recall several facts which would motivate our result and make its statement more precise. First, recall that given a trefoil parameter $p \in P$, $f_p : \overline{U_p} \rightarrow \overline{U_p}$ denotes the first-return map for F_p for the cross-section $U_p \subseteq \{\dot{y} = 0\}$ (wherever defined - see Lemma 2.1), and that $Q \subseteq \overline{H_p} \subseteq \overline{D_\alpha} \subseteq \overline{U_p}$ denotes the set given by Cor.3.1.5. By Cor.3.1.5 (and Th.3.1) there exists a continuous $\pi : Q \rightarrow \{1, 2\}^{\mathbb{N}}$ s.t. the one-sided shift $\sigma : \{1, 2\}^{\mathbb{N}} \rightarrow \{1, 2\}^{\mathbb{N}}$ satisfies $\pi \circ f_p = \sigma \circ \pi$, and σ is chaotic on $\pi(Q)$ (w.r.t. Def.3.2). Secondly, we have also proven that given **any** periodic $s \in \{1, 2\}^{\mathbb{N}}$ which is both periodic of minimal period $k > 0$ **and** distinct from the constant $\{1, 1, 1, \dots\}$, $\pi^{-1}(s)$ contains a periodic point for f_p of minimal period k . Now, further recall that by Cor.3.1.5 we have $Q \subseteq I$, with I denoting the maximal invariant set of f_p in $\overline{U_p} \setminus \rho$ (with the curve ρ defined as in the discussion preceding Cor.3.1.5). As shown earlier, $\overline{U_p} \setminus \rho$ is composed of two subsets, U_1, U_2 , with which we defined the symbolic coding given by π (see the illustration in Fig.53 or Fig.51). Moreover, since $P_{In} \notin \rho$, $P_{In} \in U_1$.

Now, given any $v \in P, v \neq p$, let $f_v : \overline{U_v} \rightarrow \overline{U_v}$ denote the first-return map for the vector field F_v (wherever defined) - with U_v as in Lemma 2.1. Since the cross-sections U_v vary smoothly when we vary $v \in P$ (see the discussion preceding Lemma 2.1), when F_p is continuously deformed to F_v the curve $\rho \subseteq \overline{U_p}$ is continuously deformed to $\rho_v \subseteq \overline{U_v}$. Hence, since ρ divides $\overline{U_p}$ to U_1, U_2 , we conclude ρ_v divides $\overline{U_v}$ to $U_{1,v}, U_{2,v}$ (see the illustration in Fig.53). This motivates us to define a symbolic coding on I_v , the invariant set of f_v in $\overline{U_v} \setminus \rho_v$ - provided I_v is non-empty, there exists a function $\pi_v : I_v \rightarrow \{1, 2\}^{\mathbb{N}}$ (not necessarily continuous, or surjective) s.t. $\pi_v \circ f_v = \sigma \circ \pi_v$ (again, with $\sigma : \{1, 2\}^{\mathbb{N}} \rightarrow \{1, 2\}^{\mathbb{N}}$ denoting the one-sided shift). We now prove:

Theorem 4.1. *With the notations above, let $p \in P$ be a trefoil parameter, and let $s \in \{1, 2\}^{\mathbb{N}}$ be periodic of minimal period k that is **not** the constant $\{1, 1, 1, \dots\}$. Then, for $v \in P$ sufficiently close to p we have:*

- $s \in \pi_v(I_v)$.
- $\pi_v^{-1}(s)$ contains at least one periodic point $x_s \in I_v$ for f_v , of minimal period k .
- The functions f_v, f_v^2, \dots, f_v^k are all continuous at x_s .
- π_v is continuous at $x_s, f_v(x_s), \dots, f_v^{k-1}(x_s)$.

Proof. As remarked earlier, we prove Th.4.1 with the aid of the Fixed-Point Index (see [5]). Therefore, in order to give a sketch of the proof, let us first recall its definition - let $V \subseteq \mathbb{R}^2$ be an **open** set, and let $f : V \rightarrow \mathbb{R}^2$ be continuous s.t. the set $\{x \in V | f(x) = x\}$ is compact. The **Fixed-Point Index** of f would be defined as the degree of $f(x) - x$ on V - in particular, when f has no fixed points in V its Fixed-Point Index is 0 (see Ch.VII.5.5 in [5]). Now, let $f_t : V \rightarrow \mathbb{R}^2, t \in [0, 1]$ be a homotopy of continuous maps, and for every $t \in [0, 1]$ set $F_t = \{x \in V | f_t(x) = x\}$. As proven in Ch.VII.5.8 in [5], provided $\cup_{t \in [0, 1]} F_t \times \{t\}$ is compact in $V \times [0, 1]$, the fixed point index is invariant under the homotopy. Or in other words, given homotopies as described above, if the Fixed-Point Index for f_0 is non-zero, the same is true for f_1 , i.e. f_1 has at least one fixed-point in V .

With these ideas in mind, let us sketch the proof of Th.4.1 - let $s \in \{1, 2\}^{\mathbb{N}}$ be periodic of minimal period $k \geq 1$, which is **not** the constant $\{1, 1, 1, \dots\}$, and let $\overline{H_p}$ and $Q \subseteq \overline{H_p}$ be as in Th.3.1 - as proven in Th.3.1, there exists a continuous $\pi : Q \rightarrow \{1, 2\}^{\mathbb{N}}$ s.t. $s \in \pi(Q)$ and $D_s = \pi^{-1}(s)$ is connected, and homeomorphic to a convex set (see Prop.3.5. Now, let $F = \{x \in D_s | f_p^k(x) = x\}$ - we will prove Th.4.1 by constructing a topological disc $B \subseteq \overline{H_p}$ s.t. the following holds:

- F is a compact subset of B .
- f_p^k is continuous on B .
- The Fixed-Point Index of f_p^k on B is 1.
- When we vary the parameter p to another $v \in P$, B is varied smoothly to another topological disc, B_v .

After proving the existence of a topological disc satisfying these properties, we show that given any $v \in P$ sufficiently close to P , $f_p^k : B_p \rightarrow \overline{U_p}$ and $f_v^k : B_v \rightarrow \overline{U_v}$ are homotopic - thus their fixed-point indices coincide, from which Th.4.1 would follow. To begin, recall the cross-section $D_\alpha \subseteq U_p$ (see Lemma 2.15) - by Cor.2.2.1, Lemma 2.15 and Th.2.2, the first-return map $f_p : \overline{D_\alpha} \rightarrow \overline{D_\alpha}$ is well-defined and satisfies $f_p(\overline{D_\alpha}) \subseteq \overline{D_\alpha}$. Now, recall W_{In}^u denoting the unstable, two dimensional manifold for the saddle-focus P_{In} , while W_{Out}^s denotes the stable, two dimensional invariant manifold of the saddle-focus P_{Out} . By Prop.2.3, D_α is a topological disc in the cross-section U_p , satisfying $\partial D_\alpha = \bar{l} \cup L$ - with L being a collection of subarcs on $(W_{In}^u \cup W_{Out}^s) \cap U_p$.

Additionally, recall l denotes the arc $\{(x, -\frac{x}{a}, \frac{x}{a}) | x \in (0, c - ab)\}$ (see the illustration in Fig.26) - and that we denote by $[P_{In}, \delta_0)$ the half open (and conversely, by (P_{In}, δ_0) the half-open) arc on l connecting P_{In} and the point δ_0 (see Prop.3.5). Similarly, let $[\delta_0, P_{Out}]$ denote the closed arc on l connecting δ_0, P_{Out} , and $[f_p(\delta_0), \delta_0]$ the closed arc connecting the points $\delta_0, f_p(\delta_0)$ on l . Moreover, recall the set $\Delta_1 \subseteq f_p^{-2}(l)$ (see Cor.3.4). Finally, recall the

cross-section $H_p \subseteq D_\alpha$ (see Prop.3.3), and that $\partial H_p = f_p^{-1}(l) \cup [P_{In}, \delta_0] \cup L$ (see the illustration in Fig.39). Finally, recall the point $\delta_1 \in [P_{In}, \delta_0]$ given by Cor.3.4, and the point $\delta_0 = \delta \cap l$ (see Prop.3.2) - since $\delta \subseteq f_p^{-1}(l)$ it follows $\delta_0 \in l \cap f_p^{-1}(l)$ hence $f_p^{-1}(\delta_0) \in f_p^{-1}(l) \cap f_p^{-2}(l)$.

Now, denote by J the arc on ∂H_p which connects δ_1 with δ_0 through l , and then connects δ_0 with $f_p^{-1}(\delta_0)$ through $f_p^{-1}(l)$ (by the connectedness of $f_p^{-1}(l)$, the arc J exists - see Prop.3.1.3 and the illustration in Fig.54). With the aid of the notions above and the ideas introduced in the proof of Prop.3.4 and Lemma 3.4, we first prove the following technical result:

Lemma 4.1. *Let $p \in P$ be a trefoil parameter. Then, if T is a periodic trajectory for the vector field F_p (which is not a fixed-point), then $T \cap J = \emptyset$ - or, equivalently, the first-return map $f_p : \overline{D_\alpha} \rightarrow \overline{D_\alpha}$ has no periodic orbits intersecting J .*

Proof. Recall the set $\mu_1 = f_p^{-2}(\delta) \cap \Delta_1$ introduced in the proof of Cor.3.4, with δ, δ_0 as in Prop.3.2. We first prove μ_1 is an arc, s.t. $\mu_1 \setminus l$ includes a curve in H_p connecting $f_p^{-1}(\delta_0)$ and δ_1 (with δ_1 as in Cor.3.4 - see the illustration in Fig.54). To this end, recall that by Cor.3.4 μ_1 is the arc on Δ_1 connecting $\Gamma_1 = f_p^{-2}([\delta_0, P_{Out}])$ with $\delta_1 \in [P_{In}, \delta_0]$ (see the illustration in Fig.54). Since $f_p^{-1}(l) \subseteq \partial H_p$ (see Prop.3.3), because $\delta \cap l = \{\delta_0\}$ it follows $f_p^{-1}(\delta) \cap f_p^{-1}(l) = \{\delta_0\}$. Therefore, because $f_p(\mu_1) \subseteq \delta$, $\delta_0 \in f_p(\mu_1)$ we conclude that once μ_1 leaves $f_p^{-1}(\delta_0)$ it enters the interior of H_p and **does not** hit ∂H_p before hitting $\overline{H_p} \setminus f_p^{-1}(l)$. Therefore, since $\mu_1 \subseteq \Delta_1 \subseteq f_p^{-2}(l)$, by Cor.3.4 it follows that once μ_1 leaves $f_p^{-1}(\delta_0)$ it never hits ∂H_p before hitting δ_1 . Therefore, there exists a component $\gamma_1 \subseteq (\mu_1 \setminus \partial H_p)$ s.t. $\gamma_1 \cap \partial H_p = \{\delta_1, f_p^{-1}(\delta_0)\}$.

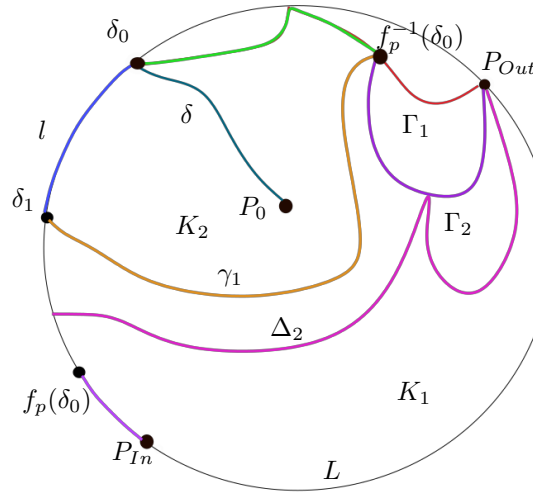


FIGURE 54. With previous notations, $J = \rho \cup \beta$, while $\Delta_1 = \gamma_1 \cup \Gamma_1$ (for simplicity, in this scenario $\gamma_1 = \mu_1$). The curves Γ_1, Γ_2 both lie strictly inside K_1 .

Now, consider K_1, K_2 the components of $\overline{H_p} \setminus \mu_1$, and recall the regions T_1, T_2 from the proof of Prop.3.5, defined by $\overline{H_p} \setminus \Delta_1$ - by definition, $D_1 \subseteq K_1$, $J \subseteq \partial K_2$. In particular, $\partial H_p \cap \partial K_2 \cap l = [\delta_1, \delta_0]$, i.e., the sub-arc of $J \cap l$ connecting δ_1, δ_0 . Conversely, $\partial K_2 \cap \partial H_p \setminus l$ is the arc ρ on J connecting $\delta_0, f_p^{-1}(\delta_0)$ (see the illustration in Fig.54). Now, using a similar argument to the one used to prove Cor.3.4, it follows that **for every** $n \geq 1$, we have $f_p^{-n}(\rho) \subseteq \Gamma_n$, $\Gamma_n \subseteq D_1$. Now, by $\rho \subseteq f_p^n(\Gamma_n)$, $\rho \subseteq \partial K_2$ and by $\Gamma_n \subseteq D_1 \subseteq K_1$, since $K_1 \cap K_2 = \emptyset$ it follows there can be no periodic orbits in ρ - as a consequence there are no periodic orbits for f_p in $f_p(\rho)$ - and since ρ is the arc on $f_p^{-1}(l)$ connecting $\delta_0, f_p^{-1}(\delta_0)$ it follows $f_p(\rho) = [f_p(\delta_0), \delta_0]$, i.e., the arc on l connecting $f_p(\delta_0), \delta_0$ (see Fig.54).

Now, recall that by Lemma 3.4, δ_1 lies in $[P_{In}, \delta_0] \setminus f_p(\delta)$ - by definition, $f_p(\delta) = (P_{In}, f_p(\delta_0))$ (see Prop.3.2). Further recall that P_{In} is a saddle-focus with an unstable two-dimensional manifold transverse to $\{\dot{y} = 0\}$ at P_{In} - which implies that given $x \in \overline{H_p}$, $x \neq P_{In}$, $f_p^{-1}(x) \neq P_{In}$. Therefore, because $\delta_1 \in f_p^{-1}(\delta)$, as $P_{In} \notin \delta$ (see Prop.3.2) it follows $\delta_1 \neq P_{In}$ - which, by the discussion above, implies $\delta_1 \in (f_p(\delta_0), \delta_0)$. Or, in other words, the arc $[\delta_1, \delta_0] \subseteq l$ connecting δ_1, δ_0 satisfies $[\delta_1, \delta_0] \subseteq f_p(\rho)$. By definition, $J = [\delta_1, \delta_0] \cup \rho$, therefore, since there are no periodic orbits for f_p in ρ it follows there are no periodic orbits for f_p in J either, and Lemma 4.1 follows. \square

Having proven Lemma 4.1, we can now begin studying the periodic dynamics of f_p in the set Q in more depth. To begin, choose some $s \in \{1, 2\}^{\mathbb{N}}$, $s = \{i_0, \dots, i_k, i_0, \dots\}$ periodic of minimal period k , s.t. $i_0 = 2$. Let us now

recall that per the notations in Prop.3.5 (and in more generality, Th.3.1), there exists a component D_s of Q s.t. $\pi(D_s) = s$, $\pi^{-1}(s) = D_s$ - and since we chose s to be periodic of minimal period k , by Cor.3.1.4 we know there exists at least one point $x_s \in D_s$ of minimal period k for f_p . As described earlier, in order to compute the Fixed Point Index of f_p^k on x_s we must first locate a neighborhood $B \subseteq H_p$ of x_s s.t. f_p^k has no fixed points in ∂B . We do so now -

Lemma 4.2. *Let $p \in P$ be a trefoil parameter, and let $s \in \{1, 2\}^{\mathbb{N}}$, $s = \{2, i_1, i_2, i_3, \dots\}$ be periodic of minimal period $k > 1$. Then, there exists an open set $B \subseteq H_p$ s.t. the following holds:*

- B is a topological disc.
- For every $j \in \{1, \dots, k\}$, f_p^j is continuous on \overline{B} .
- For every $i \neq j$, $i \in \{1, \dots, k-1\}$, $f_p^j(\overline{B}) \cap f_p^i(\overline{B}) = \emptyset$.
- $D_s \subseteq \overline{B}$.
- f_p^k has no fixed points in ∂B .
- Given any $\omega \in \{1, 2\}^{\mathbb{N}}$ of minimal period $j \leq k$, if $D_\omega \cap B \neq \emptyset$, then $s = \omega$ - i.e., D_s is the only component of Q which is periodic of minimal period k which lies in B .

Proof. Recall that by its definition in Prop.3.5, for every $n \geq 1$ we have $f_p^n(D_s) \cap l = \emptyset$. Therefore, by the compactness of D_s , for every $n \geq 1$, the Euclidean Distance (in $\overline{D_\alpha}$) between D_s , and $I_n = \overline{f_p^{-n}(l)}$ must be positive. Now, recall the closed domains D_{i_0, \dots, i_n} introduced in Prop.3.5, with which we approximated D_s - by their construction in the proof of Prop.3.5, it followed immediately that $\partial D_{i_0, \dots, i_n}$ is a (finite) collection of arcs in $\cup_{n \geq 0} I_n$ (see the illustration in Fig.55). Therefore, it follows that provided n is sufficiently large, we have $\partial D_{i_0, \dots, i_n} \cap (\cup_{1 \leq j \leq 5k} f_p^{-j}(l) I_j) = \emptyset$. Now, recall that by the periodicity of s and the construction of D_s in Prop.3.5 it follows $f_p^r(D_s) \cap D_s \neq \emptyset$ only when $r = jk$ (for some $j \geq 1$). Therefore, provided we choose $n > 0$ to be sufficiently large, for every $i, j \in \{1, \dots, k-1\}$, $i \neq j$ we have $f_p^i(D_{i_0, \dots, i_n}) \cap f_p^j(D_{i_0, \dots, i_n}) = \emptyset$ - and moreover, for every $0 \leq i \leq k$ the function f_p^i is continuous on D_{i_0, \dots, i_n} .

Additionally, it should also be noted that because we chose $s = \{2, i_1, i_2, \dots\}$, in the notations introduced in the proof of Prop.3.5 it follows $D_s \subseteq D_2$ (see the proof of Prop.3.5) - as such, the domain D_{i_0, \dots, i_n} connects the two components of $J \setminus \{\delta_0\}$ (with J as in Lemma 4.1 - see Remark 3.3). As such, since D_{i_0, \dots, i_n} is trapped in D_2 by its construction, it follows $D_{i_0, \dots, i_n} \cap l \subseteq J$. Moreover, per the construction of D_{i_0, \dots, i_n} in the proof of Prop.3.5, D_{i_0, \dots, i_n} is the result of a finite number of intersections of Jordan domains - as such, by Kerekjarto's Theorem it is also a Jordan Domain (see [1], and the illustration in Fig.55).

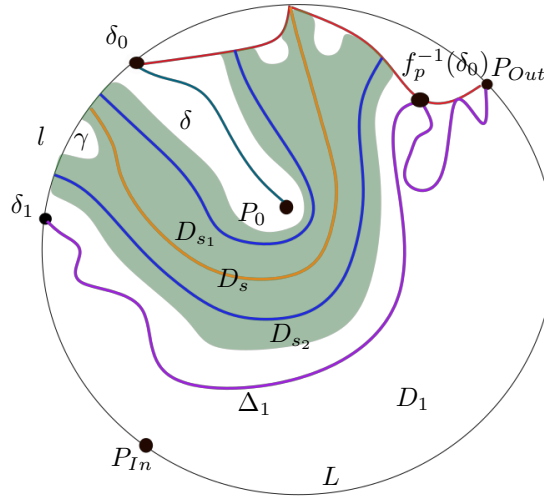


FIGURE 55. The set D_{i_0, \dots, i_n} is denoted by the green colored region, while B is the subset of D_{i_0, \dots, i_n} trapped between D_{s_1}, D_{s_2} and containing D_s .

To continue, choose two periodic symbols s_1, s_2 of minimal periods strictly greater than k s.t. $D_{s_1}, D_{s_2} \subseteq D_{i_0, \dots, i_n}$, and let B denote the **interior** of the component of $D_{i_0, \dots, i_n} \setminus (D_{s_1} \cup D_{s_2})$ s.t. $D_s \subseteq B$ (by the definition of D_{i_0, \dots, i_n} in the proof of Prop.3.5, there must exist such $s_1, s_2 \in \{1, 2\}^{\mathbb{N}}$). By the discussion above, since $B \subseteq D_{i_0, \dots, i_n}$, it must satisfy the following properties:

- For every $i \neq j$, $i \in \{1, \dots, k-1\}$, $f_p^j(\overline{B}) \cap f_p^i(\overline{B}) = \emptyset$.

- B is a topological disc.
- For every $1 \leq i \leq k$, f_p^i is continuous on \overline{B} .
- $D_s \subseteq \overline{B}$.
- $\partial B \cap (\cup_{1 \leq j \leq 5k} I_j) = \emptyset$.
- Every point in ∂B lies either in D_{s_1}, D_{s_2} , the arc J from Lemma 4.1, or $\cup_{j > 5k} I_j$. In particular, $\overline{B} \cap \delta = \emptyset$ (see the illustration in Fig.55).

Now, let $\omega \in \{1, 2\}^{\mathbb{N}}$ be periodic of minimal period **at most** k . For every such ω , by the compactness of both D_s, D_ω , the Euclidean distance between D_s, D_ω must be non-zero - and since there is at most a finite number of such ω , we can choose D_{i_0, \dots, i_n} s.t. given $D_\omega \subseteq Q \cap D_{i_0, \dots, i_n}$, if ω is periodic of minimal period k then $\omega = s$. Now, by our choice of s_1, s_2 to be periodic of minimal period **greater** than k , it follows that for $j, i \in \{0, \dots, k\}$, $r \in \{1, 2\}$ we have $f_p^i(D_r) \cap f_p^j(D_r) = \emptyset$. As such, f_p^k has no fixed points in $\partial B \cap (D_{s_1} \cup D_{s_2})$. Additionally, since we chose D_{i_0, \dots, i_n} s.t. $\partial D_{i_0, \dots, i_n} \cap (\cup_{1 \leq j \leq 5k} I_j) = \emptyset$, f_p^k cannot have any periodic points in $\partial B \cap (\cup_{1 \leq j \leq 5k} I_j) = \emptyset$ as well. Finally, by Lemma 4.1, f_p^k has no periodic points in $\partial B \cap J$, therefore all in all we conclude f_p^k has no periodic points in ∂B and Lemma 4.2 follows. \square

Remark 4.2. *In fact, we can say more - let us first recall the regions K_1, K_2 introduced in the proof of Lemma 4.1. By the arguments above, it follows $B \subseteq K_2$ - and since $\Gamma_n = f_p^{-n}([P_{Out}, \delta_0]) \subseteq K_1$ for every $n > 1$, it immediately follows that for every $n > 1$ we have $\partial B \cap \Gamma_n = \emptyset$. Or, in other words, since $f_p^{-1}(l) = \delta \cup \Gamma_1$ and because $f_p^{-n}(\Gamma_1) = \Gamma_{n+1}$ it follows that any arc $\gamma \subseteq \partial B$ which **does not** lie on either J, D_{s_1}, D_{s_2} is a pre-image of δ - i.e., $\gamma \subseteq \cup_{j \geq 0} f_p^{-j}(\delta)$.*

Having proven Lemma 4.2 we immediately derive the following result:

Corollary 4.1.1. *Let $p \in P$ be a trefoil parameter - then, with the assumptions and notations of Lemma 4.2, the set $F = \{x \in B \mid f_p^k(x) = x\}$ is non-empty and compact.*

Proof. By the continuity of f_p^k on B , F_0 is closed. Since by Lemma 4.2 there are no fixed points for f_p^k in ∂B , it is also compact. Moreover, because $D_s \subseteq B$ by Cor.3.1.4 $F \neq \emptyset$ and the assertion follows. \square

As stated in the beginning of the proof, we will prove Th.4.1 by applying the Fixed-Point Index, as it is invariant under homotopies - and to this end, we need first to compute the said index on periodic orbits in the set Q , given by Th.3.1. To do so, we will now prove the dynamics of f_p on $\overline{H_p}$ can be continuously deformed to those of a Smale Horseshoe map $H : ABCD \rightarrow \mathbf{R}^2$, acting on some rectangle $ABCD$. Therefore, using Lemmas 4.1 and 4.2, we now prove the following Proposition:

Proposition 4.3. *Let $p \in P$ be a trefoil parameter, let $s \in \{1, 2\}^{\mathbb{N}}$ be periodic of minimal period k , $s = \{2, i_1, i_2, \dots\}$, and let D_s denote the corresponding component in Q . Finally, let B denote the topological disc constructed in Lemma 4.2 s.t. $D_s \subseteq \overline{B}$ - then, the Fixed-Point Index of f_p^k on B is positive.*

Proof. Recall the imposition of $f_p(H_p)$ on H_p , as in Fig.48, let $s \in \{1, 2\}^{\mathbb{N}}$, D_s be as above, and let B be as in Lemma 4.2 (in particular, recall D_s includes x_s , a periodic point for f_p of minimal period k - see Cor.3.1.4). Before diving into the technical details of the proof, let us first give a rough sketch of it - as stated, the proof is based upon constructing a very specific continuous deformation of the dynamics of $f_p : \overline{H_p} \rightarrow \overline{D_\alpha}$ to those of a Smale Horseshoe map $H : ABCD \rightarrow \mathbf{R}^2$ (with $ABCD$ denoting some topological rectangle which can be continuously deformed to the slit disc $\overline{H_p}$). As we will see, this deformation will induce a homotopy $g_t : B \rightarrow \mathbf{R}^2$, $t \in [0, 1]$ s.t. $g_0 = f_p$, $g_1 = H$ - and by the hyperbolicity of H on its non-wandering set, it will then follow the Fixed-Point Index of H^k on B is 1. Now, denoting $F_t = \{x \in B \mid g_t^k(x) = x\}$ (by definition, $F_0 = F$ from Cor.4.1), it will be clear from our construction of $\{g_t\}_{t \in [0, 1]}$ that the set $\cup_{t \in [0, 1]} F_t \times \{t\}$ is compact in $B \times [0, 1]$ - therefore, by the invariance of the Fixed-Point Index under homotopies it would follow the Fixed-Point Index of $f_p^k = g_0^k$ on B is also 1.

Therefore, per the sketch of proof above, let us begin with homotoping f_p to a Smale Horseshoe map. Let us first recall the cross-sections $\overline{H_p}, \overline{D_\alpha}$ introduced in Prop.3.3 and Lemma 2.15, and recall we have $\overline{H_p} \subseteq \overline{D_\alpha}$, and that $f_p : \overline{H_p} \setminus \delta \rightarrow \overline{D_\alpha}$ is continuous (with δ as in Prop.3.2) - see Remark 3.1. We will do so in three consecutive stages, s.t. at each stage we carefully construct another part of the homotopy. We begin with the following one:

4.1. Stage I - constructing the deformation $\{g_t\}_{t \in [0, \frac{1}{8}]}$. Before constructing the deformation, we first study the set ∂B - as we will see, this will give us a clear motivation how to construct the deformation $\{g_t\}_{t \in [0, \frac{1}{8}]}$. As stated earlier, by its construction in Lemma 4.2 and Remark 4.2, ∂B is made out of arcs on the curve J , arcs on D_{s_1}, D_{s_2} and arcs γ on $\cup_{j > k} f_p^{-j}(\delta)$ (see Lemma 4.2 and Remark 4.2) - see the illustration in Fig.55. As such, $\partial B \setminus (D_{s_1} \cup D_{s_2})$ is composed from a collection of arcs in $M = J \cup (\cup_{j > k} f_p^{-j}(\delta))$ - moreover, any component of $M \setminus J$ is an arc γ in $\cup_{j > k} f_p^{-j}(\delta)$, s.t. γ is an arc with endpoints on J (see the illustration in Fig.55). As such, since the components of ∂B are strongly dependent on the dynamics of f_p , it follows that when we continuously

deform the map $f_p : \overline{H_p} \rightarrow \overline{D_\alpha}$ to some $g : \overline{H_p} \rightarrow \overline{D_\alpha}$, the deformation induces a continuous deformation of B to another domain, B' .

To make things more precise, given a continuous deformation $\{g_t\}_{t \in [0, \frac{1}{8}]}$, $g_t : \overline{H_p} \setminus \delta \rightarrow \overline{D_\alpha}$ s.t. $g_0 = f_p$, and write $B = B_0$ - since the deformation is continuous, because B_0 is generated by the dynamical properties of f_p it follows B_0 is continuously deformed to a domain $B_t, t \in (0, \frac{1}{8}]$ (at least provided the deformation is sufficiently well-behaved). As we will prove, recalling the set J (see the discussion before Lemma 4.1), we can choose such a deformation s.t. for every $t \in [0, \frac{1}{8}]$ B_t is defined and g_t^k has no fixed-points in ∂B_t - and moreover, for $t = \frac{1}{8}$ we have $\partial B_{\frac{1}{8}} \subseteq D_{s_1, \frac{1}{8}} \cup D_{s_2, \frac{1}{8}} \cup J$. In other words, we prove there exists a deformation of f_p s.t. B is continuously deformed to $B_{\frac{1}{8}}$ s.t. no new fixed points for g_t^k are added, and moreover, the boundary arcs of $\partial B \cap (\cup_{j>k} f_p^{-j}(\delta))$ are all removed. Moreover, we will also prove the maps $g_t^k : \overline{B_t} \rightarrow \overline{D_\alpha}$ are homotopic.

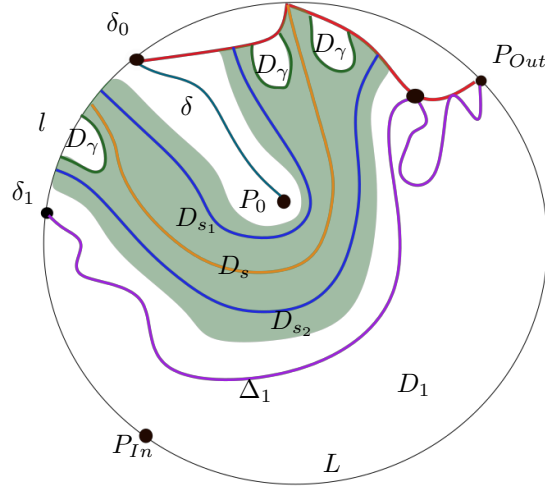


FIGURE 56. The set B is the subset of the green region, trapped between D_{s_1}, D_{s_2} and containing D_s (the orange curve). The dark green curves correspond to curves $\gamma \subseteq \cup_{j>k} f_p^{-j}(\delta)$, while D_γ are the regions trapped between γ and J .

To begin, consider an arc $\gamma \subseteq \partial B \cap (\cup_{j>k} f_p^{-j}(\partial H_p))$ as above (see the illustration in Fig.55). By the discussion above, γ is a component of $f_p^{-j}(\delta)$ for some $j > k$ - i.e., there exists some $j > 0$ s.t. $f_p^j(B) \cap \delta \neq \emptyset$. Moreover, $J \cup \gamma$ form the boundary of a Jordan domain, D_γ (see the illustration in Fig.56. Now, recall we have the inclusion $\overline{H_p} \setminus \overline{D_\alpha}$ and that $f_p(\overline{H_p}) \subseteq \overline{D_\alpha}$.

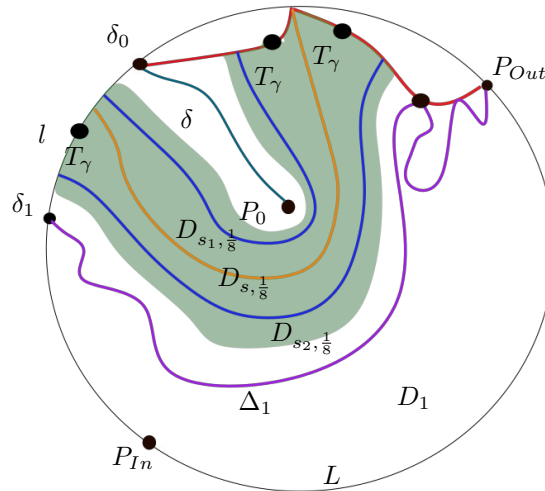


FIGURE 57. The set $B_{\frac{1}{8}}$ is the subset of the green region, trapped between $D_{s_1, \frac{1}{8}}, D_{s_2, \frac{1}{8}}$ and containing $D_{s, \frac{1}{8}}$ (the orange curve). The domains D_γ were contracted to the points T_γ .

Now, define the homotopy $\{g_t\}_{t \in [0, \frac{1}{8}]}$, $g_t : \overline{H_p} \setminus \delta \rightarrow \overline{D_\alpha}$ s.t. the following conditions hold:

- For every $t \in [0, \frac{1}{8}]$, g_t is conjugate on $\overline{H_p} \setminus \delta$ to $f_p = g_0$.
- For every $\gamma \subseteq \partial B$ as described above, the homotopy contracts D_γ to a singleton on J . That is, when t goes from 0 to $\frac{1}{8}$, D_γ is contracted to a singleton $T_\gamma \in J$ (see the illustration in Fig.57).
- For every $t \in [0, \frac{1}{8}]$, g_t is injective on $\overline{H_p} \setminus \delta$, and $P_0 \notin g_t(\overline{H_p} \setminus \delta)$ (see the illustration in Fig.57).

Now, recall the construction of the set Q from the proof of Th.3.1 (see Prop.3.5). Since g_t , $t \in (0, \frac{1}{8})$ is conjugate to f_p on $\overline{H_p} \setminus \delta$ the arguments used to prove Prop.3.5 and Cor.3.1.4 also apply for g_t , $t \in [0, \frac{1}{8}]$ - from which it follows that since g_t varies continuously in t , so does the set Q . Or, in other words, given any $t \in [0, \frac{1}{8}]$, there exists a g_t -invariant set $Q_t \subseteq \overline{H_p} \setminus \delta$, and a continuous map $\pi_t : Q_t \rightarrow \{1, 2\}^{\mathbb{N}}$ s.t. the following holds:

- $\pi_t \circ g_t = \sigma \circ \pi_t$, with $\sigma : \{1, 2\}^{\mathbb{N}} \rightarrow \{1, 2\}^{\mathbb{N}}$ denoting the one-sided shift.
- Given any periodic $\omega \in \{1, 2\}^{\mathbb{N}}$, $\omega \in \pi_t(Q_t)$.
- For any periodic ω , $\pi_t^{-1}(\omega) = D_{\omega, t}$ is compact, and connects the two components of $\partial H_p \setminus \{P_0, P_{In}\}$.
- $\pi_0 = \pi$ and $Q_0 = Q$, with Q, π as in Th.3.1.
- Given any periodic $\omega \in \{1, 2\}^{\mathbb{N}}$, when we vary g_t to g_r , $D_{\omega, t}$ is continuously deformed to $D_{\omega, r}$ (see the illustration in Fig.57).

In fact, we can say more. Since $\{g_t\}_{t \in [0, \frac{1}{8}]}$ vary continuously, it follows the same is true for $\cup_{n \geq 0} g_t^{-n}(\partial H_p)$. Now, because the set B is bounded by arcs on $\cup_{n \geq 0} f_p^{-n}(\partial H_p)$ and D_{s_1}, D_{s_2} by $D_{s_i, 0} = D_{s_i}$, $i = 1, 2$ and $g_0 = f_p$, it follows the set B also varies continuously. That is, writing $B = B_0$, the homotopy g_t , $t \in [0, \frac{1}{8}]$ induces a continuous deformation of B_t , $t \in [0, \frac{1}{8}]$. As such, since $B = B_0$ is a topological disc, for every $t \in [0, \frac{1}{8}]$ B_t would be simply connected, homeomorphic to a topological disc - and in particular, for every $t \in [0, \frac{1}{8}]$ $D_{s_1, t}, D_{s_2, t}$ intersect ∂B_t (see the illustration in Fig.57). Now, recall Lemma 4.2 proves that for every $j \in \{1, \dots, k\}$, f_p^j is defined and continuous on \overline{B} - and that for every $i, j \in \{0, \dots, k-1\}$ we have $f_p^i(\overline{B}) \cap f_p^j(\overline{B}) = \emptyset$. Additionally, recall $\gamma \subseteq \partial B_0 = \partial B$ - therefore, it follows that we can deform $f_p = g_0$ to $g_{\frac{1}{8}}$ s.t. the following extra conditions are **also** satisfied by the homotopy $\{g_t\}_{t \in [0, \frac{1}{8}]}$:

- For every γ as defined above, $T_\gamma \in \partial B_{\frac{1}{8}}$ (see the illustration in Fig.57).
- For every $j \in \{1, \dots, k\}$, g_t^j is defined and continuous on $\overline{B_t}$.
- For every $i, j \in \{0, \dots, k-1\}$ we have $g_t^i(\overline{B_t}) \cap g_t^j(\overline{B_t}) = \emptyset$.
- Recall the definition of $\Gamma_n = f_p^{-n}([\delta_0, P_{Out}])$ - because $B \cap \Gamma_n = \emptyset$ for every $n > 1$ (see Remark 4.2), we choose the continuous deformation $\{g_t\}_{t \in [0, \frac{1}{8}]}$ s.t. for every $n > 1$, $g_t^{-n}([\delta_0, P_{Out}]) \cap \overline{B_t} = \emptyset$ (that is, $g_t^{-n}(J) \cap \overline{B_t} = \emptyset$ for every $t \in -[0, \frac{1}{8}]$ - see the illustration in Fig.57).

As a consequence, $g_t^k : \overline{B_t} \rightarrow \overline{D_\alpha}$ defines a homotopy of continuous maps. Additionally, because B_t vary continuously in $t \in [0, \frac{1}{8}]$ and because $T_\gamma \in J$ for every γ it follows $\partial B_{\frac{1}{8}} \subseteq J \cup D_{s_1, \frac{1}{8}} \cup D_{s_2, \frac{1}{8}}$. In particular, it follows the arguments of Lemma 4.2 and Lemma 4.1 both apply to $B_{\frac{1}{8}}$. Or, in other words, writing $F_{\frac{1}{8}} = \{x \in B_{\frac{1}{8}} | g_{\frac{1}{8}}^k(x) = x\}$ it follows $F_{\frac{1}{8}}$ is compact in the (open) topological disc $B_{\frac{1}{8}}$.

Analogously, for every $t \in [0, \frac{1}{8}]$ define $F_t = \{x \in B_t | g_t^k(x) = x\}$ - since for every $t \in [0, \frac{1}{8}]$ the function g_t is conjugate to $f_p = g_0$ on $\overline{H_p} \setminus \delta$, it follows that because $F = F_0$ is compact in $B = B_0$, the same is true for F_t in B_t , $t \in [0, \frac{1}{8}]$ (i.e., F_t lies in a positive distance from ∂B_t). We now claim the set $Fix(\frac{1}{8}) = \cup_{t \in [0, \frac{1}{8}]} F_t \times \{t\}$ is compact in $B(\frac{1}{8}) = \cup_{t \in [0, \frac{1}{8}]} B_t \times \{t\}$. Since the set $Fix(\frac{1}{8}) = \cup_{t \in [0, \frac{1}{8}]} F_t \times \{t\}$ is already closed in $\overline{H_p} \times [0, \frac{1}{8}]$, it would suffice to prove there are no sequences $\{(x_n, t_n)\}_n \subseteq Fix(\frac{1}{8})$ satisfying **both** $x_n \rightarrow \partial B_{\frac{1}{8}}$, $t_n \rightarrow \frac{1}{8}$. We do so by contradiction - assume there exists such a sequence, and let $(x, \frac{1}{8})$ be its partial limit in $\partial B_{\frac{1}{8}} \times \{\frac{1}{8}\}$. Now, recall $f_p = g_0$ is deformed continuously to $g_{\frac{1}{8}}$. Moreover, recall that by our construction of the homotopy $\{g_t\}_{t \in [0, \frac{1}{8}]}$, g_t^j is continuous on $\overline{B_t}$ for every $t \in [0, \frac{1}{8}]$. Therefore, since for every $n > 1$ we have $g_{t_n}^k(x_n) = x$, by the continuous deformation of $f_p = g_0$ to $g_{\frac{1}{8}}$ it follows $g_{\frac{1}{8}}^k(x) = x$, i.e., $g_{\frac{1}{8}}^k$ has a fixed point in $\partial B_{\frac{1}{8}}$. As we already proved this cannot occur, we have a contradiction and we conclude $Fix(\frac{1}{8})$ is compact in $B(\frac{1}{8}) = \cup_{t \in [0, \frac{1}{8}]} B_t \times \{t\}$.

Therefore, all in all, we have proven there exists a homotopy $\{g_t\}_{t \in [0, \frac{1}{8}]}$, $g_t : \overline{H_p} \setminus \delta \rightarrow \overline{D_\alpha}$ s.t. every component γ in $\partial B \setminus (J \cup D_{s_1} \cup D_{s_2})$ is removed by the homotopy. Moreover, the homotopy varies $B = B_0$ to B_t s.t. the fixed-points of g_t^k , $t \in [0, \frac{1}{8}]$ remain away from ∂B_t - namely, the set $Fix(\frac{1}{8})$ is compact in $B(\frac{1}{8}) = \cup_{t \in [0, \frac{1}{8}]} B_t \times \{t\}$. As must be remarked at this stage, by the discussion at the beginning of the proof of Th.4.1, it follows the Fixed-Point Indices of $f_p^k = g_0^k$ on $B = B_0$ and that of $g_{\frac{1}{8}}^k$ on $B_{\frac{1}{8}}$ **coincide** (however, we still need to compute it - which will be done in Stage III).

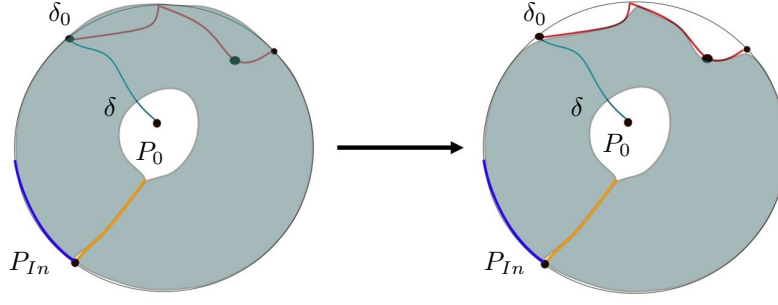


FIGURE 58. The homotopy deforming $g_{\frac{1}{8}}(\overline{H_p} \setminus \delta)$ (the grey area) on the left to $g_{\frac{1}{4}}(\overline{H_p} \setminus \delta)$ on the right, with the blue and orange curves corresponding to the double-sided limits at δ . As can be seen, $g_{\frac{1}{4}}(\overline{H_p} \setminus \delta) \subseteq \overline{H_p}$.

4.2. Stage II - constructing $\{g_t\}_{t \in [\frac{1}{8}, \frac{3}{4}]}$. Having constructed the deformation $\{g_t\}_{t \in [0, \frac{1}{8}]}$ we now extend the homotopy to the interval $[\frac{1}{8}, \frac{1}{2}]$ - and we do so in two steps: first we extend $\{g_t\}_{t \in [0, \frac{1}{8}]}$ to $[\frac{1}{8}, \frac{1}{2}]$, and then to $[\frac{1}{2}, \frac{3}{4}]$. After that, we prove that B_t varies continuously for $t \in [0, \frac{3}{4}]$, and that throughout the deformation, no new fixed-points are generated in ∂B_t . In particular, we will conclude this section by showing the set of fixed points for $\{g_t^k\}_{t \in [0, \frac{3}{4}]}$ is compact in $\cup_{t \in [0, \frac{3}{4}]} B_t \times \{t\}$.

To begin, first continuously deform $g_{\frac{1}{8}}$ to $g_{\frac{1}{4}}$ by pushing $g_{\frac{1}{8}}(\partial H_p \setminus \delta)$ inside $\overline{H_p}$, as depicted in Fig.58 - that is, the homotopy $g_t : \overline{H_p} \setminus \delta \rightarrow \overline{D_\alpha}$, $t \in [\frac{1}{8}, \frac{1}{4}]$ is a continuous deformation s.t. $g_{\frac{1}{4}}(\overline{H_p} \setminus \delta) \subseteq \overline{H_p}$ (see the illustration in Fig.58). Like we did for $t \in [0, \frac{1}{8}]$, we extend the homotopy to $t \in [\frac{1}{8}, \frac{1}{4}]$ the homotopy s.t. the following two conditions are satisfied for every $t \in [0, \frac{1}{4}]$:

- $P_0 \notin g_t(\overline{H_p} \setminus \delta)$.
- g_t is injective on $\overline{H_p} \setminus \delta$.

Now, having constructed the continuous deformation $\{g_t\}_{t \in [0, \frac{1}{4}]}$, extend it to $[\frac{1}{4}, \frac{1}{2}]$ as follows - blow up δ to an open set, thus blowing up all the components of $\cup_{j>0} g_t^{-j}(\delta)$, $\frac{1}{2} > t > \frac{1}{4}$ to open sets (see the illustration in Fig.59). This also has the effect of continuously extending g_t , $\frac{1}{2} > t > \frac{1}{4}$ to δ , as illustrated in Fig.59, which turns $g_t(\overline{H_p})$ into the Banana-shaped figure in Fig.59 (i.e., we blow up δ to a Jordan arc with two endpoints, C, D on ∂H_p - see the illustration in Fig.59). Moreover, choose the homotopy $g_t : \overline{H_p} \setminus \delta \rightarrow \overline{D_\alpha}$ s.t. $P_0 \notin g_t(\overline{H_p})$, $t \in [\frac{1}{4}, \frac{1}{2}]$ - therefore, again, using similar arguments to those in Stage I we conclude the set $Q = Q_0$ is continuously deformed to Q_t , $t \in [0, \frac{1}{2}]$. That is, given $\omega \in \{1, 2\}^{\mathbb{N}}$, the components D_ω are continuously deformed to $D_{\omega, t}$. In particular, there exists a continuous map $\pi_t : Q_t \rightarrow \{1, 2\}^{\mathbb{N}}$ s.t. for $t \in [0, \frac{1}{4}]$:

- $\pi_t \circ g_t = \sigma \circ \pi_t$, with $\sigma : \{1, 2\}^{\mathbb{N}} \rightarrow \{1, 2\}^{\mathbb{N}}$ denoting the one-sided shift.
- Given any periodic $\omega \in \{1, 2\}^{\mathbb{N}}$, $\omega \in \pi_t(Q_t)$.
- For any periodic ω , $\pi_t^{-1}(\omega) = D_{\omega, t}$ is compact, and connects the two components of $\partial H_p \setminus \{P_0, P_{In}\}$.
- $\pi_0 = \pi$ and $Q_0 = Q$, with Q, π as in Th.3.1.
- Given any periodic $\omega \in \{1, 2\}^{\mathbb{N}}$, when we vary g_t to g_r , $D_{\omega, t}$ is continuously deformed to $D_{\omega, r}$.
- Similar arguments to those used in Stage I now imply the set $B = B_0$ is continuously deformed to B_t when we vary t from 0 to $t \in (0, \frac{1}{2}]$.

We now extend the homotopy $\{g_t\}_{t \in [0, \frac{1}{2}]}$ to $[\frac{1}{2}, \frac{3}{4}]$, by deforming $g_{\frac{1}{2}}$ to a rectangle map. To do so, open up the fixed point P_{In} to an interval $[A, B] = I_{In}$ s.t. $g_t : \overline{H_p} \rightarrow \overline{D_\alpha}$, $t \in [\frac{1}{2}, \frac{3}{4}]$ is an isotopy **and** $g_{\frac{3}{4}}$ satisfies $g_{\frac{3}{4}}(I_{In}) \subseteq I_{In}$ and $g_{\frac{3}{4}}(\delta) \subseteq I_{In}$ (see the illustration in Fig.60). Moreover, choose the isotopy s.t. for every $t \in [\frac{1}{2}, \frac{3}{4}]$, we have $g_t(P_0) \notin g_t(\overline{H_p})$. Now, denote by $[C, D]$ the arc generated on $\delta \cap \partial H_p$ by blowing up δ (for $t > \frac{1}{4}$), and let $g_{\frac{3}{4}} : \overline{H_p} \rightarrow \overline{D_\alpha}$ be the map illustrated in Fig.60. After choosing an AB and CD sides, we can now re-draw $g_{\frac{3}{4}}$ as a rectangle map, as illustrated in Fig.61.

Now, let us recall that by the construction of $Q = Q_0$ in Prop.3.5, its components lie away from both P_{In}, δ - therefore, because by our construction $P_0 \notin g_t(\overline{H_p} \setminus \delta)$, $t \in [0, \frac{3}{4}]$, we conclude again that $Q = Q_0$ is continuously deformed to Q_t , $t \in [0, \frac{3}{4}]$. As a consequence, again the set B is deformed to B_t , $t \in [0, \frac{3}{4}]$ - in particular, because \overline{B} lies away from P_{In}, δ for $f_p = g_0$ (see the proof of Lemma 4.2), it follows that when we vary $f_p = g_0$ to $g_{\frac{3}{4}}$, the set $B = B_0$ is continuously deformed to $B_{\frac{3}{4}}$. And because we constructed the homotopy in Stage I s.t.

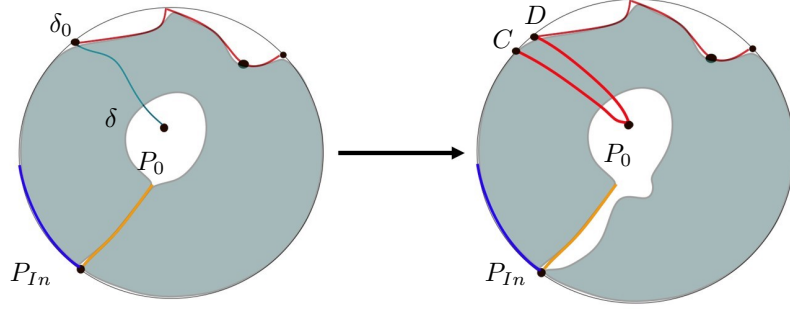


FIGURE 59. The homotopy deforming $g_{\frac{1}{4}}(\overline{H_p} \setminus \delta)$ (the grey area) on the left to $g_{\frac{1}{2}}(\overline{H_p} \setminus \delta)$ on the right, with the blue and orange curves corresponding to the double-sided limits at δ for $g_{\frac{1}{4}}$. As can be seen, the homotopy splits the curve δ to the arc $[C, D]$, s.t. the blue and orange line now denote $g_{\frac{1}{2}}(\delta)$ (with $P_{In} = g_{\frac{1}{2}}(P_0)$).

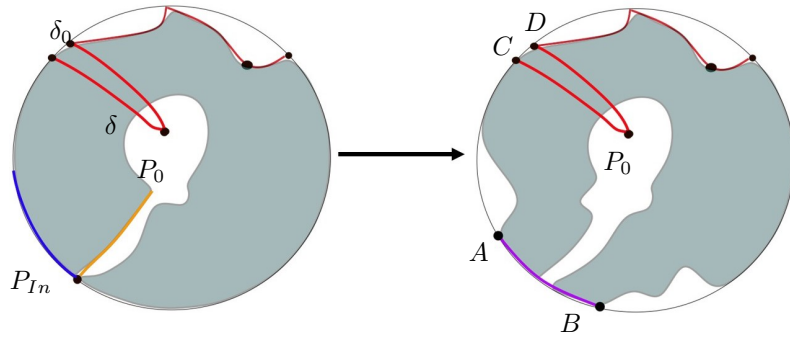


FIGURE 60. The homotopy deforming $g_{\frac{1}{2}}(\overline{H_p} \setminus \delta)$ (the grey area) on the left to $g_{\frac{3}{4}}(\overline{H_p} \setminus \delta)$ on the right. As can be seen, the homotopy stretches the fixed point P_{In} on the boundary to an interval $I_{In} = [A, B]$ s.t. $g_{\frac{3}{4}}(C, D) \subseteq I_{In}$.

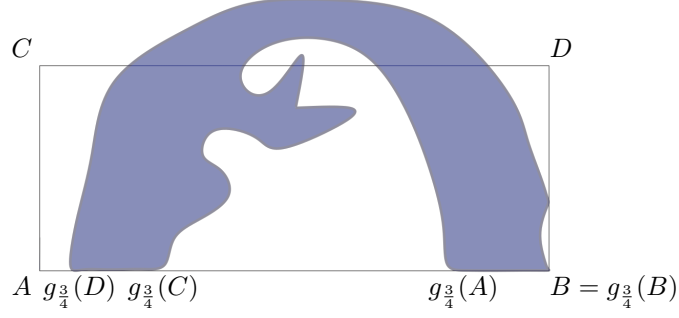
$\partial B_{\frac{1}{8}} \subseteq J \cap D_{s_1, \frac{1}{8}} \cup D_{s_2, \frac{1}{8}}$, on top of the properties listed above, we can further choose the homotopy $\{g_t\}_{t \in [0, \frac{3}{4}]}$ s.t. the following conditions are satisfied:

- $g_t : \overline{B_t} \rightarrow \overline{D_\alpha}$, $t \in [0, \frac{3}{4}]$ is a homotopy of continuous maps.
- Since $g_{\frac{j}{8}}^j$ is continuous and defined on $\overline{B_{\frac{1}{8}}}$ for every $j \in \{1, \dots, k\}$, we choose the homotopy s.t. for $\frac{3}{4} \geq t > \frac{1}{8}$ g_t^j is also defined and continuous on $\overline{B_t}$ (i.e., for $j \in 1, \dots, k$, $g_t^j(\overline{B_t}) \subseteq \overline{H_p}$).
- Since for every $i, j \in \{0, \dots, k-1\}$, $i \neq j$ we have $g_{\frac{i}{8}}^i(\overline{B_{\frac{1}{8}}}) \cap g_{\frac{j}{8}}^j(\overline{B_{\frac{1}{8}}}) = \emptyset$, we choose the homotopy s.t. for $\frac{3}{4} \geq t > \frac{1}{8}$ we also have $g_t^i(\overline{B_t}) \cap g_t^j(\overline{B_t}) = \emptyset$.
- For $\frac{3}{4} \geq t > \frac{1}{8}$, the action of g_t^k on $\overline{B_t}$ is conjugate to that of $g_{\frac{k}{8}}^k$ on $\overline{B_{\frac{1}{8}}}$.
- For every $t \in [0, \frac{3}{4}]$, the map g_t is injective on $\overline{H_p} \setminus \delta$.

To conclude Stage II, let us remark that again, similar arguments to those used in Stage I imply that setting $F_t = \{x \in B_t | g_t^k(x) = x\}$ and $Fix(\frac{3}{4}) = \cup_{t \in [0, \frac{3}{4}]} F_t \times \{t\}$, $Fix(\frac{3}{4})$ is compact in $\cup_{t \in [0, \frac{3}{4}]} B_t \times \{t\}$. To see why, recall we already proved in Stage I that $Fix(\frac{1}{8})$ is compact in $B(\frac{1}{8})$, therefore, because $g_t : \overline{B_t} \rightarrow \overline{D_\alpha}$, $t \in (\frac{1}{8}, \frac{3}{4}]$ is conjugate to $g_{\frac{1}{8}} : \overline{B_{\frac{1}{8}}} \rightarrow \overline{D_\alpha}$ it follows that for every $t \in [0, \frac{3}{4}]$, the set $F_t = \{x \in B_t | g_t^k(x) = x\}$ is compact in B_t . Therefore, using a similar argument to the one used to prove $Fix(\frac{1}{8})$ is compact in $B(\frac{1}{8})$ we conclude $Fix(\frac{3}{4})$ is compact in $B(\frac{3}{4})$.

4.3. Stage III - constructing $\{g_t\}_{t \in [\frac{3}{4}, 1]}$ and concluding the proof. Having constructed the homotopy $\{g_t\}_{t \in [\frac{3}{4}, 1]}$, we can now extend it to $[\frac{3}{4}, 1]$ and then conclude the proof. To this end, let us consider the components of $Q_{\frac{3}{4}}$ - similarly to the argument in the proof of Prop.3.5, every component $D_{\omega, \frac{3}{4}}$, $\omega \in \{1, 2\}^N$ in $Q_{\frac{3}{4}}$ is homeomorphic to a convex set, thus contractible. Because $g_{\frac{3}{4}}$ is a rectangle map of the rectangle $\overline{H_p} \setminus \delta = ABCD$ (see Fig.61), the argument used to prove Prop.3.5 now implies the following - for every $t \in [0, \frac{3}{4}]$ there exists a g_t -invariant $Q_t \subseteq \overline{H_p}$ and a continuous map $\pi_t : Q_t \rightarrow \{1, 2\}^N$ s.t. the following conditions are satisfied (with $Q_0 = Q$, $\pi_0 = \pi$ from Th.3.1):

- $\pi_t \circ g_t = \sigma \circ \pi_t$, with $\sigma : \{1, 2\}^N \rightarrow \{1, 2\}^N$ denoting the one-sided shift.

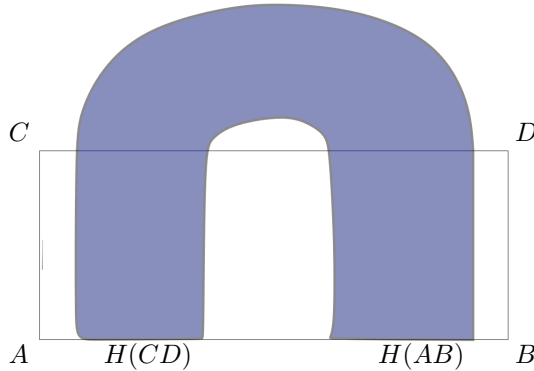
FIGURE 61. $g_{\frac{3}{4}}(\overline{H_p} \setminus \delta)$ sketched as a rectangle map.

- Given any periodic $\omega \in \{1, 2\}^{\mathbb{N}}$, $\omega \in \pi_t(Q_t)$.
- For any periodic ω , $\pi_t^{-1}(\omega) = D_{\omega,t}$ is compact, and connects the two components of $\partial H_p \setminus \{P_0, P_{I_n}\}$.
- $\pi_0 = \pi$ and $Q_0 = Q$, with Q, π as in Th.3.1.
- Given **any** periodic $\omega \in \{1, 2\}^{\mathbb{N}}$ (which is not the constant $\{1, 1, 1, \dots\}$), when we vary g_t to g_r , $D_{\omega,t}$ is continuously deformed to $D_{\omega,r}$.

However, unlike Prop.3.5, this time we can say more about the invariant set of $g_{\frac{3}{4}}$ in $ABCD$. Using similar arguments to the proof of Prop.3.5 we conclude there exists an invariant set $I \subseteq ABCD$ and a continuous, surjective map $\xi : I \rightarrow \{1, 2\}^{\mathbb{Z}}$ s.t. the following holds:

- $\xi \circ g_{\frac{3}{4}} = \zeta \circ \xi$, with $\zeta : \{1, 2\}^{\mathbb{N}} \rightarrow \{1, 2\}^{\mathbb{Z}}$ denoting the double-sided shift.
- Given $s \in \{1, 2\}^{\mathbb{Z}}$, $\xi^{-1}(s)$ is convex - hence, contractible.
- If $s \in \{1, 2\}^{\mathbb{Z}}$ is periodic of minimal period k (which is not the constant $\{\dots, 1, 1, 1, \dots\}$), $\xi^{-1}(s)$ contains a periodic point x_s of minimal period k - and moreover, $x_s \in D_{s, \frac{3}{4}}$, i.e., $x_s \in Q_{\frac{3}{4}}$.
- Conversely, given a periodic $s \in \{1, 2\}^{\mathbb{N}}$ of minimal period k , $s = \{i_0, i_1, \dots\}$ (which is not the constant $\{1, 1, 1, \dots\}$) all the periodic points in $D_{s, \frac{3}{4}}$ lie in $\xi^{-1}(s')$, $s' = \{\dots, i_k, i_0, i_1, \dots\}$.

Armed with this information, we now homotope $g_{\frac{3}{4}} : ABCD \rightarrow \overline{D_\alpha}$ to a Smale Horseshoe map $g_1 = H : ABCD \rightarrow \overline{D_\alpha}$. To do so, let R denote the maximal invariant set of $g_{\frac{3}{4}}$ in the rectangle $ABCD$ - first, homotope $g_{\frac{3}{4}}$ to $g_{\frac{7}{8}}$ by removing every component of $R \setminus I$, and then, homotope $g_{\frac{7}{8}}$ to $g_1 = H$ by crushing every component of I to a singleton. In particular, if $C \subseteq I$ a component of I which contains a periodic point x_C , crush C to x_C - as such, it now follows $g_1 = H$ is a Smale Horseshoe map, hence hyperbolic on its invariant set in $ABCD$ (see the illustration in Fig.62).

FIGURE 62. The map $g_1 = H$, a Smale Horseshoe map.

Now, let $\{g_t\}_{t \in [0,1]}$ denote the homotopy $g_t : \overline{H_p} \setminus \delta \rightarrow \overline{D_\alpha}$ (for $t > \frac{1}{2}$, δ is simply the CD side of the rectangle $ABCD$) - again, similar arguments to those used in Stages *I* and *II* imply we can choose the homotopy s.t. that the following conditions are satisfied:

- Recalling $D_s = D_{s,0}$ (see the discussion at the beginning of the proof), we always have $D_{s,t} \subseteq \overline{B_t}$. In particular, D_s is deformed continuously to $D_{s,1}$.
- In particular, because $s = \{2, i_1, i_2, \dots\}$ is periodic of minimal period k , a similar argument to that of Cor.3.1.4 implies that given $t \in [0, 1]$, there exists a fixed point for g_t^k in $D_{s,t}$.
- Moreover, every component $D_{\omega,t}$ of Q_t is continuously deformed to a unique component $D_{\omega,1}$ of Q_t , $t \in [0, 1)$. In particular, the deformation **does not** generate any new periodic points in Q_t , for $t > \frac{3}{4}$.

- Given two symbols in $\{1, 2\}^{\mathbb{N}}$, $\omega_1 \neq \omega_2$, we have $D_{\omega_1,1} \cap D_{\omega_2,1} = \emptyset$.
- Recall we denote by $\sigma : \{1, 2\}^{\mathbb{N}} \rightarrow \{1, 2\}^{\mathbb{N}}$ the one-sided shift. Therefore, for $t \in [0, 1]$ it follows $g_t(D_{\omega,t}) \subseteq g(D_{\sigma(\omega),t})$. As a consequence, if the minimal period of $\omega \in \{1, 2\}^{\mathbb{N}}$ is d , then for every $0 \leq i, j < d$, if $i \neq j$ then $g_t^i(D_{\omega,t}) \cap g_t^j(D_{\omega,t}) = \emptyset$.

Now, recall the component D_s , the compact component of $Q = Q_0$ s.t. $\pi_0(D_s) = s \in \{1, 2\}^{\mathbb{N}}$, a periodic symbol of minimal period $k > 0$ s.t. $s = \{2, i_1, i_2, \dots\}$. Furthermore, recall the construction of B in Lemma 4.2, the topological disc s.t. $D_s \subseteq \overline{B}$. As a consequence from the discussion above, similar arguments to those used in Stages *I* and *II* imply the homotopy $\{g_t\}_t \in t \in [0, 1]$ induces a continuous deformation of $B = B_0$ to B_1 s.t. $g_t^k : \overline{B_t} \rightarrow \overline{D_\alpha}$, $t \in [0, 1]$ is a homotopy. Moreover, again we can choose the homotopy s.t.:

- For every $t \in [0, 1]$, B_t is an open topological disc.
- For every $t \in [0, 1]$, $\overline{D_{s,t}} \subseteq \overline{B_t}$.
- For every $t \in [0, 1]$ and every $j \in \{0, \dots, k\}$, g_t^j is defined and continuous on $\overline{B_t}$.
- For every $t \in [0, 1]$ and every $i, j \in \{1, \dots, k-1\}$, $i \neq j$, we have $g_t^j(\overline{B_t}) \cap g_t^i(\overline{B_t}) = \emptyset$.
- Given $j \in \{1, \dots, k\}$, $1 \geq t > \frac{3}{4}$, we always have $g_t^j(\partial B_t \cap J) \subseteq H_p$, i.e., $g_{\frac{3}{4}}^j(\partial B_t \cap J)$ is **strictly interior** to the rectangle $ABCD$. Because $J \subseteq \partial H_p \setminus \delta$, it follows that $g_t^j(\partial B_t \cap J) \cap (\partial B_t \cap J) = \emptyset$, i.e., g_t^j , $j \in \{1, \dots, k\}$ has no fixed points in $\partial B_t \cap J$.

By the results of Stages *I* and *II*, we already know the set $Fix(\frac{3}{4}) = \cup_{t \in [0, \frac{3}{4}]} F_t \times \{t\}$ is compact in $B(\frac{3}{4}) = \cup_{t \in [0, \frac{3}{4}]} B_t \times \{t\}$ (with $F_t = \{x \in B_t | g_t^k(x) = x\}$). We now prove that for every $t \in [\frac{3}{4}, 1]$, g_t^k has no fixed points in ∂B_t . To see why it is so, first consider $B_{\frac{3}{4}}$ - by Stages *I* and *II*, $\partial B_{\frac{3}{4}}$ is made out of two disjoint sub-arcs in J , along with subsets of $D_{s_1, \frac{3}{4}}, D_{s_2, \frac{3}{4}}$ - therefore, when we homotope $g_{\frac{3}{4}}$ it follows, again, that we can choose the homotopy s.t. for every $t \in [\frac{3}{4}, 1]$, ∂B_t is composed of precisely two arcs on J , along with subsets of $D_{s_1, t}, D_{s_2, t}$. Now, let us recall that by the construction of $B = B_0$ in Lemma 4.2, s_1, s_2 are both periodic of minimal period **greater** than k - therefore, the discussion above combined with the results of Stages *I* and *II* imply that for every $t \in [0, 1]$, $D_{s_1, t}, D_{s_2, t}$ admit no periodic points for g_t of minimal period $j \leq k$. Now, recall we constructed the homotopy $g_t : B_t \rightarrow \overline{D_\alpha}$ s.t. for $t \in (\frac{3}{4}, 1]$ g_t^k has no fixed points in $\partial B_t \cap J$. Additionally, by construction, for $t \geq \frac{1}{8}$ we have $\partial B_t \subseteq J \cup D_{s_1, t} \cup D_{s_2, t}$ - hence, it g_t^k , $t \in (\frac{3}{4}, 1]$ has no fixed points in ∂B_t . As a consequence, the set $F_t = \{x \in B_t | g_t^k(x) = x\}$ is compact in the topological disc B_t for $t \in (\frac{3}{4}, 1]$.

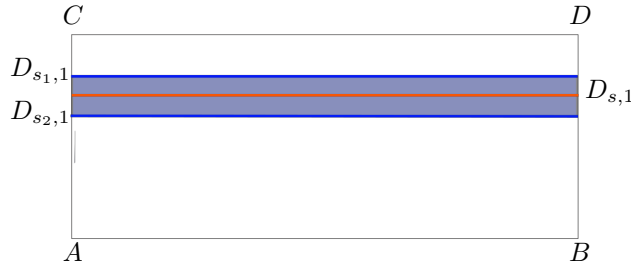


FIGURE 63. The set B_1 inside $ABCD$. The blue lines correspond to $D_{s_1,1}$ and $D_{s_2,1}$ while the orange line corresponds to $D_{s,1}$.

However, we already know that $t \in [0, \frac{3}{4}]$, F_t is compact in B_t (with $B = B_0$). Therefore, because $g_t^k : \overline{B_t} \rightarrow \overline{D_\alpha}$ is a homotopy, it follows the set $Fix(1) = \cup_{t \in [0, 1]} F_t \times \{t\}$ has no accumulation points in $\cup_{t \in [0, 1]} \partial B_t$ - for if there was such an accumulation point (x, t_0) at some $\partial B_{t_0} \times \{t_0\}$, $t_0 \in [0, 1]$, by the continuity of the deformation it would immediately follow $g_{t_0}^k(x) = x$, i.e., x is a fixed point for $g_{t_0}^k$. Since we proved in Stages *I, II, III* that g_t^k has no fixed points in ∂B_t for t in $[0, \frac{1}{8}]$, $[\frac{1}{8}, \frac{3}{4}]$, and $[\frac{3}{4}, 1]$ (respectively), this is a contradiction - hence, we conclude $Fix(1)$ is a closed set in $B(1) = \cup_{t \in [0, 1]} B_t \times \{t\}$. Therefore, by Ch.VII.5.8 in [5], it follows the Fixed-Point Index is constant along $g_t^k : B_t \rightarrow \overline{D_\alpha}$, $t \in [0, 1]$ - or, put simply, the fixed-point index of $f_p^k = g_0^k$ on $B = B_0$ is the same as that of g_1^k on B_1 - denoted by $Ind(f_p)$.

Now, recall $g_1 = H : ABCD \rightarrow \overline{D_\alpha}$ is a Smale Horseshoe map, hence hyperbolic on its invariant set. In particular, since H is a \cap -Horseshoe map, given a point $x \in ABCD$ in the invariant set of H , the differential $D_x H$ has one positive eigenvalue $\lambda_1 > 1$ and another $\lambda_2 \in (0, 1)$ - therefore, if j is the minimal period of x , the degree of $H^j - Id$, $deg(H^j(x) - x)$, is 1. Therefore, given $x \in F_1$ of minimal period k , because the fixed points of H^k are all isolated from one another, by the additivity of the Fixed-Point Index (see Ch.VII.5.6 in [5]) we conclude $Ind(f_p) = \sum_{x \in F_1} deg(H^k(x) - x)$ is a non-negative quantity (since there is at most a finite number of fixed points for H^k in $ABCD$, $Ind(f_p)$ is finite). However, as proven earlier, $D_{s,1} \subseteq \overline{B_1}$ (see the illustration in Fig.63)- and moreover, as proven earlier in Stage *III*, D_s contains a fixed point x_s for H^k - by the discussion

above, $x_s \in D_{s,1} \setminus \partial B_1$, i.e., $x_s \in F_1$. Therefore, it follows $\deg(H^k(x_s) - x_s)$ is 1, hence $\text{Ind}(f_p)$ is positive and Prop.4.3 follows. \square

Remark 4.3. *With just a little more work, one can prove the Fixed-Point Index of f_p^k on B is in fact 1 - i.e., that in fact we have $\{x_s\} = F_1$.*

Having proven Prop.4.3, we now conclude the proof of Th.4.1. To do so, recall we assume $p \in P$ is a trefoil parameter (see Def.3.2), and recall the cross-sections U_p and D_α (see the discussion before Lemma 2.1 and Lemma 2.15, respectively). Additionally, let us recall we chose a periodic $s \in \{1, 2\}^{\mathbb{N}}$, $s = \{2, i_1, i_2, \dots\}$ of minimal period k . Moreover, we constructed an open set B s.t. f_p^j , $j \in \{1, \dots, k\}$ is **continuous** on \overline{B} , s.t. $D_s \subseteq \overline{D_s}$ - by Prop.4.3, the Fixed-Point Index of f_p^k on B is positive. Additionally, since $\overline{B} \subseteq \overline{H_p}$, by $\overline{H_p} \subseteq \overline{D_\alpha}$ (see Prop.3.3) and by Prop.3.2 it follows that given any $x \in \overline{B}$, $f_p^j(x)$ is strictly interior to the cross-section $\overline{D_\alpha} \subseteq \overline{U_p}$. That is, the flow line connecting $x, f_p(x), \dots, f_p^k(x)$ **always** intersects the cross-section transversely.

Now, recall that given any $v \in P$, the cross-section $\overline{U_p}$ is smoothly deformed to $\overline{U_v}$ (see the discussion before Lemma 2.1) - since $\overline{B} \subseteq \overline{U_p}$, let us denote by $\overline{B_v}$, $v \in P$ the induced deformation of \overline{B} . As a consequence, by previous paragraph we conclude that given $v \in P$ sufficiently close to p , the trefoil parameter, when we perturb the vector field F_p to F_v , $v \in P$, for every $s \in B$, $j \in \{1, \dots, k\}$ $f_p^j(s)$ is **transverse** to U_v - which, by the compactness of \overline{B} implies f_p^k is homotopic to f_v^k on $\overline{B_v}$. We now claim:

Lemma 4.3. *Let $p \in P$ be a trefoil parameter. Then, there exists a neighborhood $p \in O \subseteq P$, s.t. $\forall v \in O$, f_p^k has no fixed points in ∂B_v .*

Proof. Assume the assumption is incorrect - that is, assume there exists a sequence $\{(x_n, v_n)\}_n \subseteq \cup_{v \in P} B_v \times \{v\}$ s.t. the following hold:

- $(x_n, v_n) \in \cup_{v \in P} B_v \times \{v\}$ for every n .
- $f_{v_n}^k(x_n) = x_n$.
- $x_n \rightarrow \partial B$ (in \mathbb{R}^3).

Let $x \in \partial B$ be the limit (or partial limit) of x_n - since by construction $\overline{B} \subseteq \overline{H_p}$, by $\overline{H_p} \subseteq \overline{D_\alpha}$ it follows by Th.2.2 the trajectory of x is bounded. Since the vector fields $\{F_{v_n}\}_n$ tend smoothly to F_p in the C^∞ metric and because x_n lies on a periodic trajectory for F_{v_n} , it follows x must also be a periodic trajectory for F_p - which, by definition, must intersect ∂B . This is a contradiction to Lemma 4.2, hence there is no such sequence - that is, there exists a neighborhood $O \subseteq P$ of p s.t. for every $v \in O$, f_v^k has no fixed points in ∂B_v . \square

As a consequence of Lemma 4.3, for $v \in P$ sufficiently close to a trefoil parameter $p \in P$, we conclude $f_p^k : \overline{B} \rightarrow \overline{U_p}$, $f_v^k : \overline{B_v} \rightarrow \overline{U_v}$ are homotopic. As such, for every $v \in O$, the fixed-point index of f_v^k on B_v is positive - i.e., f_v^k has a fixed-point x_v in B_v , which lies on some periodic trajectory T_v for B_v . Moreover, since the flow lines connecting $x \in B_v$ with $f_v(x), \dots, f_v^k(x)$ always intersect $\overline{U_v}$ transversely it follows f_v, \dots, f_v^k are all continuous - hence, because $x_v \in B_v$ it follows all the intersection points of T_v with $\overline{U_v}$ are transverse intersection points. Additionally, since we constructed B s.t. $f_p^i(\overline{B}) \cap f_p^j(\overline{B}) = \emptyset$ for every $i \neq j$, $i, j \in \{0, \dots, k-1\}$ it follows that provided v is sufficiently close to B_v , we also have $f_v^i(\overline{B_v}) \cap f_v^j(\overline{B_v}) = \emptyset$ - hence, all in all, we conclude that provided $v \in P$ is sufficiently close to the trefoil parameter p , the minimal period of x_v w.r.t. f_v is k .

We can now conclude the proof of Th.4.1. To do so, recall we originally chose $s \in \{1, 2\}^{\mathbb{N}}$ s.t. it is periodic of minimal period k , $s = \{2, i_1, i_2, \dots\}$ and **not** the constant $\{1, 1, 1, \dots\}$. Additionally, recall the curve ρ_v which divides the cross-section U_v to $U_{1,v}, U_{2,v}$ - and additionally, recall the invariant set I_v , and the map $\pi_v : I_v \rightarrow \{1, 2\}^{\mathbb{N}}$ (see the discussion before Th.4.1). Finally, recall we constructed B in Lemma 4.2 s.t. $B \subseteq D_{i_0, \dots, i_n}$, $n > k$, which immediately implies that given $i \in \{0, \dots, n\}$, $f_p^i(\overline{B}) \cap \rho = \emptyset$ (with ρ as in Cor.3.1.5). By Lemma 4.2, $D_s \subseteq \overline{B}$ - and by Cor.3.1.4, there exists a periodic point $x_s \in D_s$ of minimal period k for f_p satisfying $\pi(x_s) = s$ (with π as in Th.3.1 and Cor.3.1.5). As a consequence, since ρ is smoothly deformed to ρ_v when the vector field F_p is deformed to F_v , it follows that provided $v \in P$ is sufficiently close to a trefoil parameter p , we have $f_v^i(\overline{B_v}) \cap \rho_v = \emptyset$, $i \in \{0, \dots, n\}$. As a consequence, because $n > k$ and because $x_v \in B_v$ is periodic of minimal period k for f_v , by the definition of π_v in page 52 it follows $\pi_v(x_s) = s$. Finally, because all the intersection points of the periodic trajectory T_v with $\overline{U_v}$ are transverse we conclude π_v is continuous at x_s .

Therefore, all in all, we have proven that given any periodic $s \in \{1, 2\}^{\mathbb{N}}$ of minimal period k , $s = \{2, i_1, i_2, \dots\}$ and given any $v \in P$ sufficiently close to a trefoil parameter $p \in P$, we have the following:

- There exists a periodic point of minimal period k , $x_v \in \overline{U_v} \setminus \rho_v$ s.t. $\pi_v(x_v) = s$.
- π_v is continuous at $x_v, f_v(x_v), \dots, f_v^{k-1}(x_v)$.

- f_v, \dots, f_v^k are continuous at x_v .

Now, by the definition of π_v in page 52, we know $\pi_v \circ f_v = \sigma \circ \pi_v$, with $\sigma : \{1, 2\}^{\mathbb{N}} \rightarrow \{1, 2\}^{\mathbb{N}}$ denoting the one-sided shift. As a consequence, recalling we denote by I_v the invariant set of f_v in $\overline{U_v} \setminus \rho_v$, given a periodic $s = \{2, i_1, i_2, \dots\}$ of minimal period k , it follows that provided $v \in P$ is sufficiently close to a trefoil parameter $p \in P$, $s, \sigma(s), \dots, \sigma^k(s)$ are all in $\pi_v(I_v)$. However, this implies that given **any** periodic $s \in \{1, 2\}^{\mathbb{N}}$ of minimal period k that is **not** the constant $\{1, 1, 1, \dots\}$, for any $v \in P$ sufficiently close to p we have:

- There exists a periodic point $y_v \in \overline{U_v} \setminus \rho_v$ of minimal period k s.t. $\pi_v(y_v) = s$.
- π_v is continuous at $y_v, f_v(y_v), \dots, f_v^{k-1}(y_v)$.
- f_v, \dots, f_v^k are continuous at y_v .

Therefore, all in all, the proof of Th.4.1 is now complete. \square

Remark 4.4. As must be stated, given $v \in P$, the set $\pi_v(I_v)$ is **never** empty. As remarked in the discussion before Cor.3.1.5, the curve ρ **does not** include the fixed point P_{In} . As such, the same is true for ρ_v - or in other words, for every $v \in P$, $P_{In} \in U_{1,v}$. Since P_{In} is a fixed-point, it follows $P_{In} \in I_v$ **and** consequentially that the constant $\{1, 1, 1, \dots\}$ is in $\pi_v(I_v)$.

Remark 4.5. In [13], the fixed-point index was applied to prove the existence of infinitely many periodic trajectories in the Rössler System (albeit in a non-heteroclinic setting).

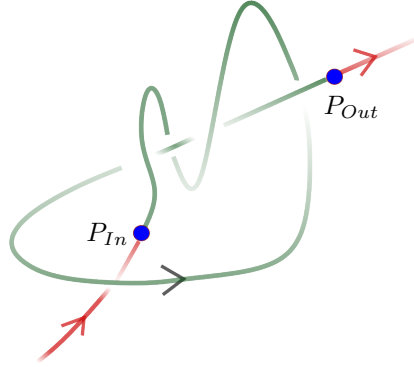


FIGURE 64. A heteroclinic knot more complex than a trefoil.

Before we conclude this paper, there are several remarks about Th.4.1 which must be made. The first is that its proof gives us a heuristic how the periodic dynamics are created (and destroyed) for vector fields in the parameter space P around trefoil parameters - namely, by colliding with the curve ρ_v , i.e., similarly to one dimensional saddle-node bifurcations in discrete-time dynamics. The second remark is that even though Th.4.1 guarantees the persistence of periodic symbolic dynamics for perturbations of trefoil parameters in the Rössler System, it **does not** guarantee the persistence of periodic trajectories in the set Q (see Th.3.1). In other words, even though the periodic, symbolic dynamics for the first-return map $f_p : \overline{U_p} \rightarrow \overline{U_p}$ (wherever defined) persist under sufficiently small perturbations in the parameter space, we do not know if the periodic trajectories in Q **also** survive such perturbations.

These two remarks (and the questions they raise) can be studied rigorously. In a series of future papers it will be proven that by applying ideas from [9],[7] and [8], it is possible to both classify the knot-types of periodic trajectories generated at trefoil parameters - and prove their persistence under perturbations in the parameter space P . Moreover, it will also be proven that the one-dimensional heuristic above about the creation (and destruction) of periodic orbits for the first-return map can be justified - namely, using Kneading Theory it will be shown that the discrete-time dynamics of the Rössler System around trefoil parameters in P can be described by those of the Logistic map. Meanwhile, we conclude this paper with the following conjecture:

Conjecture 1. Let $p \in P$ be a heteroclinic parameter for the Rössler System (not necessarily trefoil parameter - see Def.3.1) then, provided the heteroclinic knot it generates is complex at least like a trefoil, its first-return map $f_p : \overline{U_p} \rightarrow \overline{U_p}$ is chaotic w.r.t. Def.1.1.

REFERENCES

- [1] M.H.A. Newman. *Elements Of The Topology Of Plane Sets Of Points*. Cambridge, at the University Press, 1954.
- [2] E.N Lorenz. “Deterministic Nonperiodic Flow”. In: *Journal of the Atmospheric Sciences* 20 (1963), pp. 130–141.
- [3] L. Shilnikov. “A case of the existence of a denumerable set of periodic motions”. In: *Sov. Math. Dok.* 6 (1967), pp. 163–166.
- [4] S. Smale. “Differentiable dynamical systems”. In: *Bull. Amer. Math. Soc.* 73 (1967), pp. 747–817.
- [5] A. Dold. *Lectures on Algebraic Topology*. Springer, 1972.
- [6] O.E. Rössler. “An equation for continuous chaos”. In: *Physics Letters A* 57 (1976), pp. 397–398.
- [7] K.T. Alligood, J.M. Paret, and J.A. Yorke. “Geometric Dynamics”. In: Springer Verlag, 1983. Chap. 1 - *An index for the continuation of relatively isolated sets of periodic orbits*.
- [8] J.S. Birman and R.F. Williams. “Knotted periodic orbits in dynamical systems II: Knot holders for fibered knots”. In: *Contemporary Mathematics* 20 (1983), pp. 1–60.
- [9] K.T. Alligood and J.A. Yorke. “Families of periodic orbits: Virtual periods and global continuability”. In: *Journal of Differential Equations* 55 (1984), pp. 59–71.
- [10] P. Gaspard, R. Kapral, and G. Nicolis. “Bifurcation Phenomena near Homoclinic Systems: A Two-Parameter Analysis”. In: *Journal of Statistical Physics* 35 (5/6) (1984), pp. 597–727.
- [11] J. Banks et al. “On Devaney’s Definition of Chaos”. In: *The American Mathematical Monthly* 99 (1992), pp. 332–334.
- [12] C. Letellier, P. Dutertre, and B. Maheu. “Unstable periodic orbits and templates of the Rössler system: Toward a systematic topological characterization”. In: *Chaos* 5, 271 (1995).
- [13] P. Zgliczynski. “Computer assisted proof of chaos in the Rössler equations and in the Hénon map”. In: *Nonlinearity* 10(1) (1997), pp. 243–252.
- [14] V.V Bykov. “On systems with separatrix contour containing two saddle-foci”. In: *Journal of Mathematical Sciences* 95 (1999), pp. 2513–2522.
- [15] M.T. Teryokhin and T.L. Paniflova. “Periodic Solutions of the Rössler System”. In: *Russian Mathematics* 43 (8) (1999), pp. 66–69.
- [16] J. Kennedy and J.A. Yorke. “Topological Horseshoes”. In: *Transactions of the American Mathematical Society* 353 (2001), pp. 2513–2530.
- [17] John W. Milnor. *Topology from the Differentiable viewpoint*. New Jersey: World Scientific, 2001.
- [18] X.S. Yang, Yu Y., and Zhang S. “A new proof for existence of horseshoe in the Rössler system”. In: *Chaos, Solitons, and Fractals* 18 (2003), pp. 223–227.
- [19] V. Araujo and M. Jose Pacifico. *Three-Dimensional Flows*. Springer, 2010.
- [20] J.C. Gallas. “The Structure of Infinite Periodic and Chaotic Hub Cascades in Phase Diagrams of Simple Autonomous Flows”. In: *International Journal of Bifurcation and Chaos* 20(2) (2010), pp. 197–211.
- [21] M.F.S. Lima and J. Llibre. “Global dynamics of the Rössler system with conserved quantities”. In: *J. Phys. A: Math. Theor.* 44 (2011).
- [22] R. Barrio, F. Blesa, and S. Serrano. “Topological Changes in Periodicity Hubs of Dissipative Systems”. In: *Phys. Rev. Lett.* 108, 214102 (2012).
- [23] R. Barrio, A. Shilnikov, and L.P. Shilnikov. “Chaos, CNN, Memristors and beyond – a festschrift for Leon Chua”. In: World Scientific, 2013. Chap. 33 - *Symbolic Dynamics and Spiral Structures due to the Saddle Focus Bifurcations*.
- [24] R. Barrio, F. Blesa, and S. Serrano. “Unbounded dynamics in dissipative flows: Rössler model”. In: *Chaos* 242 (2014).
- [25] M. Rosalie. “Templates and subtemplates of Rössler attractors from a bifurcation diagram”. In: *Journal of Physics A: Mathematical and Theoretical, IOP Publishing* 49(31) (2016).
- [26] M.R. Cândido, D. D. Novaes, and C. Valls. “Periodic solutions and invariant torus in the Rössler system”. In: *Nonlinearity* 33 4512 (2020), pp. 66–69.
- [27] S. Malykh et al. “Homoclinic chaos in the Rössler model”. In: *Chaos* 30 (2020).
- [28] T. Pinsky. *Around Smale’s 14th Problem*. URL: <https://arxiv.org/abs/2202.01687>.